



University of
Stavanger

Faculty of Science and Technology

MASTER'S THESIS

Study program/ Specialization: Master in petroleum technology/ Production Engineering	Spring semester, 2012 Open
Writer: Jelena Grimstad (Writer's signature)
Faculty supervisor: Svein M. Skjæveland External supervisor(s): Ingebret Fjelde	
Title of thesis: Temperature effects in low salinity water flooding	
Credits (ECTS): 30	
Key words: - Enhanced oil recovery - LowSal - Aging - Waterflooding - Temperature - PHREEQC	Pages: 68 + enclosure: 33 Stavanger, 15/06/2012

Acknowledgements

I would like to thank my supervisor, Ingebret Fjelde for his advice and guidance through this master thesis. I would also like to thank PhD student Aruoturo Omekeh, the most patient person I've ever met.

Special thanks go to my parents and friends for their support and encouragement during my graduate studies.

Abstract

In the past years it has been observed that low salinity floods often lead to production of additional oil recovery. Several theories have been proposed as explanation for improved oil recovery, though the key mechanism is still under discussion.

Different effects of temperature in conducted experiments with low salinity injections have been reported. Generally, additional oil recovery with increased temperature is explained by changing oil properties and wettability modifications. An experiment in 2009 by Cissokho, H.Bertin et al. showed that incremental oil recovery was highest at moderate temperatures rather than high.

In this study, temperature effects on low salinity flooding were investigated by a simulation based on experimental results. Simulations included two mechanisms: equilibrium of phases and ion exchange. A PHREEQC model was used to analyze the temperature effects on interaction of low salinity water with a reservoir rock from a North Sea.

Observed results showed that:

- The total amount of divalent ions in low salinity brine is affected by changes in temperature though the dependency is not straight forward/ linear and is affected by ionic strength of brine, composition and composition of reservoir rock. Therefore each case should be treated separately.
- Aging of rock, brine and oil and LSWF have to be conducted at the same temperatures to avoid possible precipitation/dissolution of minerals as a result of change in temperature.
- The first aging between the brine, rock and oil happens at reservoir temperature. It is important to establish equilibrium between rock, brine and oil at new temperature before the flooding experiment at the same temperature is carried out. New aging establishes more representative wettability conditions allowing estimation of relative permeability and oil saturation that gives a good match between the simulation and experimental data.
- The simulation results have to be compared with experimentally measured changes in ionic concentrations in brines as well as precipitated minerals to be able to tune the rates together with saturation indexes.

Contents

Acknowledgements.....	2
Abstract.....	3
Contents	4
Nomenclature.....	6
Introduction.....	7
1. Theory.....	9
1.1 Methods of oil recovery/Recovery mechanisms	9
1.1.1 Primary oil recovery	10
1.1.2 Secondary oil recovery	10
1.1.3 Tertiary oil recovery (EOR)	11
1.1.4 Low salinity waterflooding as secondary and tertiary oil recovery.....	13
1.2 Wettability	17
1.2.1 Factors affecting wettability of rocks	22
1.2.1.1 COBR interaction	22
1.2.1.2 Temperature.....	22
1.2.1.3 Pressure	23
1.2.1.4 Multivalent cations	23
1.2.2 Wettability in experiments with low salinity waterflooding	23
1.3 Proposed mechanisms for low salinity water injection	28
1.3.1 Migration of fines	28
1.3.2 Increase in pH.....	29
1.3.3 Multicomponent Ionic Exchange	30
1.3.4 Double layer effect mechanism	32
1.3.5 Chemical mechanism.....	32
1.4 Temperature effects in low salinity waterflooding.....	35
2. Investigation of temperature effects on low salinity waterflooding.....	36
2.1 PHREEQC program	36
2.2 Mechanisms chosen to be simulated in the PHREEQC	37
2.3 Proposed schemes.....	39
2.3.1 Static.....	39
2.3.1.1 Description of the experiments.....	39
2.3.1.2 Description of models for simulation of static experiment	41
2.3.1.3 Programming of static modeling	43
2.3.1.4 Comparison of experiment vs simulation.....	45
2.3.1.5 Simulations with different brines	52

2.3.2 Dynamic	59
2.3.2.1 Programming procedure and difficulties encountered.....	60
3. Discussion.....	62
4. Conclusions.....	65
References.....	66
Appendices.....	69
A.1 Simulation based on experimental values	69
A.2 Simulation based on experimental values with defined reaction rate.....	74
A.3 Simulation based on reaction between FW (0.1) and reservoir rock.....	80
A.4 Simulation based on reaction between FW (0.01) and reservoir rock.....	86
A.5 Simulation based on reaction between NaCl (0.1) and reservoir rock	92
A.6 Simulation based on reaction between NaCl (0.01) and reservoir rock	97

Nomenclature

OOIP: Original Oil in Place

EOR: Enhanced Oil Recovery

IFT: Interfacial tension

COBR: Crude Oil Brine Rock

LSW: Low Salinity Water

LSWF: Low Salinity Water Flooding

STOOIP: Stock Tank Original Oil In Place

SCAL: Special Core Analysis Laboratory

HTHP: High Temperature High Pressure

AN: Acid Number

BN: Base Number

CEC: Cation Exchange Capacity

LowSal: Low Salinity

SW: Sea Water

FW: Formation Water

FW (0.1): Formation Water diluted by 10 times

FW (0.01): Formation Water diluted by 100 times

NaCl (0.1): NaCl brine with the ionic strength of formation water diluted by 10 times

NaCl (0.01): NaCl brine with the ionic strength of formation water diluted by 100 times

Introduction

Low-salinity waterflooding was described as an emerging enhanced-oil-recovery (EOR) technique in which the salinity of the injected water is controlled to improve oil recovery vs. conventional, higher-salinity waterflooding (Jerauld, Webb et al. 2008). Others described low salinity waterflooding as a promising technique for improving oil recovery in mixed-to-oil-wet sandstone reservoirs by improving the microscopic sweep efficiency by reduction in remaining oil saturation (Nasralla and Nasr-El-Din (2011), Vledder, Gonzalez et al. (2010), Mahani, Sorop et al. (2011)).

Many researchers observe, both in laboratory experiments and field tests, an increase in ultimate oil recovery using low salinity water both in secondary and tertiary flooding though the underlying mechanism is still not identified (Soraya, Malick et al. (2009), Agbalaka, Dandekar et al. (2009). Already in 1967 Bernard G.G revealed the effect of low salinity water injection on recovery of oil from cores containing clays. In the 90`s the great number of studies carried out by Tang and his co-workers awaken the interest to low salinity waterflooding (Tang and Morrow 1997). Since then, several mechanisms have been proposed in literature, but none of them has been accepted as a “true” one. The reason for this is the complexity and significant amount of parameters involving COBR interactions (crude oil/brine/rock) and the injection fluid.

Several conditions have been listed as being necessary in order to see the low salinity effects: (Austad, Rezaeidoust et al. 2010)

- presence of clay, however Pu et al. (2008) studied low salinity injection into clay free dolomite samples and got positive results (Pu, Xie et al. 2008);
- oil must contain polar components;
- injected water salinity is between 1000-2000 ppm, but effects have been observed up to 5000 ppm;
- presence of connate water containing divalent cations;

Skrettingland et al. (2010) concluded that an initial wetting condition is a crucial property to see the effect of low salinity.

Temperature is one of the parameters that have an effect on ultimate oil production by injection of low salinity water. Experiments highlighted the changes caused by changing the

temperature of low salinity waterflooding (Alotaibi, Azmy et al. (2010a), Robertson (2010), Rivet, Lake et al. (2010), Nasralla, Alotaibi et al. (2011)).

The improved oil recovery at elevated temperatures was explained by:

- viscosity reduction of the crude oil (Agbalaka, Dandekar et al. 2009);
- wettability modification due to change in temperature (Soraya, Malick et al. 2009);

The purpose of this master thesis is to contribute with geochemical modeling based on known values from the experimental studies in order to get better understanding of what is going on in the reservoir during the low salinity waterflooding. The goal is to investigate the temperature effect during low salinity injections.

This thesis starts with the theory and fundamentals that include general theory and then concentrates on low salinity waterflooding mechanisms. The second part is explaining the geochemical modeling with PHREEQC program vs. given values from an experiment as well as simulations with different brines. Finally, all main results are presented and discussed in the discussion and conclusion sections.

1. Theory

1.1 Methods of oil recovery/Recovery mechanisms

After drilling and completing one starts with production of oil/gas. Production often happens in several stages: (Schumacher (1978), Green and Willhite (1998))

- primary production including both primary and artificial lift;
- increased production/Boost from secondary recovery;
- the later extra volume from tertiary recovery/EOR;

Production period of a well can be divided into phases, distinguished by amount of pressure/energy in the reservoir. Historically, those phases described the production in a chronological sense (Green and Willhite 1998). In the initial/early period the reservoir pressure is high, and the reservoir fluids flow to the surface through the wellbore. With time pressure starts to decline and artificial lift can be used. As production continues, reservoir pressure decreases in proportion to the net volume of fluid that leaves the formation, unless it has a contiguous aquifer. When the oil recovery rate starts to be uneconomic or to achieve better performance (higher oil recovery, shorter duration of production time, etc) secondary/tertiary recoveries are used (Zolotuchin and Ursin 2000).

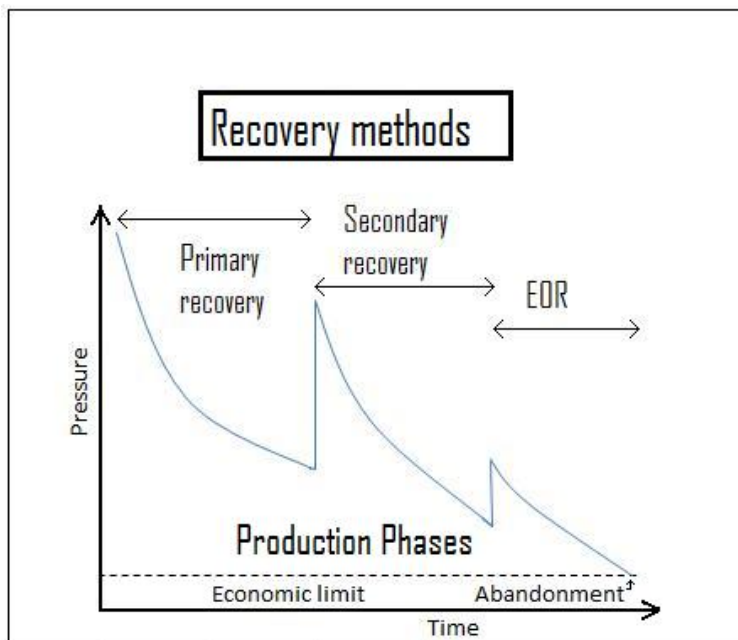


Figure 1 Production phases (based on Raymond and Leffler (2006))

1.1.1 Primary oil recovery

Primary recovery is the first stage of the oil recovery operations that uses the natural energy existing in the reservoir as a main source of energy for the displacement of oil to producing well (Green and Willhite 1998). Primary drive mechanisms/energy sources are elastic control (a depletion mechanism squeezing the oil from the reservoir due to compressibility of the oil and water saturating the porous media and shrinkage of the pores due to elastic deformation of the rock), natural water drive, solution gas drive, gas-cap drive, gravity drainage and compaction drive. Primary oil recovery is often relatively low and rarely exceeds 45% (Zolotuchin and Ursin 2000).

Reserves obtained by primary recovery depend on: (Cossé 1993)

- amount and distribution of oil/gas in place;
- characteristics of the fluids and of the rock;
- drive mechanisms and production rate;
- economic factors;

Primary production of petroleum, often but not always, consists of two phases: normal flow, where fluids are lifted only by the means of natural energy and artificial flow – fluids are lifted by means of artificial and natural energy, which include artificial gas lift and electrical pumps (Zolotuchin and Ursin 2000).

1.1.2 Secondary oil recovery

Secondary recovery is often defined as a concentrated injection of fluid into the oil reservoir, creating the second “wave” of oil from the reservoir (Schumacher 1978). It adds extra boost to the natural energy through injection of water or gas to displacement of oil to producing well (Green and Willhite 1998).

Secondary oil recovery consists of: (Schumacher 1978)

- waterflood;
- flooding by immiscible hydrocarbon gases (gas injection);

Nowadays, secondary oil recovery is synonymous with waterflooding since immiscible gas flooding is not as efficient as waterflooding (Green and Willhite 1998).

The critical design elements of a waterflood are: reservoir geometry, lithology, reservoir depth, porosity, permeability, continuity of rock properties, fluid saturations, fluid properties and relative permeabilities and water source and its chemistry (Raymond and Leffler 2006).

Primary and secondary recoveries together give up to 60% from the oil initially contained in the reservoir (Bavière 1991).

1.1.3 Tertiary oil recovery (EOR)

Traditionally, after the second oil recovery process become uneconomical, tertiary recovery is used (Green and Willhite 1998). Although due to technical and economic factors many reservoir operations are not conducted in specified order. Because of that chronologic commotion, the term tertiary oil recovery was replaced by the term “enhanced oil recovery” (Green and Willhite 1998).

Norwegian Petroleum Directorate defines enhanced oil recovery as a term used for advanced methods of reducing the residual oil saturation in the reservoir (NPD 2012).

Green and Willhite (1998) consider EOR as a process involving the injection of a fluid or fluids of some type into a reservoir. It supplies the additional energy (artificial energy) needed to displace oil to a producing well and interact with the reservoir oil/rock system to create conditions favorable for oil recovery (Green and Willhite 1998). The targets of EOR are oil remaining in place after primary/secondary oil recovery and oil which is hard to produce (Zolotuchin and Ursin 2000).

Based on both definitions, injection of low salinity water is an enhanced oil recovery. Most experiments highlight low salinity water interaction with the reservoir oil/rock system, creating the needed conditions for improved oil recovery and reducing the residual oil saturation in the reservoir. Nevertheless in some experiments low salinity injection was classified after primary/secondary/tertiary injection scheme to establish a basis for understanding. In different circumstances low salinity injection might be applied as a secondary production stage or even used as the initial production stage (Green and Willhite 1998).

Main objectives of EOR are: (Zolotuchin and Ursin 2000)

- As well as in the secondary oil recovery, EOR has to maintain the reservoir pressure at the desired level.
- Enhance displacement efficiency by reducing the residual oil saturation. Microscopic displacement efficiency expresses the mobilization of oil at the pore scale. Efficient microscopic displacement depends on several physical/chemical interactions occurring between the displacing fluid and oil. Those interactions include miscibility between the fluids, decreasing the IFT between the fluids, oil volume expansion and reducing oil viscosity (Green and Willhite 1998).
- Improve sweep efficiency by improving the mobility ratios between all displacing and displaced fluids throughout the process. Sweep efficiency is a measure or degree both horizontal and vertical to which flood have moved the displaced fluid through the reservoir before reaching the producing well. (Green and Willhite 1998).

The displacement efficiency of oil at the pore scale and the sweep efficiency at the macroscopic scale are often distinguished to analyze the way in which enhanced recovery methods operate (Bavière 1991). Some methods involve both displacements while others act mainly in one of those ways. For example alkaline flooding increases ultimate oil recovery by alternating the rock wettability, increasing the displacement efficiency, while polymer flooding affect sweep efficiency by increasing the water viscosity (Bavière 1991).

Generally, all low salinity experiments were performed with respect to microscopic displacement. In the case of low salinity waterflooding oil is displaced by an immiscible fluid, so the main forces related to displacement efficiency and acting upon the fluid droplets are capillary, viscous (contact forces) and gravity forces distributed throughout the forces. Capillary forces exerted by the fluid-fluid interface, where the droplet is bounded by another fluid phase (Bavière 1991). They depend on the physical properties of the interface as well as on the surface deformation. At pore scale capillary forces are much larger than other forces like gravity, therefore the fluid distribution is mainly controlled by capillary forces. Capillary forces limit the microscopic displacement efficiency of water (Bavière 1991).

The capillary pressure can be defined as a pressure differences across the interface of the immiscible fluids. It is influenced by the drainage and the imbibition's processes (Thakur and Satter 1998).

The capillary pressure between the two sides of the interface can be calculated from the Laplace formula: (Green and Willhite 1998)

$$P_c = P_o - P_w = \sigma_{ow}c = \frac{2 \sigma_{ow} \cos \theta}{r}$$

where:

P_c - capillary pressure, pressure difference existing across the interface

P_o - oil-phase pressure at a point just above the oil/water interface

P_w - water-phase pressure just below the oil/water interface

σ_{ow} - interfacial tension between oil and water

c – mean curvature of the interfacial tension

r - radius of the cylindrical pore channel

θ - contact angle measured through the water (wetting phase)

The capillary pressure might be positive or negative, depending on the IFT of the fluid, the relative wettability of the rocks (through θ) and the size of the capillary, r . The wetting fluid phase will always be the one with the lower pressure/lowest interfacial tension with the solid (Green and Willhite 1998).

In short cores, especially in oil wet and mixed wet systems, experimental data must be corrected for capillary end effects. It can be one of the possible sources of error during measurement of residual/remaining oil and water saturations as well as during measurements of additional oil recovery (Chukwudeme, Fjelde et al. (2011), Abeyasinghe, Fjelde et al. (2012)).

The EOR processes can be arranged in five classes: mobility-control, chemical, miscible, thermal and other processes (Green and Willhite 1998). Low salinity can be placed in the chemical or miscible class depending on which of the mechanism (out of the several suggested) is the most active.

1.1.4 Low salinity waterflooding as secondary and tertiary oil recovery

Low salinity waterflooding is generally viewed as an EOR, but in coreflood experiments it is classified as secondary (flooding from initial oil saturation) or tertiary (flooding from a remaining oil saturation) recovery for better understanding of injection sequences.

Zhang and Morrow (2006) compared low salinity secondary and tertiary recoveries with injection of reservoir brine. Five types of Berea sandstones with permeability ranged from 60 to 1100 mD with Minnelusa, CS and A crude oils were flooded. Results from secondary

recoveries with injections of low salinity brine showed increase in waterflood recovery from about 13% to 27%. In all cases of low salinity injections recoveries were higher than for injections of reservoir brine. After some discussions and investigations it was concluded that Berea 60mD was not suitable for investigation of the mechanism of enhanced oil recovery by low salinity waterflooding, probably due to high content of chlorite. Chlorite is a swelling clay and may have damaged the permeability of the rock when LSW was injected (Zhang and Morrow 2006). That conclusion may be in contrast with the Multi Ion Exchange mechanism, where the cation exchange is the main mechanism and chlorite has a high CEC, same as illite/mica. Low salinity injection in the tertiary oil recovery mode exhibited the increase in additional oil recovery up to 12% OOIP. Only the low salinity brine flooding in the tertiary mode for Berea sandstone with permeability 400mD and Minnelusa oil showed no significant ultimate oil recovery (1.1%). Zhang and Morrow (2006) concluded that COBR combination is one of the most significant factors affecting additional oil recovery, but response based only on COBR combination cannot be predicted (Zhang and Morrow 2006).

Agbalaka, Dandekar et al. (2009) studied two sets of experiments based on change in wettability state. The first set utilized Berea sandstone core plug, while other used MPU cores from Alaska. Two different oils were used in each set of experiments: pipeline blend of various crude oils from the Alaskan North Slope (TAPS oil sample) and refined oil spiked with TAPS crude oil. The first set examined the EOR potential of low salinity waterflooding, while the second set evaluated the potential of low salinity waterflood for application in secondary oil recovery. EOR potential was studied through three different injection schemes, where injection of brine was continued until no more oil production is observed. At that point salinity or temperature was changed. Observation showed that with decreasing salinity additional oil was recovered. Water breakthrough occurred at early stages and additional production of oil was at the expense of increasing water production. Researchers reported decrease in the residual oil saturation for decreasing salinity. One of the goals of the second set of experiments was to evaluate the secondary oil recovery potential of low salinity waterflooding at ambient and elevated temperatures. High salinity brine was compared with low salinity brines. Production of oil occurred only until water breakthrough after which negligible oil production was observed. Decrease in brine salinity was associated with insignificant increase in ultimate oil recovery. It was noticed that recovery efficiency was higher with change in salinity than change in temperature. Increased ultimate oil recovery

with decreased salinity was explained by wettability alteration from strongly water wet state to mixed wet system (Agbalaka, Dandekar et al. 2009).

Experiments conducted by Cissokho, H.Bertin et al. 2009 gave positive results of low salinity injections both in secondary and tertiary mode, but different response on additional oil recovery depending on concentration of diluted brine and temperatures. Consolidated core samples from the same outcrop were used for the experiments. Ten types of brine were used. One type of crude oil was used during the experiments. Their study highlighted the fact that there is no direct relationship between the pressure drop or pH increase and additional oil, and they observed that a salinity threshold must be overcome to see the low salinity effects. Oil recovery during the secondary recovery experiment was close to the oil recovery at tertiary mode (Cissokho, H.Bertin et al. 2009).

Scott M. Rivet et al. (2010) researched on 21 different waterflood using nine brines, three crude oil (A, B, C), six outcrops Berea cores and two oil reservoir cores. Four series were conducted. Experiment- A *Parallel* used 5 different brines for 5 parallel waterfloods:

- high salinity brine containing Na^+ and Ca^{2+} in secondary mode and low salinity brine with Na^+ and Ca^{2+} as tertiary waterflood;
- low salinity brine containing Na^+ and Ca^{2+} as secondary waterflood;
- low salinity brine containing Na^+ as secondary waterflood;
- low salinity brine containing Ca^{2+} as secondary waterflood;
- low salinity brine containing Li^+ as secondary waterflood;

Ultimate oil recovery for secondary low salinity waterflooding containing Na^+ and Ca^{2+} was highest and low salinity brine containing Li^+ as secondary waterflood had lowest recovery compared to the high salinity waterflood. The difference in oil recoveries for secondary low salinity brine injections containing Na^+ and Li^+ was not clearly understood since the relative replacing power for cations is relatively similar. From this part of the experiment Scott M. Rivet et al. (2010) concluded that ultimate oil recovery during the injection of low salinity water might be the result of cation exchange. No additional oil recovery during the tertiary waterflooding could be explained by secondary oil recovery stripping the clay/fine particles along the pore wall for crude oil polar components. Experiment A *series* included a sequence of two high salinity secondary, two low salinity secondary and two low salinity tertiary waterflood. Experiment B and C series included high and low salinity secondary waterflood. Low salinity injections improved ultimate oil recovery in secondary waterflood in both cases,

thought the results in tertiary recoveries were different. Experiment B-Serial had no additional recovery during tertiary flooding due to initial wettability condition (too water wet), short aging time and low clay content. Experiment C-Serial exhibited the most dramatic ultimate oil recovery due to longest aging time and the most rich clay core (Rivet, Lake et al. 2010). Several questions arisen in connection with those experiments. At some points of the experiments Scott M. Rivet et al. (2010) used the same core after restoring the high salinity connate brine. One could wonder if there was any change in sandstone structure that could affect the results of the experiments. In Experiments A-Parallel and B-Serials the aging time was only 2 days at temperatures 75 and 68 that might be not enough to establish equilibrium between sandstone, crude oil and brine water.

Gamage and Thyne (2011) have studied oil recovery in secondary and tertiary recovery modes. Berea outcrop sandstone and Minnelusa reservoir sandstone cores were used. Two types of Minnelusa crude oil were used in experiments researching the tertiary oil recovery. Berea sandstone showed increased recovery in both cases (2-8 %), but higher oil recoveries were noticed during secondary waterflood. Minnelusa sandstone showed good recovery during secondary mode and none during tertiary recovery. Migration of fines was observed in Berea waterflooding. Little pH increase was observed during Minnelusa sandstone core flooding in comparison to Berea core flooding (Gamage and Thyne 2011). No particular conclusion was derived from those experiments except the same one as Zhang and Morrow made in 2006. Different COBR combinations give different response to low salinity injections. The lack of oil recovery in tertiary mode could be explained by fast removing of oil components from the clay during the secondary recovery, since crude oil that were used represent the lighter end of the range of oil gravities in Minnelusa fields.

1.2 Wettability

Fluid distributions in porous media are affected not only by capillary, viscous and gravity forces but also by forces present at fluid/solid interfaces (Green and Willhite 1998). Wettability can be defined as a rock property related to the interaction of the rock and the fluids presented in the pores. One can observe that response when a liquid is brought into contact with a solid surface initially in contact with a gas or another liquid (Thakur and Satter 1998). The wetting phase is the phase that is adhered to the solid in the presence of another immiscible phase. Wettability is an important factor regarding fluids entrapment, flow and distribution in pore space, due to its influence on capillary pressure, fluid saturations and relative permeability characteristics, *Table 1* (Thakur and Satter (1998), Bavière 1991)). Relative permeability curves exhibit strong dependency on wettability which determines the location of the phase within the pore structure (Green and Willhite 1998). Relative permeability is defined as a ratio of the effective permeability of a fluid at a given saturation to some reference permeability, such as the absolute permeability of the rock or the effective permeability of the fluid at irreducible water saturation (Thakur and Satter 1998).

Table 1 Rules of thumb indicate the differences in the flow characteristics due to rock wettability (Bavière 1991)

	Water-Wet	Oil-Wet
Connate water saturation	Usually greater than 20 to 25% pore volume	Generally less than 15% pore volume, frequently less than 10%
Saturation at which oil and water relative permeabilities are equal	Greater than 50% water saturation	Less than 50% water saturation
Relative permeability to water at maximum water saturation; i.e., floodout	Generally less than 30%	Greater than 50% and approaching 100%

A system containing water, oil and rock can be water wet, oil wet and/or mixed wet. Wettability depends on composition of the oil phase, water phase and chemical/physical composition of the rock. When one of the fluid phases is more attracted to the rock pore surfaces than another one, system establishes different types of overall wettability (Thakur and

Satter 1998). Since overall wettability affects relative permeability and capillary pressure, it controls the ultimate recovery, *Fig 2*.

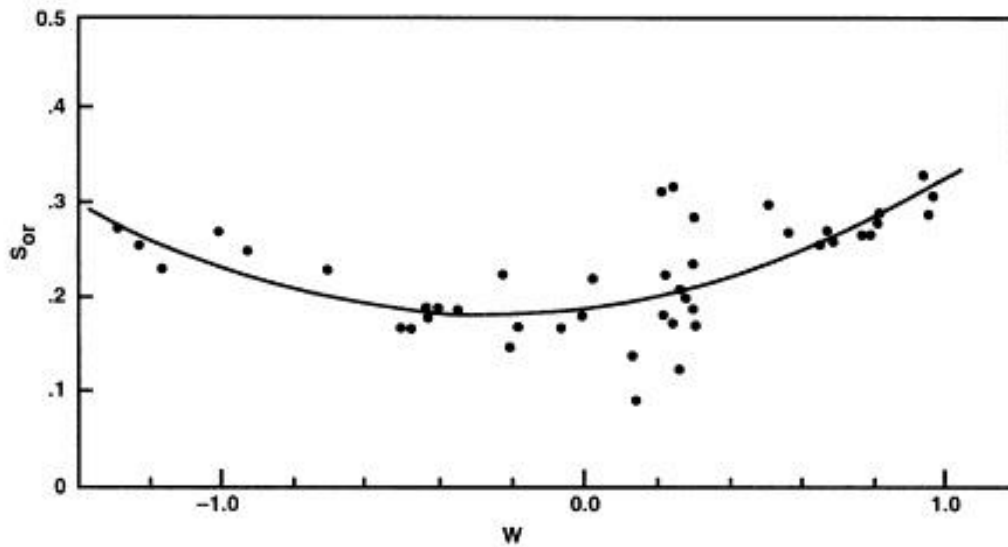


Figure 2 Dependence of oil saturation on wettability (Thakur and Satter 1998)

In a strongly water wet system, during the waterflooding, the water is taken into smaller pores, squeezing the oil into larger pores. This fluid distribution occurs because it is most energetically favorable (Anderson 1986). Water phase maintains a fairly uniform front with the oil displaced in front of it, because of the preferential wetting of the rock surface by water. Sometime, the connection of the oil in the pore with remaining oil becomes weaker and breaks off, leaving the oil drop trapped in the center of the pore, surrounded by water and rocks. The disconnected residual oil exists as small, spherical globules in the center of the larger pores or as larger patches of oil extending over many pores, *Fig 3*. Almost all remaining oil is immobile, that is why there is no additional oil recovery after water breakthrough in strongly water wet reservoirs (Agbalaka, Dandekar et al. 2008).

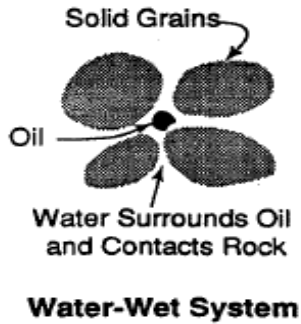


Figure 3 Residual oil in water wet system (Green and Willhite 1998)

In a strongly oil wet system, water during the waterflooding will form continuous channels or fingers through the center of larger pores, pushing oil in front of it. Remaining oil can be found in small pores and crevices as continuous film over the pore space, in pore throats and big pockets of oil trapped and surrounded by air, *Fig 4.*, (Agbalaka, Dandekar et al. 2008). Water breakthrough occurs early and most of the oil is recovered after it (Anderson 1987).

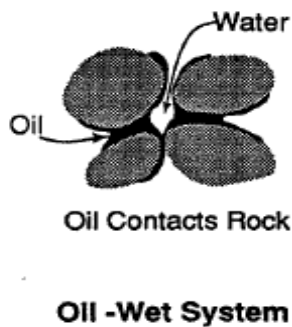


Figure 4 Residual oil in oil wet system (Green and Willhite 1998)

Mixed wettability can be described as a wettability condition varying from point to point. It results from the heterogeneity or variation in mineralogy of exposed rock surfaces or cementing-material surfaces in the pores (Green and Willhite 1998). Agbalaka et al. (2008) proposed that reservoir rock wettability is strongly affected not only by rock mineralogy and composition, but also by the adsorption or desorption of constituents in the oil phase as well as by the film deposition and spreading capability of the oleic phase. Mixed wettability is one of the definitions of the wetting states that describes the range of strongly water wet to strongly oil wet reservoirs. These wetting states include: mixed wettability, fractional

wettability, “dalmatin” wetting and speckled wetting (Agbalaka, Dandekar et al. 2008). Many reservoirs have heterogeneous wettability with variations in wettability preferences on different surfaces (Anderson 1987).

Wettability can be determined by different methods as for example: measuring the contact angle tests and Amott wettability test (Green and Willhite (1998), Thakur and Satter (1998), Agbalaka, Dandekar et al. (2008)). The conventional method of measuring the wettability when two immiscible fluids are together in a contact with a solid surface is by measuring the contact angle θ through the water phase, *Fig 5*.

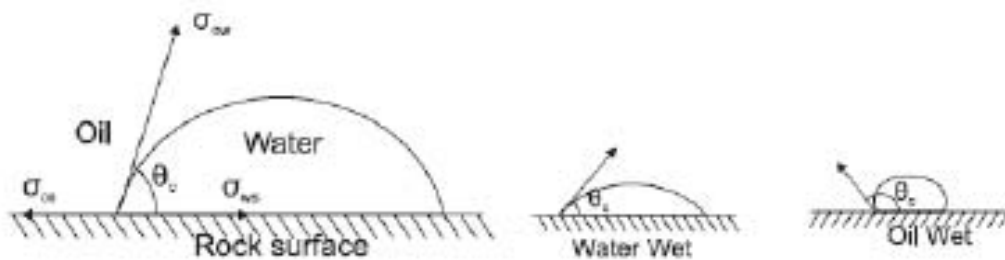


Figure 5 Contact angle θ measurement through the water phase. (Craig, 1971)

The original fluid might be displaced by the liquid moving out over the solid and stopping, when the angle between the liquid-fluid and solid-liquid interfaces reaches a certain value: a contact angle. If the liquid is spreading, while displacing the original fluid from the entire solid surface area available, a situation evidently corresponding to a contact angle of 0° , indication a strongly water wet system (Berg 1993). When contact angle is close to 90° , intermediate/neutral wettability occurs. It occurs when both fluid phases tend to wet the solid, but one phase is only slightly attracted than the other (Green and Willhite 1998). An angle close to 180° indicates a strongly oil wet rock, *Table 2*.

Contact angle values:	Wettability preference:
0-30	Strongly water wet
30-90	Preferentially water wet
90	Neutral wettability
90-150	Preferentially oil wet
150-180	Strongly oil wet

Table 2 Wettability expressed by contact angles (Rezaeidoust 2011)

Several weaknesses are connected to this method: except at the end point wetting states, the classification is strongly subjective and arbitrary and can be further divided into more classes of wettability states; length of the equilibration time cannot be reproduced at the laboratory (Agbalaka, Dandekar et al. 2008). Experimental value of the contact angle can depend on the image magnification, *Fig 6.*, (Berg 1993).

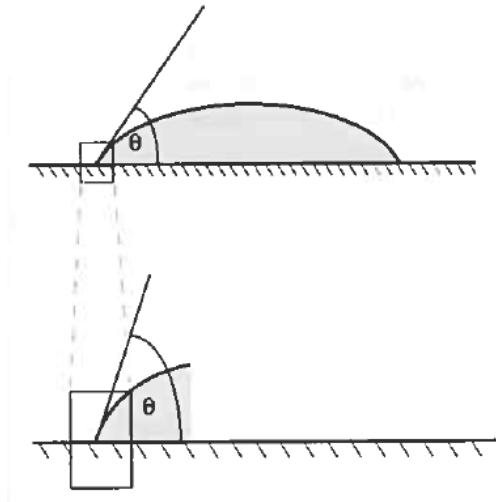


Figure 6 Large magnifications is required if the meniscus is very curved near the contact line (Berg 1993)

Amott wettability test is based on determination of Amott wettability index and derived from capillary pressure phenomena. It assumes that a strongly wetting fluid will spontaneously imbibe until the residual saturation of the non-wetting fluid is obtained and reflects the ease with which the wetting fluid will displace the non-wetting fluid. An index of 1.0 indicates a strongly wetting index, and an index of 0.0 is a strongly non-wetting fluid (Thakur and Satter 1998).

The Amott wettability neglects the hysteresis of the capillary pressure curve which can lead to the misleading results when the sample is fractionally wet (McDougall and Sorbie 1995).

Other approaches that might be used to measure the wettability are United States Bureau of Mines (USBM) wettability test, imbibitions rate test, hysteresis of the relative permeability curve and Nuclear Magnetic Relaxation (Agbalaka, Dandekar et al. 2008).

1.2.1 Factors affecting wettability of rocks

Anderson (1986) described several important factors affecting the rock wettability. In his study of wettability: the oil composition, brine chemistry, pH, ionic strength and mineral surface (COBR interaction), pressure, temperature, traces of multivalent metal cations are the parameters determining the wettability alteration (Anderson 1986).

1.2.1.1 COBR interaction

Research studies have shown that the organic matter, present in crude oil, contains the asphaltenes and resins, which are rich in polar compounds of acidic and basic nature (Anderson (1986), Buckley, Liu et al. (1998)). Buckley et al. (1998) pointed out that composition of crude oil is important to wetting alteration in two ways:

1. Polar components are those that exhibit surface activity.
2. The oil in itself is a solvent environment.

Four different mechanisms for wetting alteration by crude oil were identified:

- polar interactions in the absence of the water between oil and solid;
- surface precipitation, depending on oil properties as a solvent for the heavy fractions;
- acid/base interaction between the opposite charged interfaces;
- ion binding or specific interactions between the multivalent ions and charges sites;

A recent study revealed a crude oil-dependent low salinity effect by analyzing the aging of the same brine/rock system with different crudes having diverse physico-chemical properties (Suijkerbuijk, Hofman et al. 2012).

Brine composition together with initial pH, salinity and composition are important factors in determining wettability. They strongly affect the surface charge of the rock surface and fluid interfaces (Anderson 1986).

Minerals present in the rock can undergo wettability alterations upon adsorption of surfactants on them (Anderson 1986).

1.2.1.2 Temperature

In his major study of wettability, Anderson, W. G. claimed that increase in temperature has two different effects tending to make core more water wet (Anderson 1986):

- increases the solubility of wettability-altering compounds in oil;
- IFT and the contact angle measured through the water will decrease with increase in temperature;

1.2.1.3 Pressure

Pressure is found to be least important than, for example, temperature and there is no direct dependency between pressure and wettability (Anderson 1986).

1.2.1.4 Multivalent cations

Several studies have revealed that multivalent ion can promote oil wettability by reducing the solubility of the crude surfactants and/or promote adsorption of the mineral surfaces even at low concentrations (Anderson (1986), Bavière 1991)). Different types of cations presented in the formation water during aging of a COBR system decide the extent of wettability alteration towards more oil wet (Suijkerbuijk, Hofman et al. 2012).

1.2.2 Wettability in experiments with low salinity waterflooding

An often suggested low salinity mechanism is wettability alteration towards more water wet system, but there are contradicting experiments that exhibit opposite results.

In 2010, Skrettingland, Holt et al. conducted core flooding experiments and a single well chemical tracer test (SWCTT) field pilot to evaluate the opportunity of increased ultimate oil recovery at the Snorre field. In laboratory experiments Skrettingland et al. used cores from three formations: Upper Statfjord, Lower Statfjord and Lunde. Three different oils were used in the experiments. All flooding experiments started with sea water injection until no more oil was produced, followed by two steps of low salinity injections and two steps with low salinity NaCl injections. At the end of the experiment a high rate injection was used. No additional oil recovery was shown during both high salinity and low salinity injections. For the Statfjord formations an ultimate oil recovery of 2%-2.8% of OOIP was obtained during low salinity waterflooding as well as for low salinity of NaCl injection. Lunde cores exhibit no significant response to low salinity injections. Skrettingland, Holt et al. (2010) explained that the initial wetting conditions in the studied systems were already close to optimal for sea water injections, so it was already efficient. Therefore wettability could not be significantly altered

in a direction that favor improved oil recovery by changing the concentration and/or composition of salt in the injected water (Skrettingland, Holt et al. 2010).

Effects of low salinity waterflooding due to change of wettability from oil wet to water wet was researched both on small lab scale experimental study as well as on a field wide scale.

Nasralla, Alotaibi et al. (2011) studied the low salinity water effect on wettability in sandstone reservoirs by using the contact angle measurements technique. Mica sheets were used as a sandstone rock samples to eliminate the influence of rock heterogeneity and errors during the contact angle measurements. In order to study the dependency of wettability alteration on crude oil type, two types of crude oils were used: crude oil A and crude oil B. Deionized water and four different brines were used: formation brine, seawater, aquifer water and diluted aquifer water by 10 times. Zeta potential technique measurements using ZetaPALS technique (Phase Analysis Light Scattering) were used to investigate the impact of changing ionic strength on wettability alteration by low salinity water. Zeta potential is an electric potential at the shear plane of the double layer. (Nasralla, Alotaibi et al. 2011) Potential difference between the dispersion layer and the stationary layer of fluid attached to the dispersed particle. It's magnitude reflects the thickness of the double layer. In order to simulate different reservoir conditions, experiments were conducted at three different temperatures and two pressures. Five different experiments with crude oil A and different water salinity at 1000 psi and 212⁰F were carried out. By comparing the contact angles between oil droplets it was clear the water salinity has a great impact on the wettability. With decreasing salinity of injection water, wettability altered towards more water wet state. The results were explained by presence of water film on mica surface caused by low salinity water that did not allow adsorption of crude oil components onto the surface. The same experiments conducted with the crude oil B showed similar results as experiments with oil A, though the change of wettability for crude oil A was greater that for crude oil B. Base on those results, it was shown that the oil composition has an effect on the efficiency of low salinity water of altering the wettability. By measuring the zeta potential in solutions of crude oil A and crude oil B with brines at different salinities and compositions, researchers found clear evidence of a relation of crude oil, composition and wettability alteration. At the same experiments but with different crude oils, the amount of change of charge at oil/brine interface is different. Based on the experiments, Nasralla, Alotaibi et al. (2011) concluded that the dominant mechanism

for improving the ultimate oil recovery by low salinity water is the change of electric charge at oil/brine and brine/rock interfaces. With negative charges on both interfaces double layer expands, the repulsive forces become stronger, stabilizing the water film surrounding the rock (Nasralla, Bataweel et al. 2011).

Vledder, Gonzalez et al. (2010) investigated the wettability alteration from oil wet to water wet in the Omar field in Syria in a secondary flood mode. Two cases based on extended Buckley-Leverett theory were constructed: high salinity water flooding and low salinity water flooding. The following field observations in case of wettability alteration caused by low salinity injection were expected: at initial conditions the reservoir should be mixed-to-oil wet at a distance far from injector, while at final point the wettability should change to more water wet, close to the injector. If the location of observation point is intermediate, events such as an oil bank, high water salinity during oil banking when it passes by an observation point (production well) and/or a dual - step in watercut development (Vledder, Gonzalez et al. 2010). Field observations revealed strong oil wetness as the initial condition both from SCAL measurements and open hole logging. Final condition observation exhibited a remaining oil saturation of 15% in the flushed zone. Observations at the intermediate conditions were similar to the expected conditions. Based on the observations, Vledder, Gonzalez et al. (2010) concluded that wettability alteration from oil wet to water wet system on a reservoir scale is a reason for the incremental recovery of 10%-15% of the STOIP in the Omar field (Vledder, Gonzalez et al. 2010).

Alotaibi, Azmy et al. (2010b) studied wettability using low salinity water in sandstone reservoirs, based on proposal that the key factor in achieving the low salinity effect, such as increased oil recovery, reduced residual oil saturation, is wettability alteration. In his study, he researched the COBR interactions at different salinity level and elevated temperature conditions by determining the wettability with the help of HTHP contact angle and zeta potential technique as a function of ionic strength. Stability of solutions depending on colloidal suspensions can be measured and understood by zeta potential techniques. Two sandstone outcrops were used for this experiment: Scioto and Berea. All fluids used in this experiment were chosen to simulate the Middle East field case. Drop Shape Analysis System method was chosen as a method to measure the contact angle and interfacial tension at static conditions. Zeta Phase Analysis Light Scattering technique was used to measure zeta

potential. Researchers reported strong dependence of zeta potential on the ionic strength and clay minerals. By measuring the contact angle, Berea sandstone/crude oil/formation brine system exhibit alteration of wettability from water to oil wet condition with constant pressure and increased temperature. Alotaibi, Azmy et al. (2010b) assumed that interfacial tension of fluid/fluid and solid/fluid interfaces are affected by the ionic strength of the injected water, hence wettability and contact angle will be altered. Experiment confirmed the suggestion about wettability alteration from oil wet towards more water wet system with reducing the salinity from formation brine to sea water. Though, the wettability state changed towards intermediate state while using the fluids with elevated temperature. In oil/aquifer water/rock system wettability changed to strong water wet state because oil droplet was unstable and could hold on the rock surface for only 20 s. The contact angle was around 30° and was not significantly affected by elevated temperatures. Crude oil/formation brine/Scioto rock system exhibit an intermediate state of wettability during the whole experiment. Increasing the temperature showed no change in wettability state over time duration of 17 hours. Alotaibi, Azmy et al. (2010b) proposed that the reason for that might be the monovalent ions as Na^+ covering the rock surface, preventing the contact between the rock and crude oil. The interface will be neutrally charged preventing the adsorption of polar components in crude oil onto the clay surface. Crude oil/seawater/Scioto rock system demonstrated the wettability change towards water wet condition at low and high temperatures. Crude oil/aquifer/Scioto rock system showed unexpected results by changing the rock wettability from water wet to intermediate wet. Explanation to that result was the difference in rock mineralogy (Alotaibi, Azmy et al. 2010b). During that experiment the significance of aging time (same temperature, different aging periods) was proven by comparison of Scioto samples aged at 1 and at 5 days in the crude oil/seawater/Scioto system. Rock aged for 1 day displayed more water wet surface than a sample aged for 5 days. That might be explained by the lack of time to achieve the equilibrium between the crude oil and rock, as the heavy components of crude oil had no time to be adsorbed into the rock system. Based on those experiments it was concluded that the effect of low salinity water on wettability alteration was a function of rock mineralogy, brine salinity and temperature. However, despite the number of experiments highlighting the wettability change towards more water wet state during the injection of low salinity water, conducted experiments displayed results indicating that injection of low salinity water may not change the rock wettability into water wet state (Alotaibi, Azmy et al. 2010b).

In this paper Berea sandstone composition was described based on composition description from Kia et al (1987). That might affect the results since already in 2006 Zhang and Morrow highlighted the difficulties that might appear during usage of Berea sandstones (Zhang and Morrow 2006).

Several conclusions can be drawn from those researchers, such as:

1. Initial wettability is an important factor affecting the success rate of increment recovery by low salinity water.
2. There is a connection between ionic strength of the injected water and wettability alteration.
3. Wettability alteration during low salinity injections depends on COBR system: while Berea sandstone samples nearly always display wettability alteration towards water wet condition, other sandstone samples might have wettability alteration going towards oil or mixed wet conditions.

Many studies suggested that type of clay presented in the rock affect the adsorption of asphaltenes and resins causing the varying wettabilities (Skrettingland, Holt et al. 2010). Insufficient aging period leads to more water wet sample that might blur the end results. Temperature and pressure might have an impact on ultimate recovery during low salinity waterflooding experiments.

Based on those conclusions, the simulations done during this master thesis have to show the low salinity effect as a function of temperature.

1.3 Proposed mechanisms for low salinity water injection

Many lab work and field experiments showed a positive result for low salinity waterflooding. In recent years, it has been a common understanding that wettability alteration, together with an (underlying) physico-chemical mechanism is the reason for improved oil recovery (Suijkerbuijk, Hofman et al. 2012). Several mechanisms were presented in order to explain the COBR interactions leading to incremental oil recoveries during the injection of low salinity water, though contradictory results exist for each of it. Best known mechanisms for low salinity waterflooding are:

- “Migration of fines” by Tang and Morrow (1999)
- “pH increase” by McGuire et al. (2005)
- “Multicomponent Ionic Exchange” (MIE) by Lager et al. (2007)
- “Double layer effects” by Ligthelm et al. (2009)
- “Chemical mechanism” by Austad et al. (2010)

1.3.1 Migration of fines

In 1999 Tang and Morrow presented a theory, where the mobilization of fine particles is the main factor in the sensitivity of oil recovery to salinity in non-fired and non-acidized sandstones. Two types of oils were used: CS crude oil and refined oil. Synthetic reservoir brine, synthetic seawater and dilutions of those brines with concentrations 0.1, 0.1 with the same calcium concentration as in the original fluid and 0.01 were used. During the waterflooding experiments with different brines, researchers noticed a production of fines and increased oil recovery up to 5.8% after changing the injection brine from CS to 0.1 CS. Based on the conducted experiments they concluded that COBR interactions play a significant role in determining the sensitivity of oil recovery to brine composition. Released fine particles do not affect/damage the permeability of the samples in the same way as distilled water, but researchers reported the reduction in permeability when the injection brine salinity was less than 1550ppm. Tang and Morrow identified a number of conditions needed to observe the low salinity effects such as: presence of polar components in the crude oil and presence of initial water.

Based on the observations on wettability alteration towards increased water wetness, researchers proposed a mechanism based on the adsorption of heavy components onto the surface of the rock and release of oil together with fine particles during displacement by the

low salinity water due to the electrical double layer effect. *Fig. 7* illustrates the migration of fines.

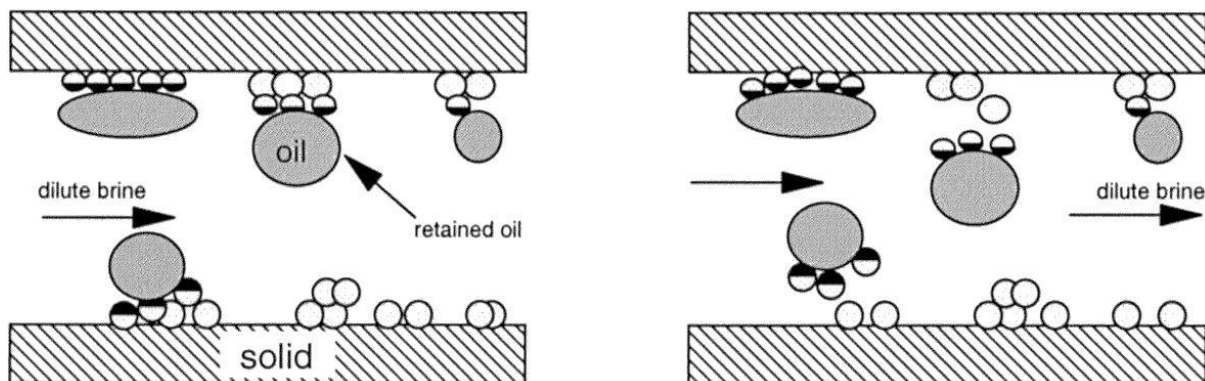


Figure 7 Oil detached to particles before injection of dilute brine and mobilization of oil during low salinity waterflooding (Tang and Morrow, 1999)

At the same time as oil components are adsorbed onto mineral surfaces, the outer surface of fine particles that coat the pore walls adheres to those polar crude oil components. During waterflooding crude oil can be released as drops together with fine particles and/or the mixed wet clay particles can be taken away with the flowing oil, tending to locate at the oil-water interface. A balance between mechanical and colloidal forces decides the release of mixed wet fines. Mechanical forces include capillary and viscous forces, while colloidal forces will depend on the balance between van der Waals attractive forces and the electrostatic repulsion.

Numerous experiments made by BP and another researchers showed increased oil recovery without observations of any fine migration and significant permeability reduction (Lager et al, 2006). In 2008 Lager et al. analyzed the results from the Alaskan reservoir and noted that the injectivity index stayed constant throughout the low salinity injection, while migration of fines would block some of the pore throats reducing the injectivity (Lager, Webb et al. 2008). Those results doubt the migration of fines as a main mechanism of low salinity waterflooding and ascribe it as a side effect (Tang and Morrow 1999).

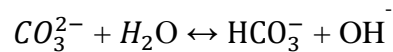
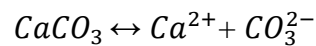
1.3.2 Increase in pH

McGuire et al. (2005) proposed a low salinity recovery mechanism based on the generation of surfactants from the residual oil at elevated pH levels in accordance with the observations on the changes in reservoir fluids, fluid/rock interactions and changes in wettability. Researchers

proposed that injection of low salinity water generates hydroxyl ions, increasing the pH up to 9 or more (McGuire, Chatham et al. 2005).

Lager et al. (2006) proposed two possible reactions increasing the pH during low salinity waterflooding experiments:

- Carbonate dissolution resulting in an excess of OH⁻



- Cation exchange between clay minerals and the invading water.

However, cation exchange is faster than carbonate dissolution and the mineral surface will exchange H⁺ present in the liquid phase with cations previously adsorbed, resulting in a pH increase.

This leads to in-situ generation of surfactants altering the interfacial and surface tension in the fluid/fluid, fluid/rock interactions as well as wettability altering. The problem of precipitation of surfactants in presence of divalent cations like calcium and magnesium is avoided by very low concentrations of these divalent cations in low salinity water..

The “increased pH” mechanism was doubted by Lager et al (2006). Researchers compared an acid number of a crude oil that gave best low salinity waterflooding result (AN<0.05) and acid number needed to generate enough surfactant to get altered wettability and emulsion formation (AN>0.2). Another fact arguing against that mechanism is presence of CO₂ in petroleum reservoirs acting as a pH buffer eliminating the possibility of pH increase up to 9 or more. Cissokho, H.Bertin et al. 2009 presented results of tertiary LowSal waterflooding, where injection of high salinity brine was followed by injection of brines with decreasing salinity. It was noticed that with each step pH and pressure drop increased but no additional oil recovery was obtained (Cissokho, H.Bertin et al. 2009)

1.3.3 Multicomponent Ionic Exchange

“Multicomponent Ionic exchange” mechanism proposed by Lager et al. (2006) based on the geochemical analysis of the low salinity effluents. It showed the importance of multicomponent ionic exchange chromatography on the water chemistry during

waterflooding. All ions in pore water compete for the mineral matrix exchange site, while natural exchangers display different selectivity for different cations. Several experiments showed the decrease of Mg^{2+} and Ca^{2+} in effluent in comparison to injected water and connate water. It supported the MIE as a main mechanism responsible for additional oil recovery during low salinity waterflooding (Lager 2006). Lager et al. stated that four of eight possible mechanisms of organic matter adsorption onto clay minerals are strongly affected by cation exchange occurring during low salinity waterflooding, illustrated in Fig 8.

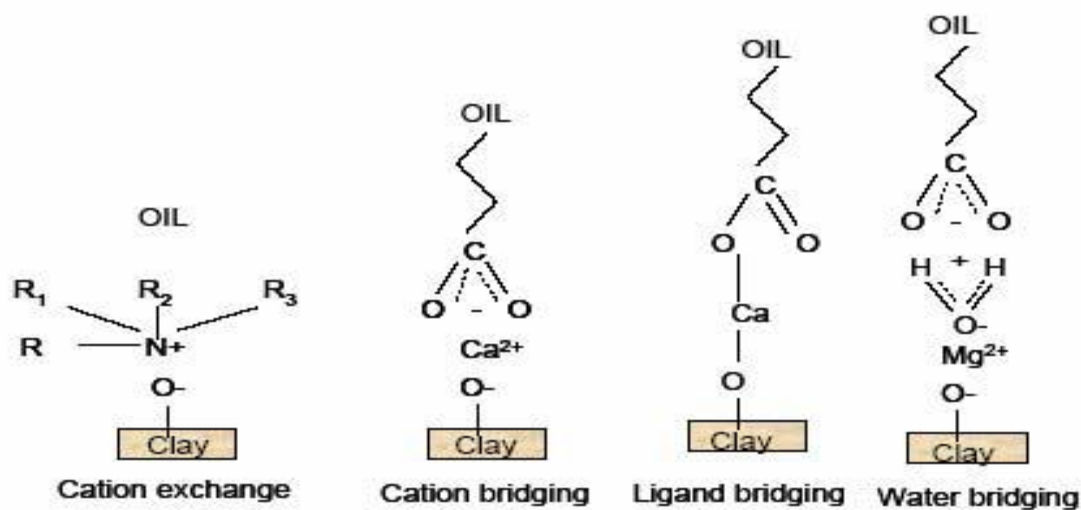


Figure 8 Mechanisms strongly affecting the cation exchange occurring during low salinity water injections (Lager et al 2006)

Basic and acidic organic minerals from the crude oil are adsorbed together with divalent cations from the formation water to the clay surface, forming organo-metallic complexes and promoting oil wetness. In the case of low salinity water injection, an electrical double layer consisting of negatively charged clay particle surrounded by an inner adsorbed layer of positive divalent Ca^{2+} and Mg^{2+} ions connected to oil droplets and an outer layer consisting of mainly negative ions (BP, 2009). When the low salinity water is injected into the reservoir, it disturbs the equilibrium, expanding the double layer, and MIE takes place replacing complexes and organic polar compounds with uncomplexed cations. It leads to more water wet system, resulting in additional oil recovery. In 2008 Lager et al. (2008) supported MIE theory by studying the produced water of a well from the Alaskan reservoir. A lack of divalent cation Mg^{2+} highlighted the interaction between the injection water and reservoir rock (Lager, Webb et al. 2008). An experiment conducted by Cissokho, H. Bertin et al. 2009 showed that injection of 100% monovalent cations (NaCl) is not a killing factor for low

salinity process, despite the fact that the relative replacing power of different cations is believed to be $\text{Li}^+ < \text{Na}^+ < \text{K}^+ < \text{Mg}^{2+} < \text{Ca}^{2+} < \text{H}^+$. Monovalent ions quantitatively displace the divalent ions, breaking the connection between oil and clay particles (Cissokho, H.Bertin et al. 2009). An experiment by Lee et al. in 2010 was presented in order to prove the MIE mechanism triggered by the expansion of the electric double layer. By using a Small Angle Scattering and X-rays techniques, researchers were able to measure the water layer thickness at the mineral surface, exhibiting the impact of cation-type on the water-layer thickness. They concluded that with a fall of salinity, water film thickness will increase and the size of the water layer for divalent ions is greater compared to monovalent cations, though different sand types showed different sensitivity to the ionic strength of the water. Based on these results, researchers interpreted it as an argument supporting MIE mechanism, where expansion of double layer is needed for the oil to be swept by the imposed flow (Lee, Webb et al. 2010).

1.3.4 Double layer effect mechanism

Double layer effects mechanism was proposed by Lighthelm et al (2009). Due to imperfections in crystal lattice, highly reactive, negatively charged clay particles, attract multivalent metal cations (Ca^{2+} , Mg^{2+}) which connect clay particles with negatively charged oil. It creates so-called an electrical double layer. Adsorbed multivalent metal cations form the inner positive charged layer and negatively charged oil form outer layer. Ion concentration of the surrounding water “decides” the screening potential of the cations. Lowering the water salinity reduces the screening potential of the cation increasing the electrostatic repulsion between the clay particle and oil. Once repulsive forces exceed the binding forces, oil particles can be desorbed from the clay surface. This mechanism is believed to modify the wettability towards increased more water wet state (Lighthelm, Gronsveld et al. 2009). If that mechanism was the only reason for ultimate oil recovery, every low salinity waterflooding would be successful.

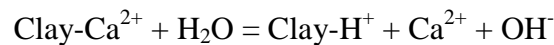
1.3.5 Chemical mechanism

Chemical low salinity mechanism by Tor Austad et al. was proposed in 2010. Based on observed experiments, several conditions were proposed in order to see the low salinity effect:

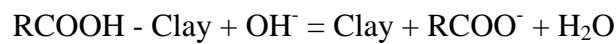
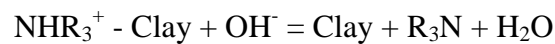
- clay properties, its type and the amount present in the rock;
- polar components in the crude oil, both acidic and basic;

- composition and pH of the initial formation brine;
- It is assumed that improved water wetness of the clay minerals present in the rock is a reason for the enhanced oil recovery effect of low salinity flooding

Initially, as in MIE mechanisms, both acidic and basic organic materials from the formation water are adsorbed onto the clay surface together with inorganic cations, especially Ca^{2+} , increasing the wetness towards more oil wet state. Depending on reservoir conditions such as pH, pressure, temperature, etc, the chemical equilibrium will be formed. In average, pH of the formation water is 5 or less due to dissolved CO_2 and H_2S . During the low salinity waterflooding, the injected water with lower ionic strength than in the formation water disturbs the chemical equilibrium. As a result of this disturbance, a net desorption of cations (Ca^{2+}) occurs. The loss of cations is compensated by adsorption of H^+ from the water close to the clay surface as in the following example:



The local increase in pH close to the clay surface triggers a reaction between adsorbed basic and acidic material, increasing the wetness towards more water wet state as displayed by following two equations:



The following illustration in *Fig. 9* describes the suggested mechanism for adsorbed basic and acidic material.

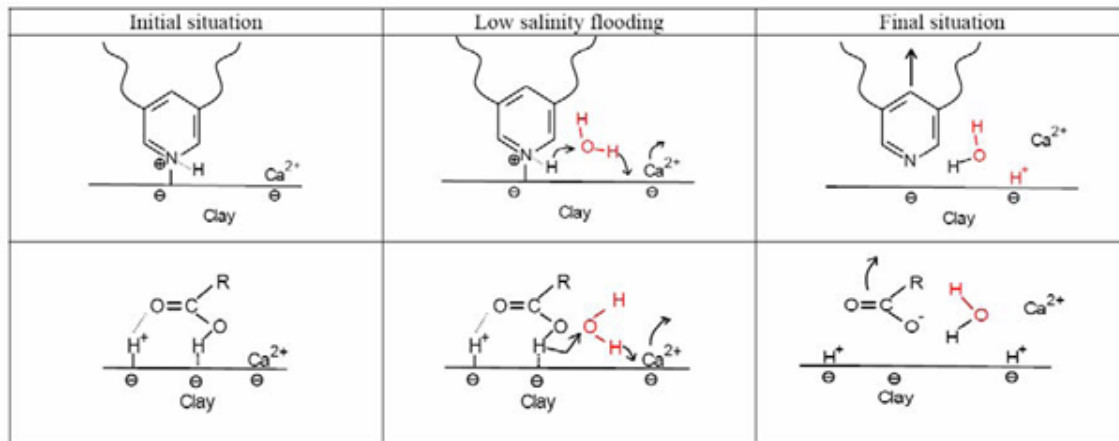


Figure 9 Proposed chemical mechanism showing the desorption of basic (upper) and acidic (lower) materials (Austad, Rezaeidoust et al. 2010)

This mechanism has difficulties to be proven by measurements of local pH change. Suijkerbuijk et al. 2012 pointed out that in most pH measurements; the pH is actually not measured because of Na^+ interference. As Na^+ ions are able to penetrate the glass electrode, creating a potential difference between the outer and inner surfaces of the electrode and replace protons, masking the true pH value (Suijkerbuijk, Hofman et al. 2012). Other experiments showed either indirect dependence of EOR at low salinity waterflooding at pH change or no dependence at all (Cissokho, H.Bertin et al. (2009), Suijkerbuijk, Hofman et al. 2012)). Another doubt is based on requirements of transition from high to low salinity. Several researchers suggested that additional oil recovery can be gained by aging the rock with the formation water containing low content of divalent cations and flooding with high salinity NaCl (Suijkerbuijk, Hofman et al. 2012).

1.4 Temperature effects in low salinity waterflooding

Cissokho, H.Bertin et al. (2009) studied the low salinity waterflooding at different temperatures in tertiary mode. Though, generally final oil recovery increases with increasing displacement temperature, no additional oil recovery was observed for high temperatures (90⁰C, 60⁰C) low salinity flooding. Surprisingly, a gain of oil production was observed at low salinity waterflood at 35⁰C (moderate temperature). Based on that, it has been suggested that the benefit of low salinity brine injection might be temperature dependent (Cissokho, H.Bertin et al. 2009).

Several studies investigating the low salinity effect at elevated temperatures have been carried out (Alotaibi, Azmy et al. (2010), Rivet, Lake et al. (2010), Nasralla, Alotaibi et al. (2011), Agbalaka, Dandekar et al. (2009), Robertson (2010), Soraya, Malick et al. (2009)). Improved oil recovery has been explained by viscosity reduction of the crude oil and/or wettability modification due to change in temperature.

2. Investigation of temperature effects on low salinity waterflooding.

In order to study the effect of temperature on low salinity waterflooding, it has been chosen to simulate the decrease in temperature during low salinity water flooding in PHREEQC program vs. experiments. Modeling was done for static and dynamic (waterflooding) conditions, investigating brine-rock interactions with FW, low salinity brines and reservoir rock containing no oil.

2.1 PHREEQC program

PHREEQC is a geochemical program written in the C programming language. It is capable of simulating a wide range of aqueous geochemical reactions including: dissolution and precipitation of phases to achieve equilibrium with the aqueous phase, surface-complexation reactions, ion-exchange reactions, effect of changing temperature and transport modeling. Transport modeling is a reactive-transport modeling simulating advection, dispersion and chemical reaction as water moves through a 1D column (PHREEQC manual, version 2).

However, PHREEQC program is a general geochemical computer program and a number of limitations have to be considered (PHREEQC manual, version 2).

Aqueous model

- Models works well for the solutions with low ionic strength, but may have problems with aqueous solutions at higher ionic strengths except the models with sodium chlorite dominating system. (SW and higher)

Ion exchange

- In many studies of ion-exchange modeling, experimental data are needed for reliable model application.

Convergence problems

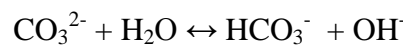
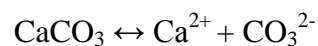
The program is not able to detect some physical impossibilities in the modeled chemical system.

2.2 Mechanisms chosen to be simulated in the PHREEQC

Two mechanisms are important for simulation of low salinity waterflooding without presence of oil phase: precipitation/dissolution of calcite and ion exchange.

It is assumed that divalent ions, especially Ca^{2+} , play an important role in low salinity waterflooding.

One of the main sources of Ca^{2+} in most sandstone is dissolved calcite. The expected dissolution reaction:



Solubility of calcite decides the concentration of Ca^{2+} in brine and is controlled by surface processes. With increase in temperature at some point the solubility will decrease since dissolution of calcite is an exothermic process. Equilibrium constants depend on temperature, therefore the rate of reaction is influenced by the temperature (PHREEQC manual, version 2).

The effect of calcite dissolution/precipitation on brine composition is quite evident, though it depends on presence of CO_2 . Increase of CO_2 results in increase on CaCO_3 dissolution, while its decrease results in CaCO_3 precipitation (PHREEQC manual, version 2). The chosen idealized case has constant partial pressure and can freely absorb CO_2 , i.e., open system.

The general rate for mineral dissolution/precipitation used in the PHREEQC for the measurement of changes in the brine concentration can be written as:

$$R = k \frac{A_0}{V} \left(\frac{m}{m_0} \right)^n g(C)$$

R – overall reaction rate [mol/L/s]

k - specific rate [mol/m²/s]

A₀–initial surface area of the solid [m²]

V – volume of solution [m³]

m₀-initial moles of solid

m-moles of solid at the given time

n – factor accounting for changes in reactive surface area during dissolution, equal to $\frac{2}{3}$

g(C) – function comprising the effect of the solution composition on the rate

The rate equation for calcite included into database (PHREEQC manual, version 2).

Example of KINETICS data block for calcite rate:

```
#
# KINETICS 1
# Calcite
# -tol 1e-8
# -m0 3.e-3
# -m 3.e-3
# -parms 5.0 0.6
Calcite
-start
1 rem Modified from Plummer and others, 1978
2 rem parm(1) = A/V, 1/m parm(2) = exponent for m/m0

10 si_cc = si("Calcite")
20 if (m <= 0 and si_cc < 0) then goto 200
30 k1 = 10^(0.198 - 444.0 / (273.16 + tc) )
40 k2 = 10^(2.84 - 2177.0 / (273.16 + tc) )
50 if tc <= 25 then k3 = 10^(-5.86 - 317.0 / (273.16 + tc) )
60 if tc > 25 then k3 = 10^(-1.1 - 1737.0 / (273.16 + tc) )
70 t = 1
80 if m0 > 0 then t = m/m0
90 if t = 0 then t = 1
100 moles = parm(1) * (t)^parm(2)
110 moles = moles * (k1 * act("H+") + k2 * act("CO2") + k3 * act("H2O"))
120 moles = moles * (1 - 10^(2/3*si_cc))
130 moles = moles * time
140 if (moles > m) then moles = m
150 if (moles >= 0) then goto 200
160 temp = tot("Ca")
170 mc = tot("C(4)")
180 if mc < temp then temp = mc
190 if -moles > temp then moles = -temp
200 save moles
-end
```

Ion exchange is generally accepted as an underlying physico-chemical mechanism at low salinity waterflooding (MIE mechanism). CEC (cation exchange capacity) shows the amount of cations that a certain mineral can exchange. Due to dependence on specific surface area, CEC is often related to clay fraction, type and generally measures in $\frac{meq}{100 g}$.

Calculated CEC of the reservoir rock is $2 \frac{meq}{100 g}$. This amount is assumed to be constant, so the calculated amount of exchangeable cations for K^+ , Ca^{2+} , Mg^{2+} , Na^+ is $4 \cdot 10^{-5}$ meq for 2 g of reservoir rock and $2 \cdot 10^{-4}$ meq for 10g.

2.3 Proposed schemes

This part of the work is aimed at simulating the equilibrium that is typically obtained during a core flooding procedure. It is common practice to age a core for a long time at reservoir temperature. During this time the core and the ageing/formation brine is expected to reach equilibrium. Typically the core is then flooded directly with fresh formation brine or any other brine at different temperature often without new aging. The schemes designed for this section is aimed at investigating any precipitation or dissolution in the ageing process. To do this, static schemes and dynamic schemes are implemented.

2.3.1 Static

This section presents modeling of static experiments, included comparisons with earlier reported experimental results.

2.3.1.1 Description of the experiments

For investigation of temperature effects on low salinity waterflooding, experiments conducted in 2011 by a bachelor student Pål Lee Gunderson were taken as a basis for simulation and comparison with a PHREEQC model. (Gundersen 2011).

In the bachelor thesis the total changes of concentrations in the static experiment between sandstone rock and low salinity brine at different temperatures was studied. Crushed oil reservoir rock was mixed with low salinity water (LSW). The samples were stored for six weeks at temperatures 20⁰C (room temperature), 38⁰ C and 80⁰C. It allowed samples to come to equilibrium between brine and reservoir rock. Experiments exhibited highest release of Ca²⁺ in reservoir rock and low salinity brine at 80⁰C. Observed results lead to a conclusion that during the interactions between rock and low salinity brine the ion exchange and dissolution might be most important factors.

Brine composition was similar the formation water (FW) in a North Sea reservoir and made from distilled water and salts, *Table 3*.

Table 3 Input data for the experiments

Salt	Formation water (FW) [g/l]	Low salinity water (LSW) or FW diluted by 100 times [g/l]
NaCl	49.59	0.496
KCl	1.04	0.010
MgCl ₂ * 6H ₂ O	2.22	0.022
CaCl ₂ * 2H ₂ O	3.74	0.037

Reservoir rock composition is similar to one shown in *Table 10*.

The experiments with mixture of low salinity water and reservoir rock measured the change in concentrations of Ca²⁺, K⁺ and Mg²⁺ at temperatures 20⁰C (room temperature), 38⁰ C and 80⁰C. pH of the mixtures at all temperatures was around 6-7, initial pH was in the region of 5.8-6.

Table 4 shows concentration of elements in brine at room temperature. The release of Ca was highest and had biggest increase with time compare to release of K and Mg. It seems that fastest release of K and Mg happened during first week and K came to equilibrium already at first week.

Table 4 Concentrations of elements in brine at room temperature (20⁰C)

Days	Seconds	Ca (mg/l)	K (mg/l)	Mg (mg/l)
0	0	13	5.4	3.0
7	604800	83	18.0	10.5
21	1814400	89	17.0	12.0
42	3628800	105	18.4	13.0

Table 5 displays concentration of elements in brine at temperature 38⁰C. At temperature 38⁰C only two samples were available. Based on given data one can conclude that Ca did not come to equilibrium after 42 days and it`s release is higher at higher temperature. Release of Mg and K is similar to increase in concentration at 20⁰C.

Table 5 Concentration of elements in brine at temperature 38⁰C

Days	Seconds	Ca (mg/l)	K (mg/l)	Mg (mg/l)
0	0	13	5.4	3.0
7	604800	85	18.5	11.0
42	3628800	132	18.0	15.8

Table 6 shows concentration of elements in brine at temperature 80⁰C. At 80⁰C calcium presented in the experiment had highest and fastest release of Ca. It will take more than 6 weeks for Ca to reach equilibrium. Concentrations of K and Mg are similar for all reactions increasing insignificantly with increase in temperature. It might indicate the low solubility of minerals containing those elements, while ion exchange does not depend on temperature increase as much as solubility.

Table 6 Concentrations of elements in brine at temperature 80⁰C

Days	Seconds	Ca (mg/l)	K (mg/l)	Mg (mg/l)
0	0	18.2	10.5	0.5
7	604800	126.0	22.6	11.0
21	1814400	205.0	20.0	16.5
42	3628800	226.0	19.0	16.9

2.3.1.2 Description of models for simulation of static experiment

To imitate static experiment, 2 schemes were proposed:

Static scheme 1: with four parallel experiments at different temperatures;

Static scheme 2: with equilibration at 20⁰C followed by increase of temperature;

Static scheme 1 represents parallel simulation at temperatures 20⁰C, 40⁰C, 60⁰C and 80⁰C, *Fig. 10*. The interaction between reservoir rock and solution continues until equilibrium was

reached. Two mechanisms were simulated in the scheme: dissolution/precipitation and ion exchange.

Solution + Rock \rightarrow (eq. at 20C)

Solution + Rock \rightarrow (eq. at 40C)

Solution + Rock \rightarrow (eq. at 60C)

Solution + Rock \rightarrow (eq. at 80C)

Figure 10 Static scheme 1

Static scheme 2 in *Fig. 11* describes the water flooding at 20⁰C coming to equilibrium and stepwise increase of temperature (40⁰C, 60⁰C and 80⁰C). At each step solution and reservoir rock come to equilibrium.

Solution + Rock \rightarrow (eq. at 20C)

↓

(eq. at 40C)

↓

(eq. at 60C)

↓

(eq. at 80C)

Figure 11 Static scheme 2

Simulations showed that both schemes gave similar results, *Fig 12*. Continuous decrease of temperature in static scheme 2 did not show any unexpected changes. This showed the possibility of simulating the temperature increase by the means of parallel simulations. Hence, for the rest of the static modeling, scheme 1 was employed.

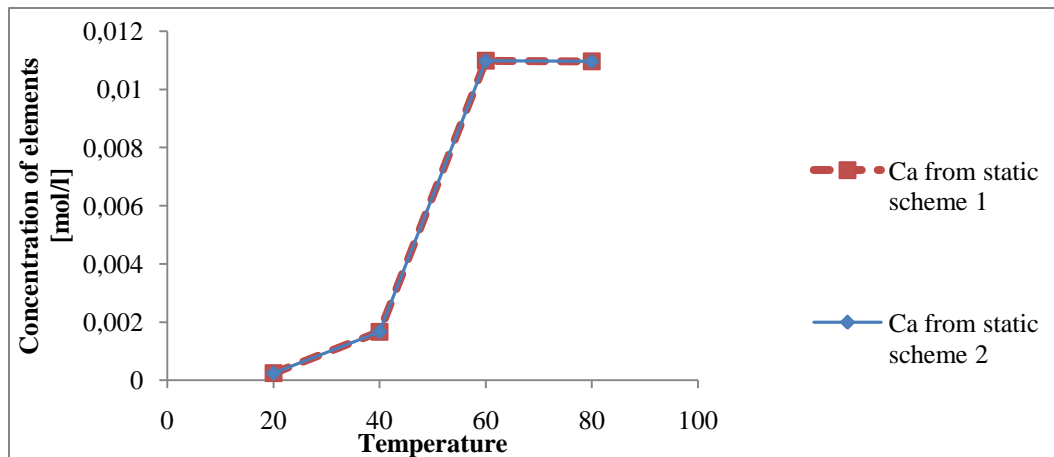


Figure 12 Example on simulations of Ca element using static schemes 1 and 2

2.3.1.3 Programming of static modeling

In order to repeat the results from the experiment, scheme 1 was used. Two databases already included in program (PHREEQC.dat and LLNL.dat) were chosen for the simulation. The PHREEQC.dat database has reduced number of minerals, which significantly decreases the simulation time. It is the smallest database. The LLNL.dat database has the highest number of minerals and temperature dependent equilibrium constants.

The simulations were done with only equilibrium and ion exchange calculations in *Data grid (1)*, Fig. 13. Simulation with PHREEQC database gave best results for concentration of Mg^{2+} and K^+ but concentration of Ca^{2+} was low.

To improve current situation, simulations with calculations of kinetic rates for different minerals were included in *Data grid (2)*. Unfortunately the PHREEQC convergence problems were encountered. Amount of moles in the simulations were too small and made it difficult for the simulator to converge. The simulation with the PHREEQC.dat kinetic rates had to be cancelled after 3 days of running due to lack of convergence.

Similar simulations, *Data grid (1)*, were conducted with LLNL.dat database. Best obtained results are shown in Fig. 14, 15 and 16. It was decided to evaluate whether better match could be found by including the kinetic rates similar to *Data grid (2)*. Sadly, convergence problem became a barrier in this case as well. Increasing number of time interval steps did not give an appropriate solution to the convergence problems encountered.

Fig. 13 shows the workflow throughout modeling of simulations. Explanations under the *Changes* column highlight variations in modeling made during the simulations to get better results.

Two types of simulation structures are used.

Data grid (1) consists of 4 grid blocks: SOLUTION, EQUILIBRIUM_PHASES, EXCHANGE, and REACTION_TEMPERATURE.

- SOLUTION data block describes the initial solutions composition, PH charge, density and temperature. Composition for LSW is taken from *Table 3*. All concentrations are converted to moles of element.
- EQUILIBRIUM_PHASES data block displays the amounts of minerals/gases that can react with the brine. To reach the equilibrium, each mineral will dissolve/precipitate. Minerals/gases are described by two types of inputs: saturation index and maximum amount that can be dissolved. The set SI for minerals is 0, meaning that minerals react to equilibrium. For gases SI equal to log of atmospheric pressure. K-feldspar and illite are allowed to dissolve only. Without that step concentration of elements is too small compared to experimental values.
- EXCHANGE data block expresses the amount and composition of exchangers. Exchangers are in equilibrium with the brine given in SOLUTION data block. The number of exchanger sites is calculated from the known CEC of the reservoir rock.
- REACTION_TEMPERATURE data block displays the range of temperatures during batch reaction steps at parallel simulations.

The second structure, *Data grid (2)* including the kinetic rate consists of 5 data blocks: SOLUTION, EQUILIBRIUM_PHASES, KINETICS, EXCHANGE and REACTION_TEMPERATURE.

The difference between simulation structures is a presence of KINETICS data block. It allows formulation and identifying kinetic reactions (general rate) and specifying reaction parameters.

The input and output for the obtained results closest to the experimental values are shown in A.1 and A.2.

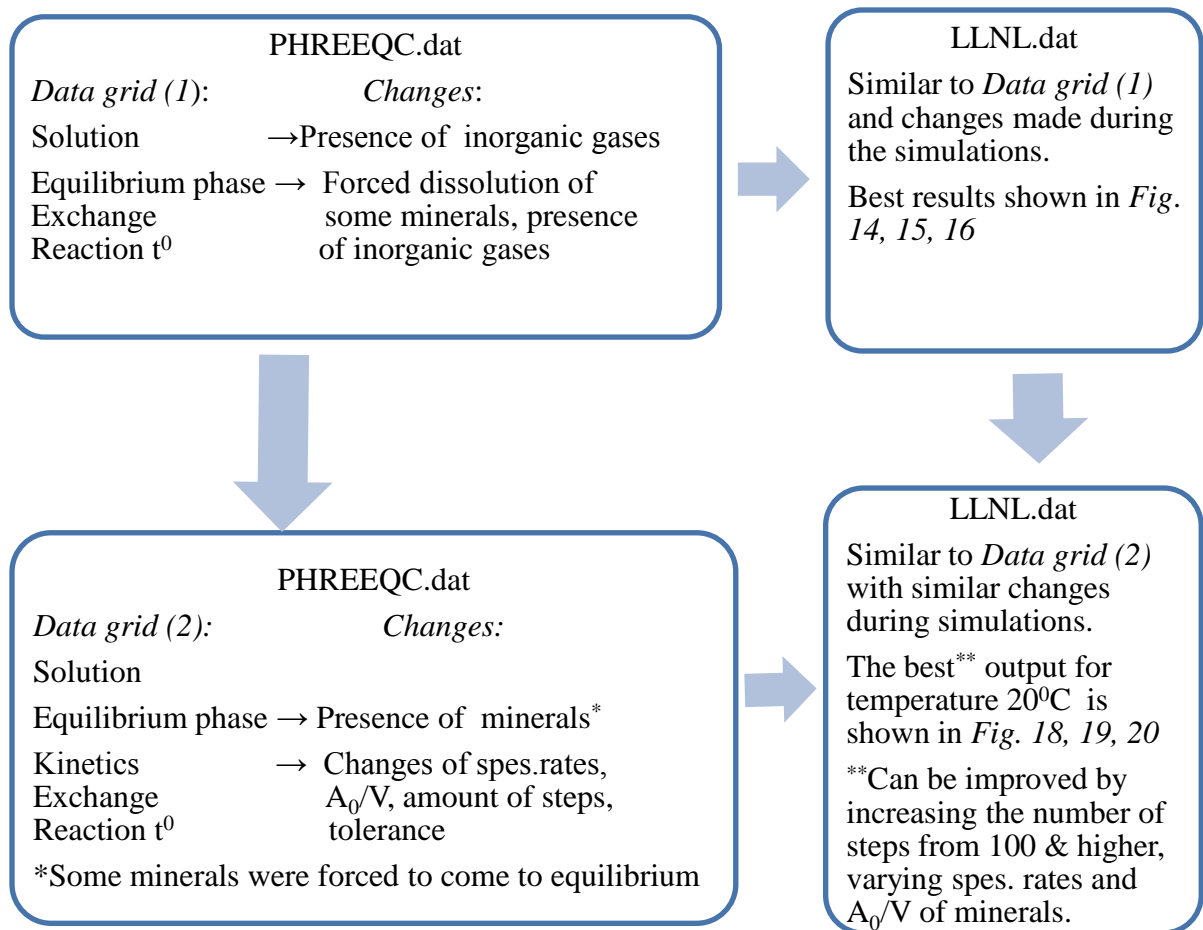


Figure 13 Workflow for simulations based on experimental data

2.3.1.4 Comparison of experiment vs simulation

The data from the experiment are presented in comparison with the simulation with *Data grid (1)* on LLNL.dat database and PHREEQC.dat. *Tables 7, 8 and 9* display the measured concentrations of elements from the experiment and concentration received with the help of modeling.

Table 7 Concentrations of Ca from experiments and simulations

Temperature	Concentrations of Ca ²⁺ [mg/l]		
	Experiment	Best simulation with LLNL.dat	Simulation with PHREEQC.dat
20	105	9.77	25.0
38	132	-	-
40	-	66.90	20.0
60	-	440.00	16.8
80	226	439.00	14.9

Table 7 gives an overview of total concentrations of Ca in brines at different temperatures from the experiment and simulations using different databases. From Fig. 14 the results from simulation with LLNL.dat display concentration of Ca 10 times less than measured concentration of Ca at the experiment at temperatures 20⁰C and 38-40⁰C. From the simulation input, calculated concentration of Ca must be higher than the one measured in the experiment since minerals were allowed to come to equilibrium in the simulation while at the experiment there was not enough time to do that. At temperatures 60⁰C and 80⁰C, Ca concentration from the simulation is two times higher than concentration from the experiment. The possible reasons that might explain the difference are found in the discussion part. Clearly, the PHREEQC.dat database cannot be used in this case, due to output concentrations incomparable to experimental values. Although, the concentration of Ca at 20⁰C calculated with PHREEQC.dat database is higher than concentration calculated with LLNL.dat database, it decreases with increase in temperature which is not in accordance with experiment.

From simulation output it is clear that retention and release of elements depend on both ion exchange and precipitation/dissolution. Removing one of those mechanisms results in dramatic decrease of total concentrations of elements in brine.

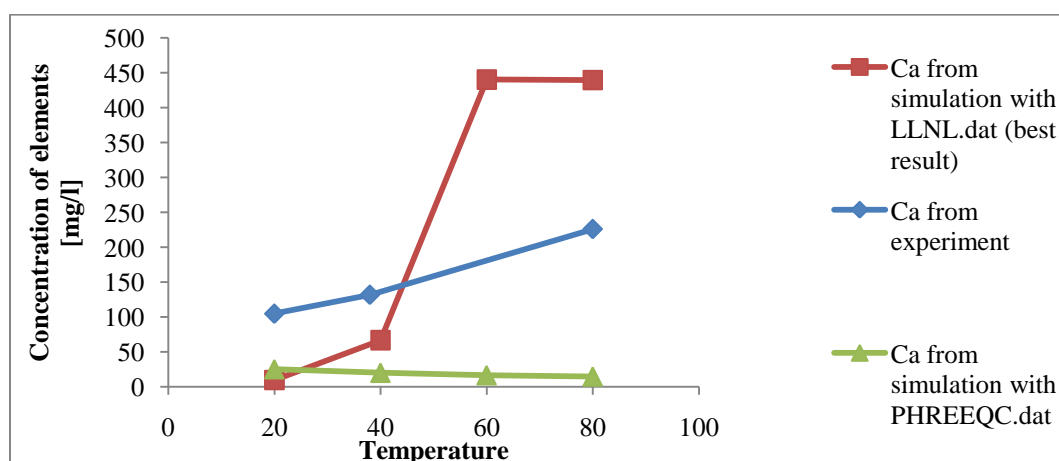


Figure 14 Concentrations of Ca from experiments and simulations

Table 8 shows the total concentration of Mg in brine at different temperatures for the experiment and simulations.

Table 8 Concentrations of Mg in brine from experiments and simulations

Temperature	Concentrations of Mg ²⁺ [mg/l]		
	Experiment	Best simulation with LLNL.dat	Simulation with PHREEQC.dat
20	13.0	2.0	1.4000
38	15.8	-	-
40	-	8.0	0.1600
60	-	15.9	0.0240
80	16.9	15.9	0.0045

The results in Fig. 15 indicate that in the experiment, the concentration of Mg increases from temperature 20⁰ C to 40⁰C and exhibits small increase from 40⁰C. The concentration of Mg from the simulation with LLNL.dat increases sharply from 20⁰C to 40⁰C and comes very close to concentration from the experiment at 60⁰C and 80⁰C. In the simulation illite and K-feldspar were allowed to dissolve only. It seems that illite is affected much more by dissolution and ion exchange than K-feldspar. Low concentration of Mg during the interactions of reservoir rock and low salinity water might be due to precipitation of minerals. Concentration calculated with PHREEQC.dat exhibit opposite trend decreasing with time.

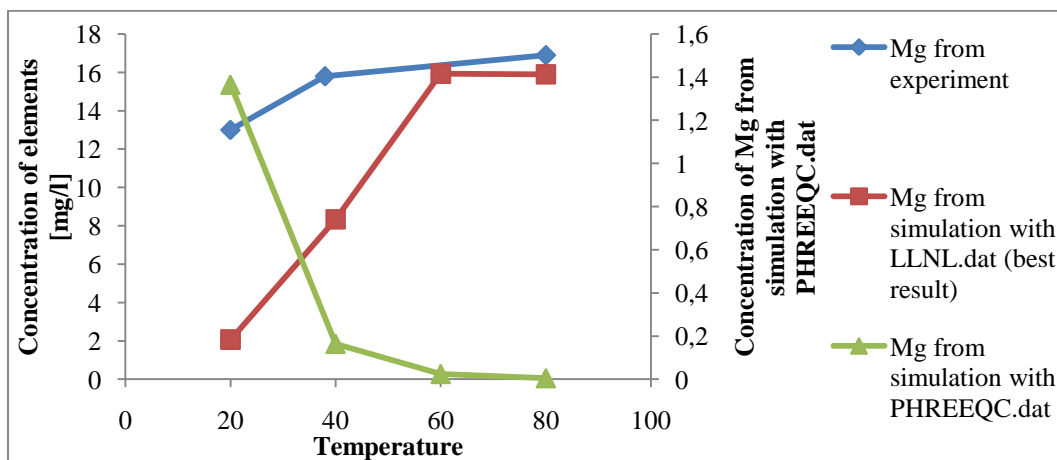


Figure 15 Concentrations of Mg in brine from experiments and simulations

Table 9 displays the concentration of K in brine at different temperatures for the experiment and simulations.

Table 9 Concentrations of K in brine from experiments and simulations

Temperature	Concentration of K ⁺ [mg/l]		
	Experiment	Best simulation with LLNL.dat	Simulation with PHREEQC.dat
20	18.4	5.00	6.0
38	18.0	-	-
40	-	7.50	6.3
60	-	8.97	6.5
80	19.0	9.00	6.8

Fig. 16 shows that release of K from the experiment does not change notably with increase in temperature. Those results point out that the solubility of minerals containing K rather constant in the temperature range investigated. The single mineral containing the K without presence of Ca and Mg is K-feldspar. So, it seems that the solubility of K-feldspar is quite constant with change in temperature. Concentration of K simulated with LLNL.dat shows an increase with increase in temperature but it is still smaller than experimental concentration. That increase with temperature might come from dissolution of illite. Concentration of K with PHREEQC.dat exhibits similar behavior as shown in the experiment but it is three times smaller.

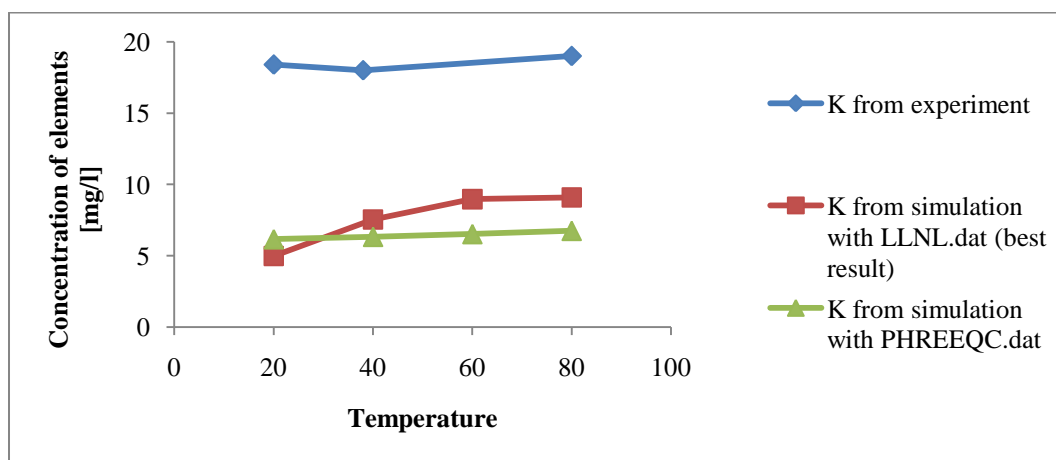


Figure 16 Concentrations of K in brine from experiments and simulations

In the experiments the pH increased from 5.8 to 7. In the simulation it increases from 5.8 to 8 at lower temperatures and decreases to 7 at higher temperatures, fig 17. The most probable reason for increase in pH is dissolution of calcite.

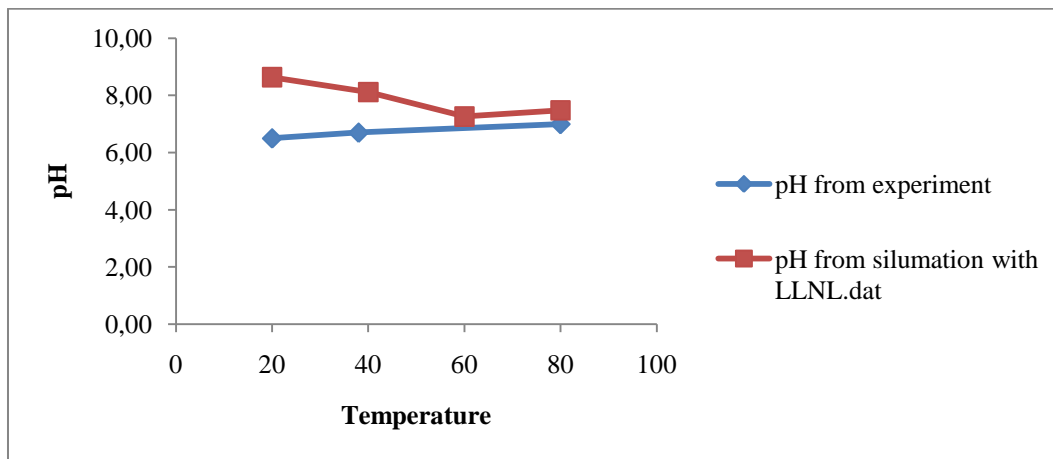


Figure 7 pH from the experiments and simulations

For checking the possibility of better matching the simulation output to experimental values at low temperatures, it was decided to use simulations including data grid with the kinetic rates *Data grid (2)*. The only successful simulation that did not get convergence problem was a simulation with LLNL.dat at 20⁰C.

As it was already described in *Tables 4* and *9*, at first week release of Ca is quite high and fast. Concentration of Ca from the simulation is slightly increased in first week and increases insignificantly with time, *Fig 18*.

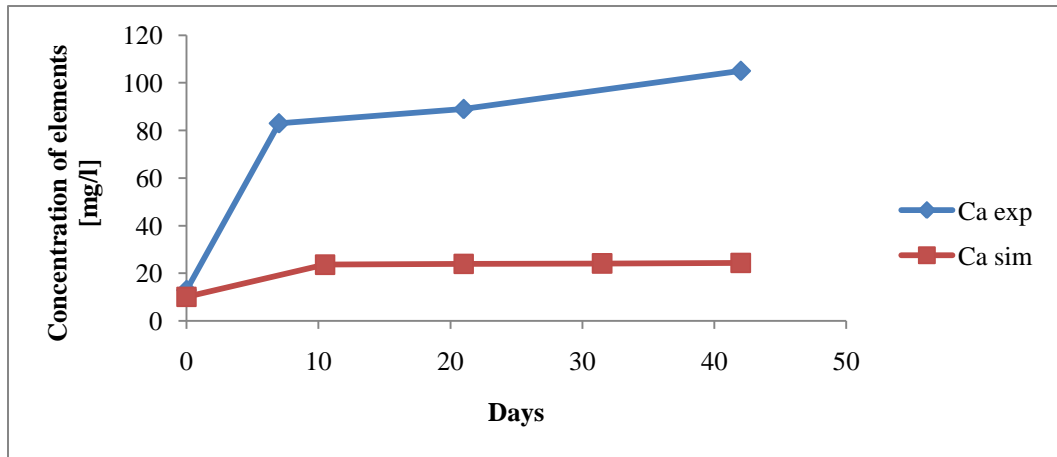


Figure 18 Concentrations of Ca from the experiment and simulation with defined reaction rate

Concentration of Mg from the experiment exhibits similar behavior as concentration of Ca. It increases quickly the first week and has a slower increase the rest of the time. As for the simulation, it seems that concentration of Mg reaches the equilibrium at the first week and does not increase further on. After 42 days it even starts to decrease, Fig 19.

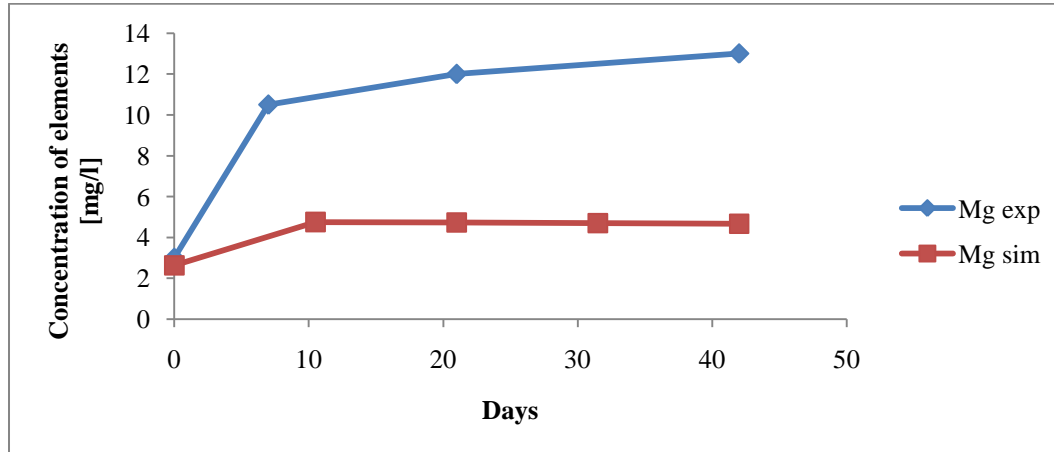


Figure 19 Concentrations of Mg from the experiment and simulation with defined reaction rate

From the Fig.20 the results from the experiment indicate fast release of K during the first week and slight increase the rest of the time. The decrease measured at day 21 is within the accepted analytical method ($\pm 15\%$). Surprisingly, the concentration of K from the simulation behaves very differently. It slightly increases at the first week and continuously reduces for the rest of the time.

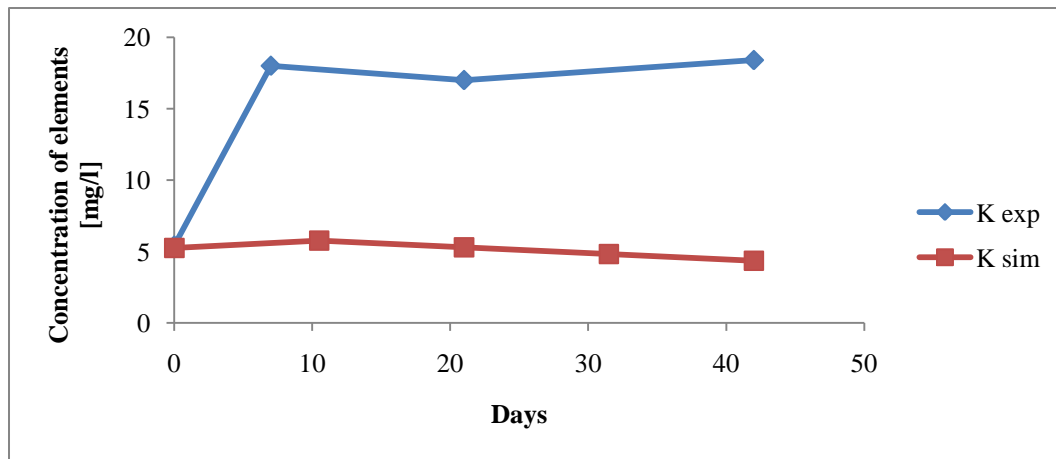


Figure 20 Concentrations of K from the experiment and simulation with defined reaction rate

2.3.1.5 Simulations with different brines

To check the temperature effect on low salinity water injections with different brines, five different brines were used in simulations. The structure, chosen for this simulation, is similar to one used for simulation of the experiment (*Data grid (1)* and static scheme 1).

The compositions of the reservoir rock and brines are given in *Tables 10* and *11*

Table 10 Composition of the reservoir rock

Mineral	Formula	mass % of minerals in reservoir rock	Total rock mass: 10g	moles
chlorite	$(\text{Fe}_5\text{Al})(\text{AlSi}_3)\text{O}_{10}(\text{OH})_8$	7.00 %	0.70	0.000981069
illite	$\text{K}_{0,6}\text{Mg}_{0,25}\text{Al}_{1,8}\text{Al}_{0,5}\text{Si}_{3,5}\text{O}_{10}(\text{OH})_2$	12.70 %	1.27	0.004206861
quartz	SiO_2	72.10 %	7.21	0.119998069
calcite	CaCO_3	0.30 %	0.03	0.000299739
k-feldspar	KAlSi_3O_8	4.50 %	0.45	0.001616777
plagioclase (albite)	$\text{NaAlSi}_3\text{O}_8$	3.30 %	0.33	0.001258471

Table 11 Brine compositions used in simulations

	FW [mmol/l]	FW(0.1) [mmol/l]	FW(0.01) [mmol/l]	NaCl(0.1) [mmol/l]	NaCl(0.01) [mmol/l]
Na	1326.22	132.62	13.26	167.95	16.80
Ca	147.94	14.79	1.48	0.00	0.00
Mg	17.46	1.75	0.17	0.00	0.00
Cl	1677.73	167.77	16.78	167.95	16.80
SO ₄ ,2-	0.89	0.09	0.01	0.00	0.00
K	5.62	0.56	0.06	0.00	0.00
Sr	8.44	0.84	0.08	0.00	0.00

FW (0.1) is FW diluted by 10 times

FW (0.01) is FW diluted by 100 times

NaCl (0.1) consists of NaCl with the ionic strength of FW diluted by 10 times

NaCl (0.01) consists of NaCl with the ionic strength of FW diluted by 100 times

Table 12 gives an overview of elements concentration in FW-reservoir rock interactions.

Table 12 Concentrations of elements in FW-reservoir rock interactions

Temperature °C	FW+Rock	Concentration of elements [mmol/l]		
	pH	Ca	K	Mg
20	7.34	189	1	30
40	7.17	287	2	73
60	6.94	332	3	93
80	6.66	331	5	93

Concentration of Ca increases with increase in temperature from 20°C to 60°C and seems to remain constant from 60°C and higher. Mg exhibits similar behavior but at smaller concentrations. Concentration of K is so small compared to Ca and Mg that one can say it is nearly constant.

Fig. 21 displays concentration of elements during interactions of FW and reservoir rock at different temperatures.

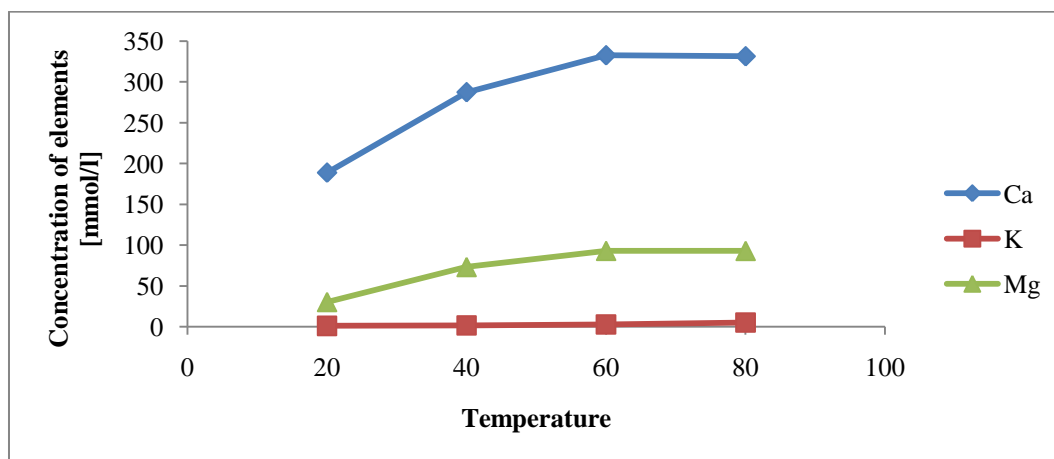


Figure 21 Concentration on elements in FW-reservoir rock interactions

It seems that dissolution and/or ion exchange increases with increase in temperature until some point when it is not affected by temperature anymore. From simulation output it looks

like both mechanisms contribute evenly at lower temperatures but at higher temperatures ion exchange has slightly higher contribution.

Table 13 shows the concentration of elements during interactions of FW(0.1) and reservoir rock at different temperatures.

Table 13 Concentrations of elements during interactions of FW(0.1) and reservoir rock

Temperature °C	FW(0.1)+Rock	Concentration of elements [mmol/l]			Conc. of minerals [mmoles]
	pH	Ca	K	Mg	Calcite
20	7.85	9.25	0.12	0.00	0.32
40	7.78	9.01	0.24	0.16	0.31
60	7.65	11.86	0.43	1.12	0.30
80	7.52	17.17	0.67	2.91	0.29

Initial concentrations of elements in brine before the brine-rock interaction are higher than the concentration of elements in brine after the batch reaction. This is due to retention of elements caused by ion exchange.

Fig. 22 shows the interaction between the FW diluted by 10 times and reservoir rock.

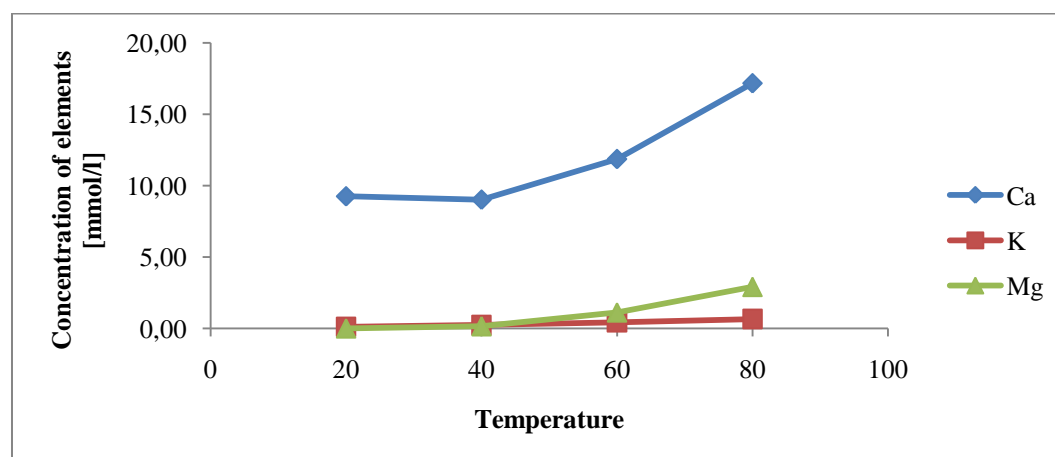


Figure 22 Concentrations of elements in FW (0.1)-reservoir rock interactions

It looks like that decrease in water strength by 10 times has affected the solubility and ion exchange of elements in FW(0.1) and reservoir rock interaction at different temperatures. Concentration of Ca and Mg is constant at temperatures 20⁰C and 40⁰C. Concentrations of Ca and Mg start to increase sharply from 40⁰C and higher. Concentration of K increases nearly twice for each temperature step, but initial concentration after the batch reaction is very low. High concentration of Ca can be explained by increased dissolution of calcite with temperature. Dissolution of minerals containing K and Mg is much lower.

Table 14 gives an overview of the concentration of elements during interactions of FW(0.01) and reservoir rock at different temperatures.

Table 14 Concentration on elements in FW (0.01)-reservoir rock interactions

Temperature °C	FW (0.01)+Rock	Concentration of elements [mmol/l]			Conc. of minerals [mmoles]
	pH	Ca	K	Mg	Calcite
20	8.41	0.401	0.013	0.000	0.3130
40	8.38	0.319	0.027	0.000	0.3130
60	8.33	0.286	0.050	0.002	0.3124
80	8.22	0.358	0.085	0.015	0.3000

The initial concentrations of elements in FW (0.01) are higher before the brine- rock interaction. Reduction in concentration in brine after interaction is caused by ion exchange.

Fig. 24 ,shows the simulations while FW diluted by 100 times reacts with reservoir rock.

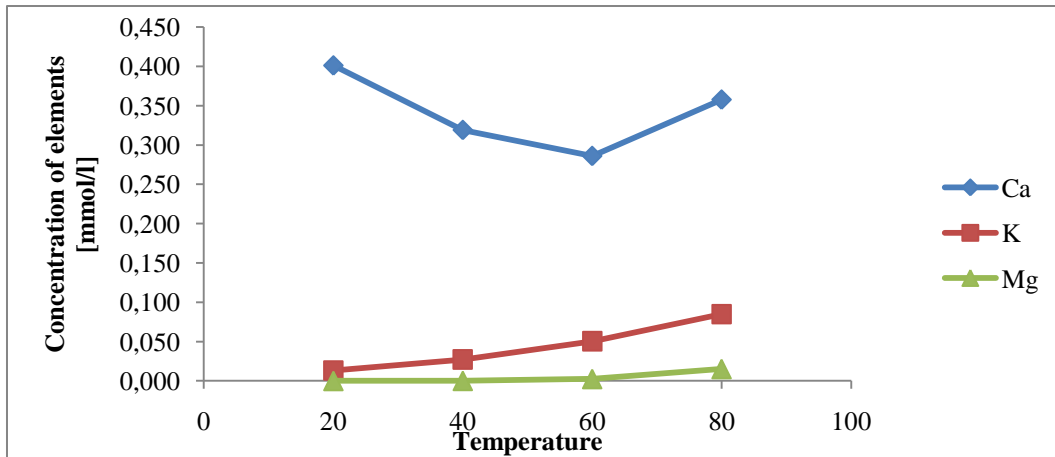


Figure 8 Concentrations of elements in FW (0.01)-reservoir rock interactions

The output of the simulation shows an intriguing behavior of elements. Surprisingly, concentration of Ca starts to decrease with increase in temperature until 60⁰C and increases at 80⁰C. That fluctuation might be explained by increased precipitation of some minerals. Mg increases insignificantly with increase in temperature and change of K concentration is larger. Dissolution of calcite is stable with increase in temperature from 20 to 40⁰C, slightly decreasing at 60⁰C and 80⁰C.

Table 15 shows the concentration of elements during interactions of NaCl (0.1) and reservoir rock at different temperatures.

Table 15 Concentration on elements in NaCl (0.1)-reservoir rock interactions

Temperature ⁰ C	NaCl (0.1)+Rock	Concentration of elements [mmol/l]			Conc. of minerals [mmoles]
	pH	Ca	K	Mg	calcite
20	8.26	1.392	0.128	0.834	0.280
40	7.98	3.511	0.254	2.157	0.262
60	7.76	7.280	0.441	4.358	0.244
80	7.59	12.426	0.680	7.211	0.226

With the change of brine composition from FW to NaCl, the behavior of elements changes as well. It looks more or less linear increase with increase in temperature.

Fig. 24 shows the reaction of NaCl with the same ion strength as in FW diluted by 10 times with reservoir rock.

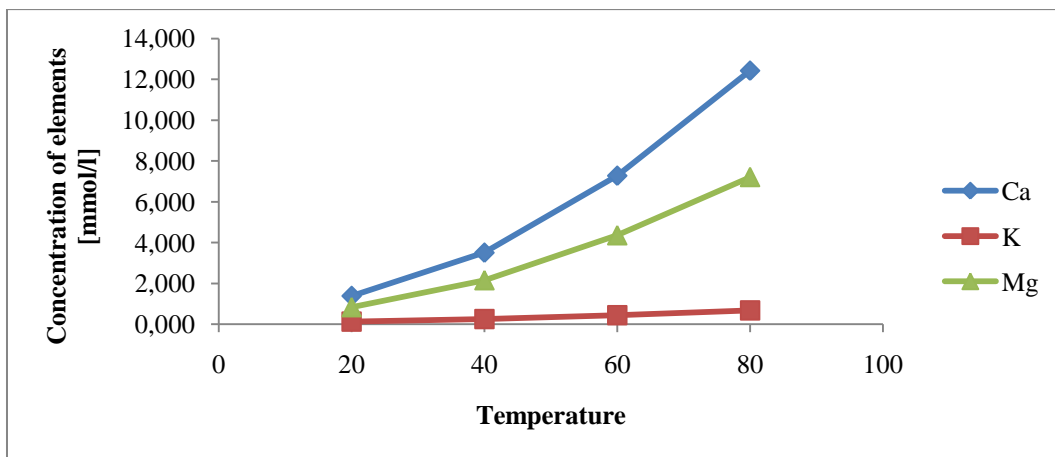


Figure 24 Concentration on elements in NaCl (0.1)-reservoir rock interactions

Concentration of K is still small, highlighting low solubility of minerals containing K. Initial concentration of elements in NaCl (0.1) is lower so there is no retention of ions. During the interactions of NaCl brines and reservoir rock dissolution of calcite increases evenly with increase in temperature.

Table 16 gives an overview of the concentration of elements during interactions of NaCl(0.01) and reservoir rock at different temperatures.

Table 16 Concentrations of elements in NaCl (0.01)-reservoir rock interactions

Temperature ⁰ C	NaCl (0.01)+Rock	Concentration of elements [mmol/l]			Conc. of minerals [mmoles]
	pH	Ca	K	Mg	calcite
20	9.02	0.033	0.018	0.013	0.282
40	8.80	0.053	0.031	0.030	0.270
60	8.59	0.096	0.053	0.058	0.259
80	8.39	0.174	0.087	0.109	0.249

Fig. 25 shows the reaction of NaCl with ion strength equal to FW diluted by 100 times with reservoir rock.

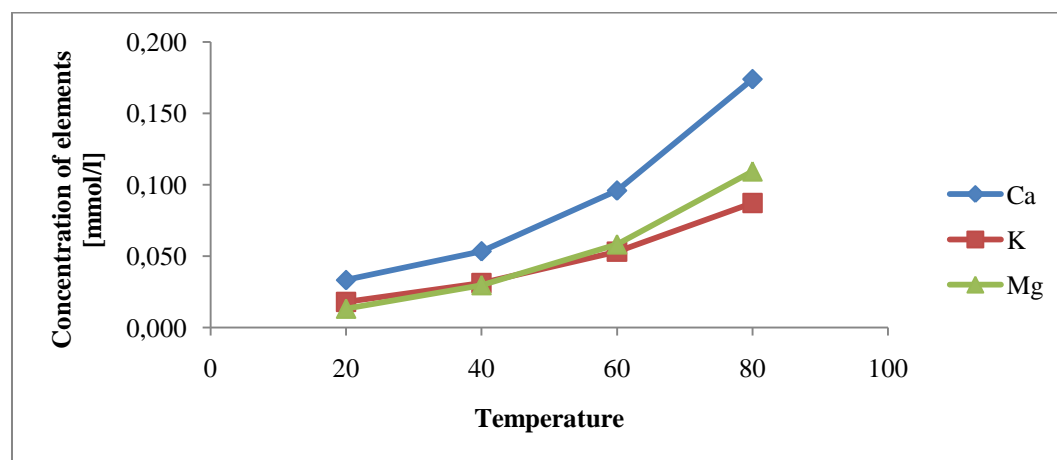


Figure 25 Concentrations of elements in NaCl (0.01)-reservoir rock interactions

With reduction in ionic strength of brine, the difference in concentrations and behavior of K and Mg is striking. At temperatures from 20⁰C to 40⁰C, the concentration of K is higher than concentration of Mg, but at higher temperatures it is opposite.

In all simulations initial brine pH increases from 6 pH up to 7.8-8 pH at 20⁰C and decrease with increase in temperature. This might be caused by lower solubility of CO₂ at higher temperatures.

2.3.2 Dynamic

Two dynamic schemes are chosen to simulate the waterflooding with decrease in temperature.

First scheme consists of 4 steps:

At first step a reservoir core is flooded with high salinity or low salinity solution at 80°C. Brine-rock interactions include ion exchange and precipitation/dissolution of minerals until equilibrium is attained.

At the second step new solution with the same composition and concentration but at lower temperature (60°C) is mixed with the core from step one. Brine-rock interactions include ion exchange and precipitation/dissolution of minerals until a new equilibrium is attained.

Steps three and four are similar to the second step except the decrease of temperature. At the third step injected brine has temperature 40°C and equilibrium is attained at 40°C, while at the last step the temperature of the injected brine is 20°C and equilibrium is attained at 20°C. From the first to the last step, scheme uses the same core, *Fig 26*.

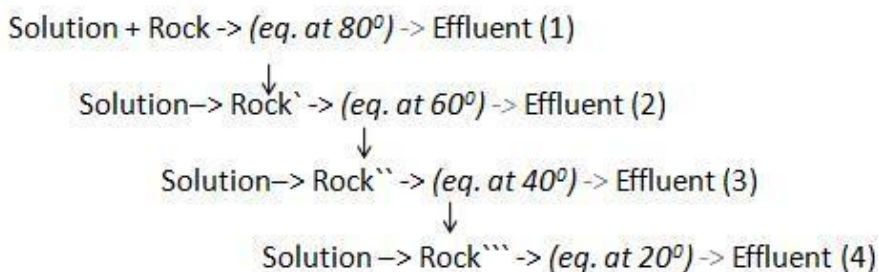


Figure 26 Scheme 1

Next scheme describes the situation of reservoir core flooded by low salinity water in succession to FW. This scheme is analogous to the previous one. In the first step reservoir core is with high salinity FW at 80°C. Afterward the core used in the first step is mixed with low salinity water at 60°C. At the third step core used at previous steps is mixed with low salinity water with temperature 40°C and in the last step core from the previous step is mixed with low salinity brine at 20°C, *Fig 27*.

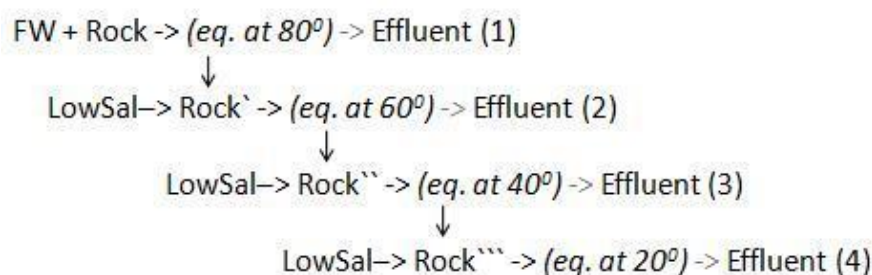


Figure 27 Scheme 2

The description of solution types are presented in *Tables 10* and *11*, flooding of solutions and their successions are shown in *Table 17*.

Table 17 The description of solution types used in dynamic schemes 1 and 2

Dynamic scheme	Flooding of reservoir core with FW or solutions with low ionic concentration directly or FW and low salinity water in succession				
1	FW	FW (0.1)	FW (0.01)	NaCl (0.1)	NaCl (0.01)
2			FW / FW (0.01)	FW / NaCl (0.1)	FW / NaCl (0.01)

2.3.2.1 Programming procedure and difficulties encountered

Manual for PHREEQC program states that PHREEQC has functions able to model several one-dimensional transport processes, combined with equilibrium and kinetic chemical reactions.

The following simulations were designed to reproduce the reduction in temperature during water flooding with different brines. Model consists of 4 Datablocks:

1. The input data sets are listed in *Tables 10* and *11*.
2. The amount and composition of the exchanger in each reservoir rock column cell is defined by the EXCHANGE 1-20 data block.
3. The REACTION_TEMPERATURE data block defines the reactions during batch-reactions steps. It is used to specify the initial temperature for the cell range (1-20) in advective-dispersive transport calculations, in Celsius.
4. The TRANSPORT data block simulated advection and dispersive mixing.

After the first step at 80⁰C, the program used the solution in the first cell as an initial solution for the whole column in the next step at temperature 60⁰C. Attempts to force the simulation to go the correct way by saving the solution in each of the cell did not succeed.

3. Discussion

The simulation model made in PHREEQC for comparison with the experiment describes the interactions between cations in brine and reservoir rock by means of precipitation/dissolution and ion exchange equilibrium. Differences between the simulation output and experimental data at 20-40⁰C might be explained by several factors:

- Brines were prepared several times during the reported experiment. There are significant variations in the initial composition of brine due to sampling. The calculated concentration of Ca ions from the LSW is 10 mg/l. The concentration of Ca from the sample used in experiment is 13mg/l, which is higher even with included 15% uncertainty.
- Core cleaning might affect the final results. If one assumes the worst case where the water in the core evaporated during storage, leaving the precipitated salts at the core surface, Soxhlet extraction may not be sufficient to remove the precipitated salts. The reservoir core was cleaned by toluene/methanol in cycles until colorless fluid extraction and dried at 120⁰C until constant weight. It might remove the residual oil but not all the salt precipitates. Water saturation in reservoir rock is 0.2. Even if only 1% of PV was occupied by FW, the amount of extra Ca from this could be 2.04 mg/l.
- A worst case of ion exchange, where the negatively charged surfaces was initially covered by only Ca ions. The release of such Ca ions can increase Ca concentration up to 160 mg/l in the added brine.
- Data from the field show that rock composition vary with depths. Description of the rock composition is not given in the bachelor thesis, but it is known that rock composition in the simulation is taken from the same North Sea reservoir and is similar to one used in the experiment.

Increased presence of Ca at 60-80⁰C most probably caused by:

- Complete dissolution of calcite at high temperatures in the simulation, this is due to the fact that rate effects were neglected in the simulation.
- Sample preparation for the ICP analysis might change the brine composition. After reaction of reservoir rock with low salinity water at high temperatures, samples were taken out and analyzed by ICP at an external laboratory. The decrease of temperature during sampling might have caused the precipitation of minerals, leading to decrease of elements in samples.

Another factor possibly affecting the results is the choice of plagioclase series members in simulations. There was no clear composition in the description of the reservoir rock, so one had to choose the plagioclase minerals and its composition. In this simulation, plagioclase was chosen as a mineral composing 100% consisting of albite. That could be misleading since plagioclase can contain both anorthite ($\text{CaAl}_2\text{Si}_2\text{O}_8$) and albite ($\text{NaAlSi}_3\text{O}_8$) in different fractions.

Simulations including defined reaction rate show that several factors affecting the dissolution/precipitation depend on temperature such as specific rate, initial surface area of the solid. Specific rate of each mineral changes with change in pH and temperature. In simulations, initial surface areas of quartz, daphnite and illite are unknown, so it is taken from the example in PHREEQC manual. Calculation of possible initial surface areas shows that the chosen example is within the range of possible areas. Formulae of reaction rate used in PHREEQC shows that increase of specific rate and initial surface area for illite results in increased reaction rate. That will increase the amount of K and Mg in brine. Increase in initial area for K-feldspar and calcite would result in increase of total amount of Mg and Ca in brine. Unfortunately, it was not possible to check due to convergence problems.

With injection of cold LSW into reservoir, temperature does not change right after the water shock front but much later. New temperature gradient/profile creates new equilibrium between LSW and reservoir rock. It affects the mineral composition and can establish new wettability. Simulations showed that in case of experiments with change in temperature after aging at reservoir temperature, there has to be a new aging at the new temperature to establish equilibrium between rock, brine and oil. It will establish more representative wettability. New wettability allows estimation of relative permeability and oil saturation that give a good match between the simulation and experimental data.

Temperature of water affects the degree of ion exchange. Generally it goes faster with increase in temperature due to increased diffusion rate of ions. At high temperatures monovalent ions replaces divalent ions with less effort. It explains increased amount of an assemblage of exchangers with increased temperature for Ca and decreased amount for K in simulations. Though, it does not explain the decreased amount for Mg. In the simulations ion exchange was forced to go to equilibrium with solution, it exhibits the dependency on initial composition of low salinity brine, its pH and temperature. Experimental values considered

increase in ion concentrations as a result of ion exchange, dissolution or a combination. It was not possible to analyze effect of each mechanism.

4. Conclusions

Simulation modeled two main mechanisms controlling the pH and total release of divalent cations: ion exchange and dissolution/precipitation. Those mechanisms considered to stand behind the LSW effects such as reduction in residual oil saturation and increased oil recovery. Both mechanisms are affected by the changes in temperature.

- Reaction of low salinity water with reservoir rock depends on the brine composition and minerals present. With change in temperature, minerals exhibit different behavior depending on ionic strength and composition of brine. Total amount of divalent ions in low salinity brine is affected by changes in temperature though the dependency is not straight forward/ linear and is affected by ionic strength of brine, composition and composition of reservoir rock. Therefore each case should be treated separately.
- Aging of rock, brine and oil and LSWF have to be conducted at the same temperatures to avoid possible precipitation/dissolution of minerals as a result of temperature change.
- Change in temperature affects wettability as well. It is important to establish equilibrium between rock, brine and oil at new temperature before the flooding experiment is carried out. Without new aging there can be wrong wettability conditions resulting in misleading values of relative permeability and oil saturation.
- Simulation results have to be compared with experimentally measured changes in ionic concentrations in brines as well as precipitated minerals to be able to tune the rates together with saturation indexes.

References

- Abeyasinghe, K. P., I. Fjelde, et al. (2012). Acceleration of Oil Production in Mixed-wet Reservoirs by Alteration of Relative Permeability Curves using Surfactants. SPE EOR Conference at Oil and Gas West Asia. Muscat, Oman, Society of Petroleum Engineers.
- Abeyasinghe, K. P., I. Fjelde, et al. (2012). Dependency of Remaining Oil Saturation on Wettability and Capillary Number. SPE Saudi Arabia Section Technical Symposium and Exhibition. Al-Khobar, Saudi Arabia, Society of Petroleum Engineers.
- Agbalaka, C., A. Dandekar, et al. (2009). "Coreflooding Studies to Evaluate the Impact of Salinity and Wettability on Oil Recovery Efficiency." Transport in Porous Media **76**(1): 77-94.
- Agbalaka, C. C., A. Y. Dandekar, et al. (2008). The Effect of Wettability on Oil Recovery: A Review. SPE Asia Pacific Oil and Gas Conference and Exhibition. Perth, Australia, Society of Petroleum Engineers.
- Alotaibi, M. B., R. Azmy, et al. (2010a). A Comprehensive EOR Study Using Low Salinity Water in Sandstone Reservoirs. SPE Improved Oil Recovery Symposium. Tulsa, Oklahoma, USA, Society of Petroleum Engineers.
- Alotaibi, M. B., R. M. Azmy, et al. (2010b). Wettability Studies Using Low-Salinity Water in Sandstone Reservoirs. Offshore Technology Conference. Houston, Texas, USA.
- Anderson, W. G. (1986). "Wettability Literature Survey- Part 1: Rock/Oil/Brine Interactions and the Effects of Core Handling on Wettability." SPE Journal of Petroleum Technology(10): 1125-1144.
- Anderson, W. G. (1987). "Wettability Literature Survey-Part 6: The Effects of Wettability on Waterflooding." SPE Journal of Petroleum Technology(12): 1605-1622.
- Austad, T., A. Rezaeidoust, et al. (2010). Chemical Mechanism of Low Salinity Water Flooding in Sandstone Reservoirs. SPE Improved Oil Recovery Symposium. Tulsa, Oklahoma, USA, Society of Petroleum Engineers.
- Bavière, M. (1991). Basic concepts in enhanced oil recovery processes. Oxford, Published for the Society of Chemical Industry by Blackwell.
- Berg, J. C. (1993). Wettability. New York, Marcel Dekker.
- Bernard, G. G. (1967). Effect of Floodwater Salinity on Recovery Of Oil from Cores Containing Clays.
- BP (August 2009). "The BP magazine of technology and innovation." Frontiers.
- Buckley, J. S., Y. Liu, et al. (1998). "Mechanisms of Wetting Alteration by Crude Oils." SPE Journal(1): 54-61.
- Chukwudeme, E. A., I. Fjelde, et al. (2011). Effect of Interfacial Tension on Water/Oil Relative Permeability and Remaining Saturation with Consideration of Capillary Pressure. SPE EUROPEC/EAGE Annual Conference and Exhibition. Vienna, Austria, Society of Petroleum Engineers.
- Cissokho, H. Bertin, et al. (2009). "Low Salinity Oil Recovery On Clayey Sandstone: Experimental Study." presented at the International Symposium of the Society of Core Analysts, Noordwijk aan Zee, The Netherlands, September.
- Cossé, R. (1993). Basics of reservoir engineering. Paris, Technip.
- Craig F.F., 1971. The reservoir engineering aspects of waterflooding. Monograph. SPE., New York, 134 s. pp.
- Gamage, P. H. S. and G. D. Thyne (2011). Comparison of Oil Recovery by Low Salinity Waterflooding in Secondary and Tertiary Recovery Modes. SPE Annual Technical Conference and Exhibition. Denver, Colorado, USA, Society of Petroleum Engineers.

- Green, D. W. and G. P. Willhite (1998). Enhanced oil recovery. Richardson, TX, Society of Petroleum Engineers.
- Gundersen, P. L. (2011). Interactions between sandstone rocks and brines during low salinity waterflooding at different temperatures BACHELOR, University of Stavanger.
- Jerauld, G. R., K. J. Webb, et al. (2008). "Modeling Low-Salinity Waterflooding." SPE Reservoir Evaluation & Engineering(6): pp. 1000-1012.
- Lager, A., K. J. Webb, et al. (2008). LoSal, Enhanced Oil Recovery: Evidence of Enhanced Oil Recovery at the Reservoir Scale. SPE/DOE Symposium on Improved Oil Recovery. Tulsa, Oklahoma, USA, Society of Petroleum Engineers.
- Lager, A., K. J. Webb, et al. (2008). LoSal, Enhanced Oil Recovery: Evidence of Enhanced Oil Recovery at the Reservoir Scale. SPE/DOE Symposium on Improved Oil Recovery. Tulsa, Oklahoma, USA, Society of Petroleum Engineers.
- Lager, A., Webb, K.J., Black C.J: (2006.). "Low salinity oil recovery-An experimental investigation" International Symposium of the Society of core analysts, SCA 2006-36. A. Lager, Webb, K.J., Black C.J: "Low salinity oil recovery-An experimental and investigation" SCA 2006-36. Trondheim, Norway.
- Lee, S. Y., K. J. Webb, et al. (2010). Low Salinity Oil Recovery: Increasing Understanding of the Underlying Mechanisms. SPE Improved Oil Recovery Symposium. Tulsa, Oklahoma, USA, Society of Petroleum Engineers.
- Ligthelm, D. J., J. Gronsveld, et al. (2009). Novel Waterflooding Strategy by Manipulation of Injection Brine Composition. EUROPEC/EAGE Conference and Exhibition. Amsterdam, The Netherlands, Society of Petroleum Engineers.
- Mahani, H., T. Sorop, et al. (2011). Analysis of Field Responses to Low-salinity Waterflooding in Secondary and Tertiary Mode in Syria. SPE EUROPEC/EAGE Annual Conference and Exhibition. Vienna, Austria, Society of Petroleum Engineers.
- McDougall, S. R. and K. S. Sorbie (1995). "The Impact of Wettability on Waterflooding: Pore-Scale Simulation." SPE Reservoir Engineering(3): 208-213.
- McGuire, P. L., J. R. Chatham, et al. (2005). Low Salinity Oil Recovery: An Exciting New EOR Opportunity for Alaska's North Slope. SPE Western Regional Meeting, Irvine, California, Society of Petroleum Engineers.
- Nasralla, R. A., M. B. Alotaibi, et al. (2011). Efficiency of Oil Recovery by Low Salinity Water Flooding in Sandstone Reservoirs. SPE Western North American Region Meeting. Anchorage, Alaska, USA, Society of Petroleum Engineers.
- Nasralla, R. A., M. A. Bataweel, et al. (2011). Investigation of Wettability Alteration by Low Salinity Water. Offshore Europe. Aberdeen, UK, Society of Petroleum Engineers.
- Nasralla, R. A. and H. A. Nasr-El-Din (2011). Impact of Electrical Surface Charges and Cation Exchange on Oil Recovery by Low Salinity Water. SPE Asia Pacific Oil and Gas Conference and Exhibition. Jakarta, Indonesia, Society of Petroleum Engineers.
- NPD (2012) from <http://www.npd.no/en/About-us/Information-services/Dictionary/>.
- PHREEQC manual, version 2 (2012) from http://wwwbrr.cr.usgs.gov/projects/GWC_coupled/phreeqc/html/final.html
- Pu, H., X. Xie, et al. (2008). Application of Coalbed Methane Water to Oil Recovery by Low Salinity Waterflooding. SPE/DOE Symposium on Improved Oil Recovery. Tulsa, Oklahoma, USA, Society of Petroleum Engineers.

- Raymond, M. and W. L. Leffler (2006). Oil and gas production in nontechnical language. Tulsa, Okla., PennWell.
- Rezaeidoost, A. (2011). Low salinity water flooding in sandstone reservoirs: a chemical wettability alteration mechanism. no. 135, UiS.
- Rivet, S., L. W. Lake, et al. (2010). A Coreflood Investigation of Low-Salinity Enhanced Oil Recovery. SPE Annual Technical Conference and Exhibition. Florence, Italy, Society of Petroleum Engineers.
- Robertson, E. P. (2010). Oil Recovery Increases by Low-Salinity Flooding: Minnelusa and Green River Formations. SPE Annual Technical Conference and Exhibition. Florence, Italy, Society of Petroleum Engineers.
- Schumacher, M. M. (1978). Enhanced oil recovery: secondary and tertiary methods. Park Ridge, NJ, Noyes Data.
- Skrettingland, K., T. Holt, et al. (2010). Snorre Low Salinity Water Injection - Core Flooding Experiments And Single Well Field Pilot. SPE Improved Oil Recovery Symposium. Tulsa, Oklahoma, USA, Society of Petroleum Engineers.
- Soraya, B., C. Malick, et al. (2009). Oil Recovery by Low-Salinity Brine Injection: Laboratory Results on Outcrop and Reservoir Cores. SPE Annual Technical Conference and Exhibition. New Orleans, Louisiana, Society of Petroleum Engineers.
- Suijkerbuijk, B., J. Hofman, et al. (2012). Fundamental Investigations into Wettability and Low Salinity Flooding by Parameter Isolation. SPE Improved Oil Recovery Symposium. Tulsa, Oklahoma, USA, Society of Petroleum Engineers.
- Tang, G. Q. and N. R. Morrow (1997). "Salinity, Temperature, Oil Composition, and Oil Recovery by Waterflooding." SPE Reservoir Engineering(4): 269-276.
- Thakur, G. C. and A. Satter (1998). Integrated waterflood asset management. Tulsa, Okla., PennWell.
- Vledder, P., I. E. Gonzalez, et al. (2010). Low Salinity Water Flooding: Proof Of Wettability Alteration On A Field Wide Scale. SPE Improved Oil Recovery Symposium. Tulsa, Oklahoma, USA, Society of Petroleum Engineers.
- Zhang, Y. and N. R. Morrow (2006). Comparison of Secondary and Tertiary Recovery With Change in Injection Brine Composition for Crude Oil/Sandstone Combinations. SPE/DOE Symposium on Improved Oil Recovery. Tulsa, Oklahoma, USA, Society of Petroleum Engineers.
- Zolotuchin, A. B. and J.-R. Ursin (2000). Introduction to petroleum reservoir engineering. Kristiansand, Høyskoleforl.

Appendices

A.1 Simulation based on experimental values

SOLUTION 1

```
temp      20
pH        5.8
pe        4
redox     pe
units     mol/l
density   0.973
Na        0.00848733744010951
Cl        0.00934120547241157
K         0.000134138162307176
Mg        0.000108198495057296
Ca        0.000251666439940144
water     0.005 # kg
```

EQUILIBRIUM_PHASES 1

```
Albite    0 0.000251694161984803
Calcite   0 5.99477255832914e-005
CO2(g)    -3.5 10
Daphnite-14A 0 0.000196213830457555
Illite    0 0.000841372137015702 dissolve_only
K-feldspar 0 0.000323355377990419 dissolve_only
O2(g)     -0.68 10
Quartz    0 0.0239996138758378
```

EXCHANGE 1

```
X          4e-005
equilibrate with solution 1
pitzer_exchange_gammas true
```

REACTION_TEMPERATURE 1-4

```
20 40 60 80
```

Beginning of initial solution calculations.

Initial solution 1.

```
-----Solution composition-----
Elements          Molality      Moles
Ca                 2.588e-004   1.294e-006
Cl                 9.606e-003   4.803e-005
K                  1.379e-004   6.897e-007
Mg                 1.113e-004   5.563e-007
Na                 8.728e-003   4.364e-005
```

```
-----Description of solution-----
pH = 5.800
pe = 4.000
Activity of water = 1.000
Ionic strength = 9.963e-003
Mass of water (kg) = 5.000e-003
Total alkalinity (eq/kg) = -1.731e-006
Total carbon (mol/kg) = 0.000e+000
Total CO2 (mol/kg) = 0.000e+000
Temperature (deg C) = 20.000
Electrical balance (eq) = 8.656e-009
Percent error, 100*(Cat-|An|)/(Cat+|An|) = 0.01
Iterations = 4
Total H = 5.552533e-001
Total O = 2.776266e-001
```

Beginning of initial exchange-composition calculations.

Exchange 1.

X 4.000e-005 mol

Species	Moles	Equiv- alents	Equivalent Fraction	Log Gamma
CaX2	1.274e-005	2.548e-005	6.371e-001	-0.169
NaX	7.064e-006	7.064e-006	1.766e-001	-0.044
MgX2	3.438e-006	6.877e-006	1.719e-001	-0.160
KX	5.770e-007	5.770e-007	1.442e-002	-0.046

Beginning of batch-reaction calculations.

Reaction step 1.

-----Phase assemblage-----

Phase	SI	log IAP	log KT	Moles in assemblage		
				Initial	Final	Delta
Albite	-0.00	2.80	2.80	2.517e-004	3.023e-004	5.064e-005
Calcite	0.00	1.90	1.90	5.995e-005	5.666e-005	-3.287e-006
CO2(g)	-3.50	-11.30	-7.80	1.000e+001	1.000e+001	-1.182e-005
Daphnite-14A	-25.99	27.65	53.64	1.962e-004	0	-1.962e-004
Illite	8.92	18.30	9.38	8.414e-004	8.414e-004	0.000e+000
K-Feldspar	4.18	3.87	-0.32	3.234e-004	3.234e-004	0.000e+000
O2(g)	-0.68	-3.53	-2.85	1.000e+001	1.000e+001	-2.467e-004
Quartz	0.00	-4.13	-4.13	2.400e-002	2.444e-002	4.363e-004

-----Exchange composition-----

X 4.000e-005 mol

Species	Moles	Equiv- alents	Equivalent Fraction	Log Gamma
CaX2	1.611e-005	3.222e-005	8.054e-001	-0.439
MgX2	3.571e-006	7.143e-006	1.786e-001	-0.383
KX	6.309e-007	6.309e-007	1.577e-002	-0.136
NaX	1.029e-008	1.029e-008	2.573e-004	-0.124
AlOHX2	5.306e-012	1.061e-011	2.653e-007	-0.493
AlX3	1.730e-014	5.189e-014	1.297e-009	-0.817
FeX2	1.044e-015	2.088e-015	5.219e-011	-0.439

-----Solution composition-----

Elements	Molality	Moles
Al	6.862e-002	3.418e-004
C	3.033e-003	1.510e-005
Ca	2.437e-004	1.214e-006
Cl	9.643e-003	4.803e-005
Fe	1.970e-001	9.811e-004
K	1.276e-004	6.357e-007
Mg	8.498e-005	4.233e-007
Na	1.079e-005	5.373e-008
Si	7.823e-005	3.897e-007

-----Description of solution-----

pH = 8.635 Charge balance
pe = 12.340 Adjusted to redox equilibrium
Activity of water = 0.996

Ionic strength = 1.481e-001
 Mass of water (kg) = 4.981e-003
 Total alkalinity (eq/kg) = 3.940e-001
 Total CO2 (mol/kg) = 3.033e-003
 Temperature (deg C) = 20.000
 Electrical balance (eq) = 8.656e-009
 Percent error, 100*(Cat-|An|)/(Cat+|An|) = 0.00
 Iterations = 58
 Total H = 5.568230e-001
 Total O = 2.804075e-001

Reaction step 2.

-----Phase assemblage-----

Phase	SI	log IAP	log KT	Moles in assemblage		
				Initial	Final	Delta
Albite	0.00	2.20	2.20	2.517e-004	3.024e-004	5.070e-005
Calcite	-0.00	1.60	1.60	5.995e-005	4.810e-005	-1.185e-005
CO2(g)	-3.50	-11.43	-7.93	1.000e+001	1.000e+001	8.462e-006
Daphnite-14A	-13.64	34.10	47.74	1.962e-004	0	-1.962e-004
Illite	11.26	18.67	7.41	8.414e-004	8.414e-004	0.000e+000
K-Feldspar	4.97	4.37	-0.60	3.234e-004	3.234e-004	0.000e+000
O2(g)	-0.68	-3.66	-2.98	1.000e+001	1.000e+001	-2.463e-004
Quartz	0.00	-3.76	-3.76	2.400e-002	2.444e-002	4.357e-004

-----Exchange composition-----

X 4.000e-005 mol

Species	Moles	Equiv- alents	Equivalent Fraction	Log Gamma
CaX2	1.756e-005	3.512e-005	8.781e-001	-0.427
MgX2	2.285e-006	4.570e-006	1.143e-001	-0.375
KX	3.046e-007	3.046e-007	7.614e-003	-0.131
NaX	4.370e-010	4.370e-010	1.092e-005	-0.120
AlOHX2	1.393e-011	2.785e-011	6.963e-007	-0.476
FeX2	2.108e-014	4.216e-014	1.054e-009	-0.427
AlX3	1.431e-014	4.293e-014	1.073e-009	-0.803

-----Solution composition-----

Elements	Molality	Moles
Al	6.858e-002	3.417e-004
C	6.790e-004	3.384e-006
Ca	1.669e-003	8.319e-006
Cl	9.638e-003	4.803e-005
Fe	1.969e-001	9.811e-004
K	1.931e-004	9.621e-007
Mg	3.430e-004	1.709e-006
Na	1.282e-006	6.390e-009
Si	1.796e-004	8.951e-007

-----Description of solution-----

pH = 8.119 Charge balance
 pe = 11.454 Adjusted to redox equilibrium
 Activity of water = 0.996
 Ionic strength = 1.202e-001
 Mass of water (kg) = 4.983e-003
 Total alkalinity (eq/kg) = 3.972e-001
 Total CO2 (mol/kg) = 6.790e-004
 Temperature (deg C) = 40.000
 Electrical balance (eq) = 8.656e-009
 Percent error, 100*(Cat-|An|)/(Cat+|An|) = 0.00

Iterations = 23
 Total H = 5.568230e-001
 Total O = 2.803928e-001

Reaction step 3.

-----Phase assemblage-----

Phase	SI	log IAP	log KT	Moles in assemblage		
				Initial	Final	Delta
Albite	0.00	1.57	1.57	2.517e-004	3.024e-004	5.070e-005
Calcite	-0.74	0.58	1.32	5.995e-005	0	-5.995e-005
CO2(g)	-3.50	-11.56	-8.06	1.000e+001	1.000e+001	5.957e-005
Daphnite-14A	-3.59	38.89	42.48	1.962e-004	0	-1.962e-004
Illite	12.17	17.72	5.55	8.414e-004	8.414e-004	0.000e+000
K-Feldspar	4.92	3.96	-0.96	3.234e-004	3.234e-004	0.000e+000
O2(g)	-0.68	-3.74	-3.06	1.000e+001	1.000e+001	-2.461e-004
Quartz	0.00	-3.47	-3.47	2.400e-002	2.443e-002	4.349e-004

-----Exchange composition-----

X 4.000e-005 mol

Species	Moles	Equiv- alents	Equivalent Fraction	Log Gamma
CaX2	1.921e-005	3.842e-005	9.606e-001	-0.419
MgX2	7.273e-007	1.455e-006	3.637e-002	-0.371
KX	1.226e-007	1.226e-007	3.064e-003	-0.127
NaX	1.150e-010	1.150e-010	2.875e-006	-0.117
AlOHX2	1.073e-010	2.146e-010	5.364e-006	-0.465
FeX2	1.440e-012	2.880e-012	7.201e-008	-0.419
AlX3	8.943e-014	2.683e-013	6.707e-009	-0.794

-----Solution composition-----

Elements	Molality	Moles
Al	6.852e-002	3.417e-004
C	7.642e-005	3.811e-007
Ca	1.098e-002	5.477e-005
Cl	9.630e-003	4.803e-005
Fe	1.967e-001	9.811e-004
K	2.294e-004	1.144e-006
Mg	6.552e-004	3.267e-006
Na	9.078e-007	4.528e-009
Si	3.401e-004	1.696e-006

-----Description of solution-----

pH = 7.261 Charge balance
 pe = 11.084 Adjusted to redox equilibrium
 Activity of water = 0.995
 Ionic strength = 1.006e-001
 Mass of water (kg) = 4.987e-003
 Total alkalinity (eq/kg) = 4.162e-001
 Total CO2 (mol/kg) = 7.642e-005
 Temperature (deg C) = 60.000
 Electrical balance (eq) = 8.656e-009
 Percent error, 100*(Cat-|An|)/(Cat+|An|) = 0.00
 Iterations = 38
 Total H = 5.568230e-001
 Total O = 2.804362e-001

Reaction step 4.

-----Phase assemblage-----

Phase	SI	log IAP	log KT	Moles in assemblage		
				Initial	Final	Delta
Albite	-0.00	0.93	0.93	2.517e-004	3.024e-004	5.068e-005
Calcite	-0.09	0.96	1.05	5.995e-005	0	-5.995e-005
CO2(g)	-3.50	-11.70	-8.20	1.000e+001	1.000e+001	5.950e-005
Daphnite-14A	-0.00	37.75	37.75	1.962e-004	1.228e-004	-7.340e-005
Illite	9.98	13.78	3.80	8.414e-004	8.414e-004	0.000e+000
K-Feldspar	4.08	2.72	-1.36	3.234e-004	3.234e-004	0.000e+000
O2(g)	-0.68	-3.79	-3.11	1.000e+001	1.000e+001	-9.256e-005
Quartz	0.00	-3.24	-3.24	2.400e-002	2.406e-002	6.524e-005

-----Exchange composition-----

X 4.000e-005 mol

Species	Moles	Equiv- alents	Equivalent Fraction	Log Gamma
CaX2	1.922e-005	3.843e-005	9.609e-001	-0.327
MgX2	7.295e-007	1.459e-006	3.648e-002	-0.298
KX	1.058e-007	1.058e-007	2.645e-003	-0.094
NaX	4.418e-010	4.418e-010	1.104e-005	-0.089
FeX2	1.211e-012	2.422e-012	6.054e-008	-0.327
AlOHX2	5.377e-013	1.075e-012	2.688e-008	-0.353
AlX3	7.647e-017	2.294e-016	5.736e-012	-0.644

-----Solution composition-----

Elements	Molality	Moles
Al	1.924e-002	9.612e-005
C	9.058e-005	4.525e-007
Ca	1.096e-002	5.477e-005
Cl	9.614e-003	4.803e-005
Fe	7.346e-002	3.670e-004
K	2.324e-004	1.161e-006
Mg	6.536e-004	3.265e-006
Na	3.736e-006	1.867e-008
Si	5.823e-004	2.909e-006

-----Description of solution-----

pH = 7.474 Charge balance
 pe = 9.785 Adjusted to redox equilibrium
 Activity of water = 0.998
 Ionic strength = 4.092e-002
 Mass of water (kg) = 4.996e-003
 Total alkalinity (eq/kg) = 1.450e-001
 Total CO2 (mol/kg) = 9.058e-005
 Temperature (deg C) = 80.000
 Electrical balance (eq) = 8.656e-009
 Percent error, 100*(Cat-|An|)/(Cat+|An|) = 0.00
 Iterations = 14
 Total H = 5.558405e-001
 Total O = 2.786578e-001

 End of simulation.

A.2 Simulation based on experimental values with defined reaction rate

RATES

```
    Quartz
start
1 rem      Modified from Plummer and others, 1978
2 rem      parm(1) = A/V, 1/m      parm(2) = exponent for m/m0
10 rate=10^-13.7*(1-SR("Quartz"))*parm(1)*(m/m0)^parm(2)
20 moles =rate * time
30 save moles
end

    Daphnite-14A
start
1 rem      Modified from Plummer and others, 1978
2 rem      parm(1) = A/V, 1/m      parm(2) = exponent for m/m0
10 rate=10^-13.7*(1-SR("Daphnite-14A"))*parm(1)*(m/m0)^parm(2)
20 moles =rate * time
30 save moles
end

    Illite
start
1 rem      Modified from Plummer and others, 1978
2 rem      parm(1) = A/V, 1/m      parm(2) = exponent for m/m0
10 rate=10^-13.7*(1-SR("Illite"))*parm(1)*(m/m0)^parm(2)
20 moles =rate * time
30 save moles
end
SOLUTION 1
    temp      20
    pH        5.8
    pe        4
    redox     pe
    units     mol/l
    density   0.973
    Na        0.00848733744010951
    Cl        0.00934120547241157
    K         0.000134138162307176
    Mg        0.000108198495057296
    Ca        0.000251666439940144
    water     0.005 # kg
EQUILIBRIUM_PHASES 1
    O2(g)     -0.68 10
    CO2(g)    -3.5 10
KINETICS 1
Calcite
    formula   CaCO3 1
    m         5.99477e-005
    m0        5.99477e-005
    parms     10 0.67
    tol       1e-008
Illite
    formula   K0.6Mg0.25Al1.8Al0.5Si3.5O10(OH)2 1
    m         0.000841372137015702
    m0        0.000841372137015702
    parms     10 0.67
    tol       1e-008
Daphnite-14A
    formula   Fe5AlAlSi3O10(OH)8 1
    m         0.000196213830457555
    m0        0.000196213830457555
    parms     10 0.67
    tol       1e-008
K-feldspar
    formula   KAlSi3O8 1
    m         0.000323355
    m0        0.000323355
    parms     10 0.67
    tol       1e-008
```

```

Albite
  formula NaAlSi3O8 1
  m       0.000251694
  m0      0.000251694
  parms   10 0.67
  tol     1e-008
Quartz
  formula SiO2 1
  m       0.0239996
  m0      0.0239996
  parms   10 0.67
  tol     1e-008
steps     3628800 in 4 steps # seconds
step_divide 1
runge_kutta 3
bad_step_max 100000
  EXCHANGE 1
    X      4e-005
    equilibrate with solution 1
    pitzer_exchange_gammas true
  REACTION_TEMPERATURE 1
    20

```

Beginning of initial solution calculations.

Initial solution 1.

-----Solution composition-----

Elements	Molality	Moles
Ca	2.588e-004	1.294e-006
Cl	9.606e-003	4.803e-005
K	1.379e-004	6.897e-007
Mg	1.113e-004	5.563e-007
Na	8.728e-003	4.364e-005

-----Description of solution-----

```

pH = 5.800
pe = 4.000
Activity of water = 1.000
Ionic strength = 9.963e-003
Mass of water (kg) = 5.000e-003
Total alkalinity (eq/kg) = -1.731e-006
Total carbon (mol/kg) = 0.000e+000
Total CO2 (mol/kg) = 0.000e+000
Temperature (deg C) = 20.000
Electrical balance (eq) = 8.656e-009
Percent error, 100*(Cat-|An|)/(Cat+|An|) = 0.01
Iterations = 4
Total H = 5.552533e-001
Total O = 2.776266e-001

```

Beginning of initial exchange-composition calculations.

Exchange 1.

X 4.000e-005 mol

Species	Moles	Equiv- alents	Equivalent Fraction	Log Gamma
CaX2	1.274e-005	2.548e-005	6.371e-001	-0.169

NaX	7.064e-006	7.064e-006	1.766e-001	-0.044
MgX2	3.438e-006	6.877e-006	1.719e-001	-0.160
KX	5.770e-007	5.770e-007	1.442e-002	-0.046

Beginning of batch-reaction calculations.

Reaction step 1.

-----Phase assemblage-----

Phase	SI log IAP	log KT	Moles in assemblage			
			Initial	Final	Delta	
CO2 (g)	-3.50	-11.30	-7.80	1.000e+001	1.000e+001	-2.854e-006
O2 (g)	-0.68	-3.53	-2.85	1.000e+001	1.000e+001	-1.683e-006

-----Exchange composition-----

X 4.000e-005 mol

Species	Moles	Equiv- alents	Equivalent Fraction	Log Gamma
CaX2	1.421e-005	2.842e-005	7.104e-001	-0.180
NaX	5.197e-006	5.197e-006	1.299e-001	-0.047
MgX2	2.976e-006	5.952e-006	1.488e-001	-0.170
KX	4.354e-007	4.354e-007	1.089e-002	-0.049
AlOHX2	3.482e-015	6.964e-015	1.741e-010	-0.188
AlX3	1.043e-017	3.129e-017	7.822e-013	-0.373
FeX2	9.144e-019	1.829e-018	4.572e-014	-0.180

-----Solution composition-----

Elements	Molality	Moles
Al	3.148e-007	1.574e-009
C	1.195e-003	5.976e-006
Ca	5.899e-004	2.949e-006
Cl	9.606e-003	4.803e-005
Fe	1.810e-004	9.048e-007
K	1.473e-004	7.367e-007
Mg	1.957e-004	9.784e-007
Na	9.103e-003	4.551e-005
Si	3.005e-005	1.503e-007

-----Description of solution-----

pH	=	8.307	Charge balance
pe	=	12.668	Adjusted to redox equilibrium
Activity of water	=	1.000	
Ionic strength	=	1.156e-002	
Mass of water (kg)	=	5.000e-003	
Total alkalinity (eq/kg)	=	1.396e-003	
Total CO2 (mol/kg)	=	1.195e-003	
Temperature (deg C)	=	20.000	
Electrical balance (eq)	=	8.467e-009	
Percent error, 100*(Cat- An)/(Cat+ An)	=	0.01	
Iterations	=	1916078	
Total H	=	5.552544e-001	
Total O	=	2.776468e-001	

Reaction step 2.

-----Phase assemblage-----

Phase	SI log IAP	log KT	Moles in assemblage		
			Initial	Final	Delta

CO2 (g)	-3.50	-11.30	-7.80	1.000e+001	1.000e+001	-2.745e-006
O2 (g)	-0.68	-3.53	-2.85	1.000e+001	1.000e+001	-1.909e-006

-----Exchange composition-----

X 4.000e-005 mol

Species	Moles	Equiv- alents	Equivalent Fraction	Log Gamma
CaX2	1.427e-005	2.854e-005	7.135e-001	-0.180
NaX	5.180e-006	5.180e-006	1.295e-001	-0.047
MgX2	2.940e-006	5.880e-006	1.470e-001	-0.170
KX	3.987e-007	3.987e-007	9.968e-003	-0.049
AlOHX2	1.721e-015	3.443e-015	8.607e-011	-0.188
AlX3	5.146e-018	1.544e-017	3.860e-013	-0.373
FeX2	1.821e-018	3.642e-018	9.106e-014	-0.180

-----Solution composition-----

Elements	Molality	Moles
Al	1.560e-007	7.798e-010
C	1.193e-003	5.966e-006
Ca	5.971e-004	2.985e-006
Cl	9.606e-003	4.803e-005
Fe	3.618e-004	1.809e-006
K	1.354e-004	6.772e-007
Mg	1.948e-004	9.741e-007
Na	9.108e-003	4.554e-005
Si	4.825e-005	2.413e-007

-----Description of solution-----

pH = 8.306 Charge balance
 pe = 12.669 Adjusted to redox equilibrium
 Activity of water = 1.000
 Ionic strength = 1.157e-002
 Mass of water (kg) = 5.000e-003
 Total alkalinity (eq/kg) = 1.582e-003
 Total CO2 (mol/kg) = 1.193e-003
 Temperature (deg C) = 20.000
 Electrical balance (eq) = 8.273e-009
 Percent error, 100*(Cat-|An|)/(Cat+|An|) = 0.01
 Iterations = 3819511
 Total H = 5.552555e-001
 Total O = 2.776488e-001

Reaction step 3.

-----Phase assemblage-----

Phase	SI	log IAP	log KT	Moles in assemblage		
				Initial	Final	Delta
CO2 (g)	-3.50	-11.30	-7.80	1.000e+001	1.000e+001	-2.625e-006
O2 (g)	-0.68	-3.53	-2.85	1.000e+001	1.000e+001	-2.135e-006

-----Exchange composition-----

X 4.000e-005 mol

Species	Moles	Equiv- alents	Equivalent Fraction	Log Gamma
CaX2	1.433e-005	2.866e-005	7.165e-001	-0.180
NaX	5.168e-006	5.168e-006	1.292e-001	-0.047
MgX2	2.906e-006	5.811e-006	1.453e-001	-0.170

KX	3.623e-007	3.623e-007	9.058e-003	-0.049
AlOHX2	1.293e-015	2.586e-015	6.465e-011	-0.188
AlX3	3.876e-018	1.163e-017	2.907e-013	-0.373
FeX2	2.746e-018	5.493e-018	1.373e-013	-0.180

-----Solution composition-----

Elements	Molality	Moles
Al	1.159e-007	5.795e-010
C	1.187e-003	5.934e-006
Ca	6.028e-004	3.014e-006
Cl	9.606e-003	4.803e-005
Fe	5.425e-004	2.713e-006
K	1.234e-004	6.171e-007
Mg	1.936e-004	9.681e-007
Na	9.112e-003	4.556e-005
Si	5.949e-005	2.974e-007

-----Description of solution-----

pH = 8.304 Charge balance
 pe = 12.671 Adjusted to redox equilibrium
 Activity of water = 1.000
 Ionic strength = 1.158e-002
 Mass of water (kg) = 5.000e-003
 Total alkalinity (eq/kg) = 1.764e-003
 Total CO2 (mol/kg) = 1.187e-003
 Temperature (deg C) = 20.000
 Electrical balance (eq) = 8.082e-009
 Percent error, 100*(Cat-|An|)/(Cat+|An|) = 0.01
 Iterations = 5713213
 Total H = 5.552566e-001
 Total O = 2.776508e-001

Reaction step 4.

-----Phase assemblage-----

Phase	SI	log IAP	log KT	Moles in assemblage		
				Initial	Final	Delta
CO2(g)	-3.50	-11.30	-7.80	1.000e+001	1.000e+001	-2.503e-006
O2(g)	-0.68	-3.53	-2.85	1.000e+001	1.000e+001	-2.361e-006

-----Exchange composition-----

X 4.000e-005 mol

Species	Moles	Equiv- alents	Equivalent Fraction	Log Gamma
CaX2	1.439e-005	2.877e-005	7.193e-001	-0.180
NaX	5.158e-006	5.158e-006	1.289e-001	-0.047
MgX2	2.872e-006	5.745e-006	1.436e-001	-0.170
KX	3.261e-007	3.261e-007	8.154e-003	-0.049
AlOHX2	1.136e-015	2.273e-015	5.682e-011	-0.188
FeX2	3.693e-018	7.386e-018	1.847e-013	-0.180
AlX3	3.422e-018	1.026e-017	2.566e-013	-0.373

-----Solution composition-----

Elements	Molality	Moles
Al	1.003e-007	5.017e-010
C	1.179e-003	5.895e-006
Ca	6.080e-004	3.040e-006
Cl	9.606e-003	4.803e-005

Fe	7.232e-004	3.616e-006
K	1.114e-004	5.569e-007
Mg	1.923e-004	9.614e-007
Na	9.116e-003	4.558e-005
Si	6.646e-005	3.323e-007

-----Description of solution-----

	pH	=	8.301	Charge balance
	pe	=	12.674	Adjusted to redox equilibrium
	Activity of water	=	1.000	
	Ionic strength	=	1.158e-002	
	Mass of water (kg)	=	5.000e-003	
	Total alkalinity (eq/kg)	=	1.944e-003	
	Total CO2 (mol/kg)	=	1.179e-003	
	Temperature (deg C)	=	20.000	
	Electrical balance (eq)	=	7.895e-009	
Percent error, 100*(Cat- An)/(Cat+ An)		=	0.01	
	Iterations	=	7593988	
	Total H	=	5.552578e-001	
	Total O	=	2.776527e-001	

End of simulation.

A.3 Simulation based on reaction between FW (0.1) and reservoir rock

```

SOLUTION 1-4
  temp      20
  pH        6 charge
  pe        4
  redox     pe
  units     mol/l
  density   1
  Na        0.1326223799
  Ca        0.0147939056
  Mg        0.0017459303
  Cl        0.1677729112
  S(6)     0.000089424
  K         0.0005620389
  Sr        0.0008438344
  water     0.0016 # kg
EQUILIBRIUM_PHASES 1-4
  Albite   0 0.001258471
  Calcite  0 0.000299739
  Daphnite-14A 0 0.000981069
  Illite   0 0.004206861
  K-feldspar 0 0.001616777
  Quartz   0 0.119998069
  CO2(g)  -3.5 10
EXCHANGE 1
  X        2e-004
  equilibrate with solution 1
  pitzer_exchange_gammas true
REACTION_TEMPERATURE 1-4
  20 40 60 80
PRINT
  alkalinity      false
  echo_input      false
-----
Beginning of initial solution calculations.
-----

Initial solution 1.

-----Solution composition-----

Elements          Molality          Moles
-----
Ca                 1.494e-002      2.390e-005
Cl                 1.694e-001      2.711e-004
K                  5.676e-004      9.081e-007
Mg                 1.763e-003      2.821e-006
Na                 1.339e-001      2.143e-004
S(6)              9.030e-005      1.445e-007
Sr                 8.521e-004      1.363e-006

-----Description of solution-----

pH = 7.048          Charge balance
pe = 4.000
Activity of water = 0.995
Ionic strength = 1.846e-001
Mass of water (kg) = 1.600e-003
Total alkalinity (eq/kg) = 1.932e-010
Total carbon (mol/kg) = 0.000e+000
Total CO2 (mol/kg) = 0.000e+000
Temperature (deg C) = 20.000
Electrical balance (eq) = 4.819e-014
Percent error, 100*(Cat-|An|)/(Cat+|An|) = 0.00
Iterations = 4
Total H = 1.776810e-001
Total O = 8.884110e-002

```

 Beginning of initial exchange-composition calculations.

Exchange 1.

X 2.000e-004 mol

Species	Moles	Equiv- alents	Equivalent Fraction	Log Gamma
NaX	6.718e-005	6.718e-005	3.359e-001	-0.132
CaX2	5.736e-005	1.147e-004	5.736e-001	-0.465
SrX2	4.198e-006	8.397e-006	4.198e-002	-0.505
MgX2	4.111e-006	8.221e-006	4.111e-002	-0.403
KX	1.488e-006	1.488e-006	7.439e-003	-0.146

 Beginning of batch-reaction calculations.

Reaction step 1.

-----Phase assemblage-----

Phase	SI	log IAP	log KT	Moles in assemblage		
				Initial	Final	Delta
Albite	-0.00	2.80	2.80	1.258e-003	1.210e-003	-4.883e-005
Calcite	-0.00	1.90	1.90	2.997e-004	3.159e-004	1.613e-005
CO2 (g)	-3.50	-11.30	-7.80	1.000e+001	1.000e+001	-1.706e-005
Daphnite-14A	0.00	53.64	53.64	9.811e-004	9.811e-004	-3.905e-009
Illite	0.00	9.38	9.38	4.207e-003	4.235e-003	2.764e-005
K-Feldspar	-0.00	-0.32	-0.32	1.617e-003	1.602e-003	-1.474e-005
Quartz	0.00	-4.13	-4.13	1.200e-001	1.201e-001	9.384e-005

-----Exchange composition-----

X 2.000e-004 mol

Species	Moles	Equiv- alents	Equivalent Fraction	Log Gamma
NaX	8.986e-005	8.986e-005	4.493e-001	-0.131
CaX2	5.034e-005	1.007e-004	5.034e-001	-0.461
SrX2	4.527e-006	9.054e-006	4.527e-002	-0.499
KX	3.621e-007	3.621e-007	1.811e-003	-0.144
MgX2	1.456e-008	2.912e-008	1.456e-004	-0.399
FeX2	1.127e-008	2.255e-008	1.127e-004	-0.461
AlOHX2	7.531e-015	1.506e-014	7.531e-011	-0.521
AlX3	1.919e-017	5.758e-017	2.879e-013	-0.851

-----Solution composition-----

Elements	Molality	Moles
Al	7.576e-008	1.212e-010
C	5.852e-004	9.360e-007
Ca	9.249e-003	1.479e-005
Cl	1.695e-001	2.711e-004
Fe	5.158e-006	8.250e-009
K	1.159e-004	1.853e-007
Mg	4.406e-006	7.048e-009
Na	1.503e-001	2.404e-004
S	9.033e-005	1.445e-007
Si	7.769e-005	1.243e-007
Sr	6.468e-004	1.035e-006

-----Description of solution-----

pH = 7.852 Charge balance
 pe = -3.392 Adjusted to redox
 equilibrium
 Activity of water = 0.994
 Ionic strength = 1.775e-001
 Mass of water (kg) = 1.599e-003
 Total alkalinity (eq/kg) = 5.885e-004
 Total CO2 (mol/kg) = 5.852e-004
 Temperature (deg C) = 20.000
 Electrical balance (eq) = 4.818e-014
 Percent error, 100*(Cat-|An|)/(Cat+|An|) = 0.00
 Iterations = 21
 Total H = 1.776258e-001
 Total O = 8.881607e-002

Reaction step 2.

-----Phase assemblage-----

Phase	SI	log IAP	log KT	Moles in assemblage		
				Initial	Final	Delta
Albite	0.00	2.20	2.20	1.258e-003	1.215e-003	-4.304e-005
Calcite	0.00	1.60	1.60	2.997e-004	3.141e-004	1.441e-005
CO2(g)	-3.50	-11.43	-7.93	1.000e+001	1.000e+001	-1.498e-005
Daphnite-14A	0.00	47.74	47.74	9.811e-004	9.811e-004	-9.023e-010
Illite	0.00	7.41	7.41	4.207e-003	4.231e-003	2.451e-005
K-Feldspar	0.00	-0.60	-0.60	1.617e-003	1.603e-003	-1.333e-005
Quartz	0.00	-3.76	-3.76	1.200e-001	1.201e-001	8.302e-005

-----Exchange composition-----

X 2.000e-004 mol

Species	Moles	Equiv- alents	Equivalent Fraction	Log Gamma
NaX	8.430e-005	8.430e-005	4.215e-001	-0.135
CaX2	5.244e-005	1.049e-004	5.244e-001	-0.475
SrX2	4.541e-006	9.081e-006	4.541e-002	-0.515
KX	6.324e-007	6.324e-007	3.162e-003	-0.149
MgX2	5.551e-007	1.110e-006	5.551e-003	-0.411
FeX2	2.568e-009	5.136e-009	2.568e-005	-0.475
AlOHX2	8.393e-016	1.679e-015	8.393e-012	-0.537
AlX3	6.509e-019	1.953e-018	9.764e-015	-0.877

-----Solution composition-----

Elements	Molality	Moles
Al	1.666e-007	2.665e-010
C	3.609e-004	5.772e-007
Ca	9.014e-003	1.442e-005
Cl	1.695e-001	2.711e-004
Fe	1.278e-006	2.044e-009
K	2.410e-004	3.855e-007
Mg	1.563e-004	2.500e-007
Na	1.502e-001	2.402e-004
S	9.033e-005	1.445e-007
Si	1.842e-004	2.947e-007
Sr	6.383e-004	1.021e-006

-----Description of solution-----

pH = 7.779 Charge balance

```

equilibrium
pe = -3.391 Adjusted to redox
Activity of water = 0.994
Ionic strength = 1.770e-001
Mass of water (kg) = 1.600e-003
Total alkalinity (eq/kg) = 3.774e-004
Total CO2 (mol/kg) = 3.609e-004
Temperature (deg C) = 40.000
Electrical balance (eq) = 5.408e-014
Percent error, 100*(Cat-|An|)/(Cat+|An|) = 0.00
Iterations = 16
Total H = 1.776320e-001
Total O = 8.881864e-002

```

Reaction step 3.

-----Phase assemblage-----

Phase	SI log IAP	log KT	Moles in assemblage		
			Initial	Final	Delta
Albite	0.00	1.57	1.258e-003	1.246e-003	-1.287e-005
Calcite	-0.00	1.32	2.997e-004	3.038e-004	4.054e-006
CO2(g)	-3.50	-11.56	1.000e+001	1.000e+001	-4.382e-006
Daphnite-14A	0.00	42.48	9.811e-004	9.811e-004	-2.701e-010
Illite	-0.00	5.55	4.207e-003	4.214e-003	7.070e-006
K-Feldspar	0.00	-0.96	1.617e-003	1.613e-003	-3.394e-006
Quartz	0.00	-3.47	1.200e-001	1.200e-001	2.347e-005

-----Exchange composition-----

X 2.000e-004 mol

Species	Moles	Equiv- alents	Equivalent Fraction	Log Gamma
NaX	6.724e-005	6.724e-005	3.362e-001	-0.140
CaX2	5.823e-005	1.165e-004	5.823e-001	-0.493
SrX2	4.348e-006	8.696e-006	4.348e-002	-0.535
MgX2	3.368e-006	6.735e-006	3.368e-002	-0.427
KX	8.615e-007	8.615e-007	4.307e-003	-0.155
FeX2	6.960e-010	1.392e-009	6.960e-006	-0.493
AlOHX2	1.700e-016	3.399e-016	1.700e-012	-0.558
AlX3	4.544e-020	1.363e-019	6.816e-016	-0.909

-----Solution composition-----

Elements	Molality	Moles
Al	3.618e-007	5.789e-010
C	2.052e-004	3.282e-007
Ca	1.186e-002	1.897e-005
Cl	1.694e-001	2.711e-004
Fe	4.717e-007	7.547e-010
K	4.292e-004	6.867e-007
Mg	1.123e-003	1.796e-006
Na	1.419e-001	2.271e-004
S	9.031e-005	1.445e-007
Si	3.581e-004	5.729e-007
Sr	7.585e-004	1.214e-006

-----Description of solution-----

```

equilibrium
pH = 7.655 Charge balance
pe = -2.984 Adjusted to redox
Activity of water = 0.995
Ionic strength = 1.803e-001

```

Mass of water (kg) = 1.600e-003
 Total alkalinity (eq/kg) = 2.376e-004
 Total CO2 (mol/kg) = 2.052e-004
 Temperature (deg C) = 60.000
 Electrical balance (eq) = 4.828e-014
 Percent error, 100*(Cat-|An|)/(Cat+|An|) = 0.00
 Iterations = 12
 Total H = 1.776669e-001
 Total O = 8.883602e-002

Reaction step 4.

-----Phase assemblage-----

Phase	SI	log IAP	log KT	Moles in assemblage		
				Initial	Final	Delta
Albite	0.00	0.93	0.93	1.258e-003	1.288e-003	2.946e-005
Calcite	0.00	1.05	1.05	2.997e-004	2.891e-004	-1.065e-005
CO2(g)	-3.50	-11.70	-8.20	1.000e+001	1.000e+001	1.046e-005
Daphnite-14A	-0.00	37.75	37.75	9.811e-004	9.811e-004	-9.079e-011
Illite	0.00	3.80	3.80	4.207e-003	4.189e-003	-1.753e-005
K-Feldspar	-0.00	-1.36	-1.36	1.617e-003	1.628e-003	1.085e-005
Quartz	0.00	-3.24	-3.24	1.200e-001	1.199e-001	-6.055e-005

-----Exchange composition-----

X 2.000e-004 mol

Species	Moles	Equiv- alents	Equivalent Fraction	Log Gamma
CaX2	6.443e-005	1.289e-004	6.443e-001	-0.519
NaX	4.878e-005	4.878e-005	2.439e-001	-0.148
MgX2	6.653e-006	1.331e-005	6.653e-002	-0.448
SrX2	4.026e-006	8.052e-006	4.026e-002	-0.564
KX	9.937e-007	9.937e-007	4.969e-003	-0.164
FeX2	2.110e-010	4.220e-010	2.110e-006	-0.519
AlOHX2	4.948e-017	9.895e-017	4.948e-013	-0.589
AlX3	4.937e-021	1.481e-020	7.405e-017	-0.954

-----Solution composition-----

Elements	Molality	Moles
Al	7.704e-007	1.233e-009
C	1.190e-004	1.905e-007
Ca	1.717e-002	2.748e-005
Cl	1.694e-001	2.711e-004
Fe	2.143e-007	3.430e-010
K	6.661e-004	1.066e-006
Mg	2.912e-003	4.660e-006
Na	1.270e-001	2.032e-004
S	9.029e-005	1.445e-007
Si	6.045e-004	9.674e-007
Sr	9.596e-004	1.536e-006

-----Description of solution-----

pH = 7.523 Charge balance
 pe = -2.580 Adjusted to redox
 equilibrium

Activity of water = 0.995
 Ionic strength = 1.869e-001
 Mass of water (kg) = 1.600e-003
 Total alkalinity (eq/kg) = 1.724e-004
 Total CO2 (mol/kg) = 1.190e-004
 Temperature (deg C) = 80.000

Electrical balance (eq) = 4.816e-014
Percent error, $100 * (Cat - |An|) / (Cat + |An|)$ = 0.00
Iterations = 12
Total H = 1.777161e-001
Total O = 8.886108e-002

End of simulation.

A.4 Simulation based on reaction between FW (0.01) and reservoir rock

```

SOLUTION 1-4
  temp      20
  pH        6 charge
  pe        4
  redox     pe
  units     mol/l
  density   1
  Na        0.01326223799
  Ca        0.00147939056
  Mg        0.00017459303
  Cl        0.01677729112
  S(6)     0.0000089424
  K         0.00005620389
  Sr        0.00008438344
  water    0.0016 # kg
EQUILIBRIUM_PHASES 1-4
  Albite    0 0.001258471
  Calcite   0 0.000299739
  Daphnite-14A 0 0.000981069
  Illite    0 0.004206861
  K-feldspar 0 0.001616777
  Quartz    0 0.119998069
  CO2(g)   -3.5 10
EXCHANGE 1
  X         2e-004
  equilibrate with solution 1
  pitzer_exchange_gammas true
REACTION_TEMPERATURE 1-4
  20 40 60 80
PRINT
  alkalinity      false
  echo_input     false

```

Beginning of initial solution calculations.

Initial solution 1.

-----Solution composition-----

Elements	Molality	Moles
Ca	1.481e-003	2.369e-006
Cl	1.679e-002	2.687e-005
K	5.626e-005	9.001e-008
Mg	1.748e-004	2.796e-007
Na	1.328e-002	2.124e-005
S(6)	8.951e-006	1.432e-008
Sr	8.447e-005	1.351e-007

-----Description of solution-----

pH	=	7.082	Charge balance
pe	=	4.000	
Activity of water	=	0.999	
Ionic strength	=	1.852e-002	
Mass of water (kg)	=	1.600e-003	
Total alkalinity (eq/kg)	=	2.002e-011	
Total carbon (mol/kg)	=	0.000e+000	
Total CO2 (mol/kg)	=	0.000e+000	
Temperature (deg C)	=	20.000	
Electrical balance (eq)	=	1.438e-020	
Percent error, 100*(Cat- An)/(Cat+ An)	=	0.00	
Iterations	=	5	
Total H	=	1.776810e-001	

Total O = 8.884058e-002

Beginning of initial exchange-composition calculations.

Exchange 1.

X 2.000e-004 mol

Species	Moles	Equiv- alents	Equivalent Fraction	Log Gamma
CaX2	7.618e-005	1.524e-004	7.618e-001	-0.217
NaX	2.455e-005	2.455e-005	1.228e-001	-0.058
SrX2	5.644e-006	1.129e-005	5.644e-002	-0.225
MgX2	5.629e-006	1.126e-005	5.629e-002	-0.203
KX	5.381e-007	5.381e-007	2.691e-003	-0.060

Beginning of batch-reaction calculations.

Reaction step 1.

-----Phase assemblage-----

Phase	SI	log IAP	log KT	Moles in assemblage		
				Initial	Final	Delta
Albite	0.00	2.80	2.80	1.258e-003	1.218e-003	-4.055e-005
Calcite	-0.00	1.90	1.90	2.997e-004	3.126e-004	1.291e-005
CO2 (g)	-3.50	-11.30	-7.80	1.000e+001	1.000e+001	-1.543e-005
Daphnite-14A	-0.00	53.64	53.64	9.811e-004	9.811e-004	-2.310e-009
Illite	-0.00	9.38	9.38	4.207e-003	4.230e-003	2.364e-005
K-Feldspar	0.00	-0.32	-0.32	1.617e-003	1.603e-003	-1.380e-005
Quartz	0.00	-4.13	-4.13	1.200e-001	1.201e-001	8.023e-005

-----Exchange composition-----

X 2.000e-004 mol

Species	Moles	Equiv- alents	Equivalent Fraction	Log Gamma
CaX2	6.500e-005	1.300e-004	6.500e-001	-0.218
NaX	5.828e-005	5.828e-005	2.914e-001	-0.058
SrX2	5.736e-006	1.147e-005	5.736e-002	-0.227
KX	2.289e-007	2.289e-007	1.145e-003	-0.061
FeX2	1.108e-008	2.215e-008	1.108e-004	-0.218
MgX2	2.114e-010	4.227e-010	2.114e-006	-0.204
AlOHX2	1.713e-014	3.426e-014	1.713e-010	-0.231
AlX3	5.006e-017	1.502e-016	7.508e-013	-0.445

-----Solution composition-----

Elements	Molality	Moles
Al	4.426e-007	7.080e-010
C	1.577e-003	2.522e-006
Ca	4.011e-004	6.416e-007
Cl	1.680e-002	2.687e-005
Fe	2.975e-007	4.759e-010
K	1.330e-005	2.128e-008
Mg	2.066e-009	3.304e-012
Na	1.755e-002	2.807e-005
S	8.954e-006	1.432e-008
Si	7.773e-005	1.243e-007

Sr 2.667e-005 4.267e-008

-----Description of solution-----

equilibrium

pH	=	8.414	Charge balance
pe	=	-3.995	Adjusted to redox
Activity of water	=	0.999	
Ionic strength	=	1.877e-002	
Mass of water (kg)	=	1.600e-003	
Total alkalinity (eq/kg)	=	1.602e-003	
Total CO2 (mol/kg)	=	1.577e-003	
Temperature (deg C)	=	20.000	
Electrical balance (eq)	=	-3.268e-018	
Percent error, 100*(Cat- An)/(Cat+ An)	=	-0.00	
Iterations	=	25	
Total H	=	1.776338e-001	
Total O	=	8.882353e-002	

Reaction step 2.

-----Phase assemblage-----

Phase	SI	log IAP	log KT	Moles in assemblage		
				Initial	Final	Delta
Albite	0.00	2.20	2.20	1.258e-003	1.218e-003	-4.024e-005
Calcite	0.00	1.60	1.60	2.997e-004	3.130e-004	1.325e-005
CO2(g)	-3.50	-11.43	-7.93	1.000e+001	1.000e+001	-1.498e-005
Daphnite-14A	0.00	47.74	47.74	9.811e-004	9.811e-004	-4.967e-010
Illite	0.00	7.41	7.41	4.207e-003	4.230e-003	2.358e-005
K-Feldspar	0.00	-0.60	-0.60	1.617e-003	1.603e-003	-1.399e-005
Quartz	0.00	-3.76	-3.76	1.200e-001	1.201e-001	7.988e-005

-----Exchange composition-----

X 2.000e-004 mol

Species	Moles	Equiv- alents	Equivalent Fraction	Log Gamma
CaX2	6.479e-005	1.296e-004	6.479e-001	-0.223
NaX	5.847e-005	5.847e-005	2.923e-001	-0.060
SrX2	5.743e-006	1.149e-005	5.743e-002	-0.232
KX	4.270e-007	4.270e-007	2.135e-003	-0.062
MgX2	1.378e-008	2.757e-008	1.378e-004	-0.209
FeX2	2.498e-009	4.996e-009	2.498e-005	-0.223
AlOHX2	1.671e-015	3.341e-015	1.671e-011	-0.236
AlX3	1.455e-018	4.365e-018	2.182e-014	-0.455

-----Solution composition-----

Elements	Molality	Moles
Al	9.849e-007	1.575e-009
C	1.086e-003	1.738e-006
Ca	3.190e-004	5.103e-007
Cl	1.680e-002	2.687e-005
Fe	5.354e-008	8.564e-011
K	2.721e-005	4.353e-008
Mg	1.064e-007	1.702e-010
Na	1.724e-002	2.757e-005
S	8.954e-006	1.432e-008
Si	1.872e-004	2.994e-007
Sr	2.228e-005	3.563e-008

-----Description of solution-----

pH = 8.381 Charge balance
 pe = -3.959 Adjusted to redox
 equilibrium
 Activity of water = 0.999
 Ionic strength = 1.822e-002
 Mass of water (kg) = 1.600e-003
 Total alkalinity (eq/kg) = 1.133e-003
 Total CO2 (mol/kg) = 1.086e-003
 Temperature (deg C) = 40.000
 Electrical balance (eq) = 1.479e-017
 Percent error, 100*(Cat-|An|)/(Cat+|An|) = 0.00
 Iterations = 13
 Total H = 1.776339e-001
 Total O = 8.882198e-002

Reaction step 3.

-----Phase assemblage-----

Phase	SI	log IAP	log KT	Moles in assemblage		
				Initial	Final	Delta
Albite	-0.00	1.57	1.57	1.258e-003	1.221e-003	-3.754e-005
Calcite	0.00	1.32	1.32	2.997e-004	3.124e-004	1.266e-005
CO2(g)	-3.50	-11.56	-8.06	1.000e+001	1.000e+001	-1.382e-005
Daphnite-14A	0.00	42.48	42.48	9.811e-004	9.811e-004	-1.191e-010
Illite	-0.00	5.55	5.55	4.207e-003	4.229e-003	2.217e-005
K-Feldspar	0.00	-0.96	-0.96	1.617e-003	1.603e-003	-1.345e-005
Quartz	0.00	-3.47	-3.47	1.200e-001	1.201e-001	7.478e-005

-----Exchange composition-----

X 2.000e-004 mol

Species	Moles	Equiv- alents	Equivalent Fraction	Log Gamma
CaX2	6.543e-005	1.309e-004	6.543e-001	-0.230
NaX	5.621e-005	5.621e-005	2.811e-001	-0.061
SrX2	5.746e-006	1.149e-005	5.746e-002	-0.238
KX	7.001e-007	7.001e-007	3.500e-003	-0.064
MgX2	3.629e-007	7.258e-007	3.629e-003	-0.214
FeX2	6.747e-010	1.349e-009	6.747e-006	-0.230
AlOHX2	2.431e-016	4.863e-016	2.431e-012	-0.242
AlX3	6.985e-020	2.096e-019	1.048e-015	-0.468

-----Solution composition-----

Elements	Molality	Moles
Al	2.020e-006	3.231e-009
C	7.225e-004	1.156e-006
Ca	2.859e-004	4.573e-007
Cl	1.680e-002	2.687e-005
Fe	1.290e-008	2.064e-011
K	5.039e-005	8.060e-008
Mg	2.469e-006	3.950e-009
Na	1.695e-002	2.712e-005
S	8.953e-006	1.432e-008
Si	3.752e-004	6.001e-007
Sr	2.061e-005	3.296e-008

-----Description of solution-----

pH = 8.335 Charge balance
 pe = -3.638 Adjusted to redox
 equilibrium
 Activity of water = 0.999

Ionic strength = 1.786e-002
 Mass of water (kg) = 1.600e-003
 Total alkalinity (eq/kg) = 8.102e-004
 Total CO2 (mol/kg) = 7.225e-004
 Temperature (deg C) = 60.000
 Electrical balance (eq) = 2.078e-017
 Percent error, 100*(Cat-|An|)/(Cat+|An|) = 0.00
 Iterations = 13
 Total H = 1.776367e-001
 Total O = 8.882257e-002

Reaction step 4.

-----Phase assemblage-----

Phase	SI	log IAP	log KT	Moles in assemblage		
				Initial	Final	Delta
Albite	-0.00	0.93	0.93	1.258e-003	1.232e-003	-2.692e-005
Calcite	0.00	1.05	1.05	2.997e-004	3.090e-004	9.212e-006
CO2(g)	-3.50	-11.70	-8.20	1.000e+001	1.000e+001	-9.870e-006
Daphnite-14A	-0.00	37.75	37.75	9.811e-004	9.811e-004	-2.270e-011
Illite	-0.00	3.80	3.80	4.207e-003	4.223e-003	1.608e-005
K-Feldspar	-0.00	-1.36	-1.36	1.617e-003	1.607e-003	-1.007e-005
Quartz	0.00	-3.24	-3.24	1.200e-001	1.201e-001	5.367e-005

-----Exchange composition-----

X 2.000e-004 mol

Species	Moles	Equiv- alents	Equivalent Fraction	Log Gamma
CaX2	6.877e-005	1.375e-004	6.877e-001	-0.239
NaX	4.635e-005	4.635e-005	2.317e-001	-0.064
SrX2	5.738e-006	1.148e-005	5.738e-002	-0.248
MgX2	1.864e-006	3.728e-006	1.864e-002	-0.223
KX	9.156e-007	9.156e-007	4.578e-003	-0.066
FeX2	2.060e-010	4.120e-010	2.060e-006	-0.239
AlOHX2	5.750e-017	1.150e-016	5.750e-013	-0.253
AlX3	6.048e-021	1.814e-020	9.072e-017	-0.487

-----Solution composition-----

Elements	Molality	Moles
Al	3.855e-006	6.168e-009
C	4.113e-004	6.580e-007
Ca	3.576e-004	5.721e-007
Cl	1.680e-002	2.687e-005
Fe	4.676e-009	7.480e-012
K	8.485e-005	1.357e-007
Mg	1.512e-005	2.419e-008
Na	1.649e-002	2.637e-005
S	8.953e-006	1.432e-008
Si	6.473e-004	1.035e-006
Sr	2.557e-005	4.091e-008

-----Description of solution-----

equilibrium
 pH = 8.224
 pe = -3.260
 Charge balance
 Adjusted to redox
 Activity of water = 0.999
 Ionic strength = 1.768e-002
 Mass of water (kg) = 1.600e-003
 Total alkalinity (eq/kg) = 5.638e-004
 Total CO2 (mol/kg) = 4.113e-004

Temperature (deg C) = 80.000
Electrical balance (eq) = 4.719e-020
Percent error, $100 * (\text{Cat} - |\text{An}|) / (\text{Cat} + |\text{An}|)$ = 0.00
Iterations = 13
Total H = 1.776489e-001
Total O = 8.882833e-002

End of simulation.

A.5 Simulation based on reaction between NaCl (0.1) and reservoir rock

```

SOLUTION 1-4
  temp      20
  pH        6 charge
  pe        4
  redox     pe
  units     mol/l
  density   1
  Na        0.1679517592
  Cl        0.1679517592
  water     0.0016 # kg
EQUILIBRIUM_PHASES 1-4
  Albite    0 0.001258471
  Calcite   0 0.000299739
  Daphnite-14A 0 0.000981069
  Illite    0 0.004206861
  K-feldspar 0 0.001616777
  Quartz    0 0.119998069
  CO2(g)    -3.5 10
EXCHANGE 1
  X          2e-004
  equilibrate with solution 1
  pitzer_exchange_gammas true
REACTION_TEMPERATURE 1-4
  20 40 60 80
PRINT
  alkalinity      false
  echo_input      false
-----
Beginning of initial solution calculations.
-----

Initial solution 1.

-----Solution composition-----

  Elements          Molality      Moles
  Cl                 1.696e-001  2.714e-004
  Na                 1.696e-001  2.714e-004

-----Description of solution-----

                                pH = 7.070      Charge balance
                                pe = 4.000
                                Activity of water = 0.994
                                Ionic strength = 1.671e-001
                                Mass of water (kg) = 1.600e-003
                                Total alkalinity (eq/kg) = -1.563e-011
                                Total carbon (mol/kg) = 0.000e+000
                                Total CO2 (mol/kg) = 0.000e+000
                                Temperature (deg C) = 20.000
                                Electrical balance (eq) = 1.864e-014
Percent error, 100*(Cat-|An|)/(Cat+|An|) = 0.00
                                Iterations = 4
                                Total H = 1.776810e-001
                                Total O = 8.884052e-002

-----
Beginning of initial exchange-composition calculations.
-----

Exchange 1.

X                2.000e-004 mol

                                Equiv-   Equivalent   Log

```

Species	Moles	alents	Fraction	Gamma
NaX	2.000e-004	2.000e-004	1.000e+000	-0.128

Beginning of batch-reaction calculations.

Reaction step 1.

-----Phase assemblage-----

Phase	SI	log IAP	log KT	Moles in assemblage		
				Initial	Final	Delta
Albite	-0.00	2.80	2.80	1.258e-003	1.312e-003	5.330e-005
Calcite	-0.00	1.90	1.90	2.997e-004	2.800e-004	-1.972e-005
CO2(g)	-3.50	-11.30	-7.80	1.000e+001	1.000e+001	1.737e-005
Daphnite-14A	-0.00	53.64	53.64	9.811e-004	9.811e-004	-1.659e-009
Illite	-0.00	9.38	9.38	4.207e-003	4.176e-003	-3.087e-005
K-Feldspar	-0.00	-0.32	-0.32	1.617e-003	1.634e-003	1.771e-005
Quartz	0.00	-4.13	-4.13	1.200e-001	1.199e-001	-1.051e-004

-----Exchange composition-----

X 2.000e-004 mol

Species	Moles	Equiv- alents	Equivalent Fraction	Log Gamma
NaX	1.516e-004	1.516e-004	7.581e-001	-0.129
CaX2	1.749e-005	3.499e-005	1.749e-001	-0.456
MgX2	6.382e-006	1.276e-005	6.382e-002	-0.396
KX	6.105e-007	6.105e-007	3.053e-003	-0.142
FeX2	5.962e-009	1.192e-008	5.962e-005	-0.456
AlOHX2	9.134e-016	1.827e-015	9.134e-012	-0.514
AlX3	1.376e-018	4.129e-018	2.065e-014	-0.844

-----Solution composition-----

Elements	Molality	Moles
Al	6.651e-008	1.064e-010
C	1.471e-003	2.355e-006
Ca	1.392e-003	2.228e-006
Cl	1.696e-001	2.714e-004
Fe	1.458e-006	2.334e-009
K	1.281e-004	2.050e-007
Mg	8.345e-004	1.336e-006
Na	1.665e-001	2.665e-004
Si	8.407e-005	1.346e-007

-----Description of solution-----

	pH =	8.262	Charge balance
	pe =	-3.815	Adjusted to redox
equilibrium	Activity of water =	0.994	
	Ionic strength =	1.705e-001	
	Mass of water (kg) =	1.601e-003	
	Total alkalinity (eq/kg) =	1.506e-003	
	Total CO2 (mol/kg) =	1.471e-003	
	Temperature (deg C) =	20.000	
	Electrical balance (eq) =	1.864e-014	
Percent error, 100*(Cat- An)/(Cat+ An)	=	0.00	
	Iterations =	20	
	Total H =	1.777428e-001	
	Total O =	8.887758e-002	

Reaction step 2.

-----Phase assemblage-----

Phase	SI log IAP	log KT	Moles in assemblage			
			Initial	Final	Delta	
Albite	0.00	2.20	2.20	1.258e-003	1.365e-003	1.063e-004
Calcite	0.00	1.60	1.60	2.997e-004	2.622e-004	-3.755e-005
CO2(g)	-3.50	-11.43	-7.93	1.000e+001	1.000e+001	3.665e-005
Daphnite-14A	0.00	47.74	47.74	9.811e-004	9.811e-004	-5.718e-010
Illite	0.00	7.41	7.41	4.207e-003	4.145e-003	-6.180e-005
K-Feldspar	0.00	-0.60	-0.60	1.617e-003	1.653e-003	3.584e-005
Quartz	0.00	-3.76	-3.76	1.200e-001	1.198e-001	-2.104e-004

-----Exchange composition-----

X 2.000e-004 mol

Species	Moles	Equiv- alents	Equivalent Fraction	Log Gamma
NaX	1.113e-004	1.113e-004	5.565e-001	-0.134
CaX2	3.193e-005	6.386e-005	3.193e-001	-0.472
MgX2	1.200e-005	2.399e-005	1.200e-001	-0.409
KX	8.345e-007	8.345e-007	4.173e-003	-0.148
FeX2	1.929e-009	3.858e-009	1.929e-005	-0.472
AlOHX2	3.018e-016	6.037e-016	3.018e-012	-0.533
AlX3	1.830e-019	5.491e-019	2.745e-015	-0.872

-----Solution composition-----

Elements	Molality	Moles
Al	1.563e-007	2.502e-010
C	5.669e-004	9.077e-007
Ca	3.511e-003	5.622e-006
Cl	1.695e-001	2.714e-004
Fe	6.433e-007	1.030e-009
K	2.542e-004	4.070e-007
Mg	2.157e-003	3.453e-006
Na	1.585e-001	2.538e-004
Si	1.910e-004	3.059e-007

-----Description of solution-----

equilibrium

	pH =	7.982	Charge balance
	pe =	-3.625	Adjusted to redox
Activity of water	=	0.994	
Ionic strength	=	1.727e-001	
Mass of water (kg)	=	1.601e-003	
Total alkalinity (eq/kg)	=	5.978e-004	
Total CO2 (mol/kg)	=	5.669e-004	
Temperature (deg C)	=	40.000	
Electrical balance (eq)	=	1.864e-014	
Percent error, 100*(Cat- An)/(Cat+ An)	=	0.00	
Iterations	=	16	
Total H	=	1.778046e-001	
Total O	=	8.890523e-002	

Reaction step 3.

-----Phase assemblage-----

Phase	SI log IAP	log KT	Moles in assemblage		
			Initial	Final	Delta

Albite	-0.00	1.57	1.57	1.258e-003	1.419e-003	1.603e-004
Calcite	-0.00	1.32	1.32	2.997e-004	2.435e-004	-5.621e-005
CO2(g)	-3.50	-11.56	-8.06	1.000e+001	1.000e+001	5.580e-005
Daphnite-14A	-0.00	42.48	42.48	9.811e-004	9.811e-004	-2.033e-010
Illite	-0.00	5.55	5.55	4.207e-003	4.114e-003	-9.329e-005
K-Feldspar	-0.00	-0.96	-0.96	1.617e-003	1.671e-003	5.428e-005
Quartz	0.00	-3.47	-3.47	1.200e-001	1.197e-001	-3.178e-004

-----Exchange composition-----

X 2.000e-004 mol

Species	Moles	Equiv- alents	Equivalent Fraction	Log Gamma
NaX	7.722e-005	7.722e-005	3.861e-001	-0.140
CaX2	4.455e-005	8.910e-005	4.455e-001	-0.491
MgX2	1.634e-005	3.268e-005	1.634e-001	-0.425
KX	9.890e-007	9.890e-007	4.945e-003	-0.154
FeX2	5.936e-010	1.187e-009	5.936e-006	-0.491
AlOHX2	9.901e-017	1.980e-016	9.901e-013	-0.556
AlX3	2.318e-020	6.954e-020	3.477e-016	-0.906

-----Solution composition-----

Elements	Molality	Moles
Al	3.503e-007	5.610e-010
C	2.588e-004	4.145e-007
Ca	7.280e-003	1.166e-005
Cl	1.694e-001	2.714e-004
Fe	3.264e-007	5.228e-010
K	4.414e-004	7.069e-007
Mg	4.358e-003	6.981e-006
Na	1.460e-001	2.339e-004
Si	3.642e-004	5.834e-007

-----Description of solution-----

equilibrium

	pH =	7.760	Charge balance
	pe =	-3.104	Adjusted to redox
	Activity of water =	0.994	
	Ionic strength =	1.778e-001	
	Mass of water (kg) =	1.602e-003	
	Total alkalinity (eq/kg) =	3.011e-004	
	Total CO2 (mol/kg) =	2.588e-004	
	Temperature (deg C) =	60.000	
	Electrical balance (eq) =	1.864e-014	
	Percent error, 100*(Cat- An)/(Cat+ An) =	0.00	
	Iterations =	16	
	Total H =	1.778676e-001	
	Total O =	8.893605e-002	

Reaction step 4.

-----Phase assemblage-----

Phase	SI log IAP	log KT	Moles in assemblage			
			Initial	Final	Delta	
Albite	0.00	0.93	0.93	1.258e-003	1.469e-003	2.103e-004
Calcite	0.00	1.05	1.05	2.997e-004	2.261e-004	-7.361e-005
CO2(g)	-3.50	-11.70	-8.20	1.000e+001	1.000e+001	7.338e-005
Daphnite-14A	0.00	37.75	37.75	9.811e-004	9.811e-004	-7.146e-011
Illite	-0.00	3.80	3.80	4.207e-003	4.084e-003	-1.224e-004
K-Feldspar	0.00	-1.36	-1.36	1.617e-003	1.688e-003	7.127e-005

Quartz 0.00 -3.24 -3.24 1.200e-001 1.196e-001 -4.172e-004

-----Exchange composition-----

X 2.000e-004 mol

Species	Moles	Equiv- alents	Equivalent Fraction	Log Gamma
CaX2	5.370e-005	1.074e-004	5.370e-001	-0.518
NaX	5.342e-005	5.342e-005	2.671e-001	-0.147
MgX2	1.905e-005	3.810e-005	1.905e-001	-0.447
KX	1.088e-006	1.088e-006	5.440e-003	-0.163
FeX2	1.891e-010	3.781e-010	1.891e-006	-0.518
AlOHX2	3.436e-017	6.872e-017	3.436e-013	-0.587
AlX3	3.133e-021	9.398e-021	4.699e-017	-0.952

-----Solution composition-----

Elements	Molality	Moles
Al	7.528e-007	1.206e-009
C	1.388e-004	2.223e-007
Ca	1.243e-002	1.991e-005
Cl	1.694e-001	2.714e-004
Fe	1.674e-007	2.682e-010
K	6.797e-004	1.089e-006
Mg	7.211e-003	1.155e-005
Na	1.296e-001	2.077e-004
Si	6.108e-004	9.787e-007

-----Description of solution-----

equilibrium

	pH =	7.592	Charge balance
	pe =	-2.659	Adjusted to redox
	Activity of water =	0.995	
	Ionic strength =	1.851e-001	
	Mass of water (kg) =	1.602e-003	
	Total alkalinity (eq/kg) =	2.016e-004	
	Total CO2 (mol/kg) =	1.388e-004	
	Temperature (deg C) =	80.000	
	Electrical balance (eq) =	1.864e-014	
	Percent error, 100*(Cat- An)/(Cat+ An) =	0.00	
	Iterations =	16	
	Total H =	1.779259e-001	
	Total O =	8.896550e-002	

End of simulation.

A.6 Simulation based on reaction between NaCl (0.01) and reservoir rock

```

SOLUTION 1-4
  temp      20
  pH        6 charge
  pe        4
  redox     pe
  units     mol/l
  density   1
  Na        0.01679517592
  Cl        0.01679517592
  water     0.0016 # kg
EQUILIBRIUM_PHASES 1-4
  Albite    0 0.001258471
  Calcite   0 0.000299739
  Daphnite-14A 0 0.000981069
  Illite    0 0.004206861
  K-feldspar 0 0.001616777
  Quartz    0 0.119998069
  CO2(g)    -3.5 10
EXCHANGE 1
  X         2e-004
  equilibrate with solution 1
  pitzer_exchange_gammas true
REACTION_TEMPERATURE 1-4
  20 40 60 80
PRINT
  alkalinity      false
  echo_input      false

```

Beginning of initial solution calculations.

Initial solution 1.

-----Solution composition-----

Elements	Molality	Moles
Cl	1.681e-002	2.690e-005
Na	1.681e-002	2.690e-005

-----Description of solution-----

```

pH = 7.087          Charge balance
pe = 4.000
Activity of water = 0.999
Ionic strength    = 1.678e-002
Mass of water (kg) = 1.600e-003
Total alkalinity (eq/kg) = 5.067e-018
Total carbon (mol/kg) = 0.000e+000
Total CO2 (mol/kg) = 0.000e+000
Temperature (deg C) = 20.000
Electrical balance (eq) = 7.555e-021
Percent error, 100*(Cat-|An|)/(Cat+|An|) = 0.00
Iterations = 5
Total H = 1.776810e-001
Total O = 8.884052e-002

```

Beginning of initial exchange-composition calculations.

Exchange 1.

```

X          2.000e-004 mol

Equiv-      Equivalent      Log

```

Species	Moles	alents	Fraction	Gamma
NaX	2.000e-004	2.000e-004	1.000e+000	-0.056

Beginning of batch-reaction calculations.

Reaction step 1.

-----Phase assemblage-----

Phase	SI	log IAP	log KT	Moles in assemblage		
				Initial	Final	Delta
Albite	-0.00	2.80	2.80	1.258e-003	1.291e-003	3.260e-005
Calcite	0.00	1.90	1.90	2.997e-004	2.828e-004	-1.696e-005
CO2(g)	-3.50	-11.30	-7.80	1.000e+001	1.000e+001	6.276e-006
Daphnite-14A	0.00	53.64	53.64	9.811e-004	9.811e-004	-1.189e-009
Illite	0.00	9.38	9.38	4.207e-003	4.188e-003	-1.879e-005
K-Feldspar	0.00	-0.32	-0.32	1.617e-003	1.627e-003	1.063e-005
Quartz	0.00	-4.13	-4.13	1.200e-001	1.199e-001	-6.405e-005

-----Exchange composition-----

X 2.000e-004 mol

Species	Moles	Equiv- alents	Equivalent Fraction	Log Gamma
NaX	1.562e-004	1.562e-004	7.810e-001	-0.065
CaX2	1.691e-005	3.381e-005	1.691e-001	-0.241
MgX2	4.677e-006	9.355e-006	4.677e-002	-0.223
KX	6.144e-007	6.144e-007	3.072e-003	-0.067
FeX2	5.620e-009	1.124e-008	5.620e-005	-0.241
AlOHX2	8.436e-016	1.687e-015	8.436e-012	-0.256
AlX3	1.271e-018	3.812e-018	1.906e-014	-0.485

-----Solution composition-----

Elements	Molality	Moles
Al	3.350e-007	5.360e-010
C	6.676e-003	1.068e-005
Ca	3.334e-005	5.336e-008
Cl	1.681e-002	2.690e-005
Fe	2.027e-007	3.244e-010
K	1.796e-005	2.874e-008
Mg	1.325e-005	2.121e-008
Na	2.381e-002	3.810e-005
Si	9.050e-005	1.448e-007

-----Description of solution-----

	pH =	9.016	Charge balance
	pe =	-4.563	Adjusted to redox
equilibrium	Activity of water	=	0.999
	Ionic strength	=	2.408e-002
	Mass of water (kg)	=	1.600e-003
	Total alkalinity (eq/kg)	=	7.110e-003
	Total CO2 (mol/kg)	=	6.676e-003
	Temperature (deg C)	=	20.000
	Electrical balance (eq)	=	-6.481e-018
	Percent error, 100*(Cat- An)/(Cat+ An)	=	-0.00
	Iterations	=	24
	Total H	=	1.777186e-001
	Total O	=	8.888667e-002

Reaction step 2.

-----Phase assemblage-----

Phase	SI log IAP	log KT	Moles in assemblage			
			Initial	Final	Delta	
Albite	0.00	2.20	2.20	1.258e-003	1.336e-003	7.724e-005
Calcite	0.00	1.60	1.60	2.997e-004	2.703e-004	-2.948e-005
CO2(g)	-3.50	-11.43	-7.93	1.000e+001	1.000e+001	2.474e-005
Daphnite-14A	0.00	47.74	47.74	9.811e-004	9.811e-004	-3.417e-010
Illite	0.00	7.41	7.41	4.207e-003	4.162e-003	-4.490e-005
K-Feldspar	0.00	-0.60	-0.60	1.617e-003	1.643e-003	2.603e-005
Quartz	0.00	-3.76	-3.76	1.200e-001	1.198e-001	-1.530e-004

-----Exchange composition-----

X 2.000e-004 mol

Species	Moles	Equiv- alents	Equivalent Fraction	Log Gamma
NaX	1.180e-004	1.180e-004	5.899e-001	-0.062
CaX2	2.939e-005	5.879e-005	2.939e-001	-0.232
MgX2	1.118e-005	2.236e-005	1.118e-001	-0.216
KX	8.622e-007	8.622e-007	4.311e-003	-0.065
FeX2	1.761e-009	3.521e-009	1.761e-005	-0.232
AlOHX2	2.525e-016	5.049e-016	2.525e-012	-0.245
AlX3	1.487e-019	4.462e-019	2.231e-015	-0.471

-----Solution composition-----

Elements	Molality	Moles
Al	8.670e-007	1.388e-009
C	2.960e-003	4.739e-006
Ca	5.348e-005	8.560e-008
Cl	1.680e-002	2.690e-005
Fe	2.999e-008	4.801e-011
K	3.118e-005	4.992e-008
Mg	2.968e-005	4.752e-008
Na	1.978e-002	3.167e-005
Si	2.105e-004	3.370e-007

-----Description of solution-----

equilibrium

pH =	8.803	Charge balance
pe =	-4.455	Adjusted to redox
Activity of water =	0.999	
Ionic strength =	2.007e-002	
Mass of water (kg) =	1.601e-003	
Total alkalinity (eq/kg) =	3.178e-003	
Total CO2 (mol/kg) =	2.960e-003	
Temperature (deg C) =	40.000	
Electrical balance (eq) =	-1.533e-019	
Percent error, 100*(Cat- An)/(Cat+ An) =	-0.00	
Iterations =	19	
Total H =	1.777708e-001	
Total O =	8.889812e-002	

Reaction step 3.

-----Phase assemblage-----

Phase	SI log IAP	log KT	Moles in assemblage		
			Initial	Final	Delta

Albite	0.00	1.57	1.57	1.258e-003	1.373e-003	1.146e-004
Calcite	0.00	1.32	1.32	2.997e-004	2.585e-004	-4.124e-005
CO2(g)	-3.50	-11.56	-8.06	1.000e+001	1.000e+001	3.915e-005
Daphnite-14A	0.00	42.48	42.48	9.811e-004	9.811e-004	-9.143e-011
Illite	0.00	5.55	5.55	4.207e-003	4.140e-003	-6.677e-005
K-Feldspar	0.00	-0.96	-0.96	1.617e-003	1.656e-003	3.894e-005
Quartz	0.00	-3.47	-3.47	1.200e-001	1.198e-001	-2.277e-004

-----Exchange composition-----

X 2.000e-004 mol

Species	Moles	Equiv- alents	Equivalent Fraction	Log Gamma
NaX	8.359e-005	8.359e-005	4.180e-001	-0.062
CaX2	4.108e-005	8.217e-005	4.108e-001	-0.232
MgX2	1.660e-005	3.320e-005	1.660e-001	-0.217
KX	1.041e-006	1.041e-006	5.206e-003	-0.064
FeX2	5.452e-010	1.090e-009	5.452e-006	-0.232
AlOHX2	8.130e-017	1.626e-016	8.130e-013	-0.245
AlX3	1.853e-020	5.560e-020	2.780e-016	-0.473

-----Solution composition-----

Elements	Molality	Moles
Al	1.918e-006	3.071e-009
C	1.304e-003	2.088e-006
Ca	9.597e-005	1.537e-007
Cl	1.680e-002	2.690e-005
Fe	7.461e-009	1.195e-011
K	5.320e-005	8.518e-008
Mg	5.823e-005	9.323e-008
Na	1.791e-002	2.868e-005
Si	4.057e-004	6.496e-007

-----Description of solution-----

equilibrium

pH	=	8.586	Charge balance
pe	=	-3.932	Adjusted to redox
Activity of water	=	0.999	
Ionic strength	=	1.836e-002	
Mass of water (kg)	=	1.601e-003	
Total alkalinity (eq/kg)	=	1.477e-003	
Total CO2 (mol/kg)	=	1.304e-003	
Temperature (deg C)	=	60.000	
Electrical balance (eq)	=	-1.092e-019	
Percent error, 100*(Cat- An)/(Cat+ An)	=	-0.00	
Iterations	=	17	
Total H	=	1.778146e-001	
Total O	=	8.891395e-002	

Reaction step 4.

-----Phase assemblage-----

Phase	SI	log IAP	log KT	Moles in assemblage		
				Initial	Final	Delta
Albite	0.00	0.93	0.93	1.258e-003	1.400e-003	1.410e-004
Calcite	0.00	1.05	1.05	2.997e-004	2.498e-004	-4.996e-005
CO2(g)	-3.50	-11.70	-8.20	1.000e+001	1.000e+001	4.900e-005
Daphnite-14A	0.00	37.75	37.75	9.811e-004	9.811e-004	-1.587e-011
Illite	-0.00	3.80	3.80	4.207e-003	4.125e-003	-8.220e-005
K-Feldspar	0.00	-1.36	-1.36	1.617e-003	1.665e-003	4.802e-005

Quartz 0.00 -3.24 -3.24 1.200e-001 1.197e-001 -2.806e-004

-----Exchange composition-----

X 2.000e-004 mol

Species	Moles	Equiv- alents	Equivalent Fraction	Log Gamma
NaX	5.872e-005	5.872e-005	2.936e-001	-0.064
CaX2	4.968e-005	9.937e-005	4.968e-001	-0.240
MgX2	2.037e-005	4.075e-005	2.037e-001	-0.224
KX	1.160e-006	1.160e-006	5.801e-003	-0.067
FeX2	1.746e-010	3.493e-010	1.746e-006	-0.240
AlOHX2	2.786e-017	5.573e-017	2.786e-013	-0.253
AlX3	2.492e-021	7.476e-021	3.738e-017	-0.488

-----Solution composition-----

Elements	Molality	Moles
Al	3.753e-006	6.010e-009
C	5.982e-004	9.581e-007
Ca	1.739e-004	2.785e-007
Cl	1.680e-002	2.690e-005
Fe	2.940e-009	4.708e-012
K	8.720e-005	1.396e-007
Mg	1.093e-004	1.750e-007
Na	1.695e-002	2.714e-005
Si	6.825e-004	1.093e-006

-----Description of solution-----

equilibrium

pH	=	8.386	Charge balance
pe	=	-3.448	Adjusted to redox
Activity of water	=	0.999	
Ionic strength	=	1.779e-002	
Mass of water (kg)	=	1.601e-003	
Total alkalinity (eq/kg)	=	8.179e-004	
Total CO2 (mol/kg)	=	5.982e-004	
Temperature (deg C)	=	80.000	
Electrical balance (eq)	=	4.090e-021	
Percent error, 100*(Cat- An)/(Cat+ An)	=	0.00	
Iterations	=	18	
Total H	=	1.778454e-001	
Total O	=	8.892748e-002	

End of simulation.
